

**OPTIMAL RESILIENT RETROFIT DESIGN OF  
HEAT-EXCHANGER NETWORKS**

by

**Alp Er Şevki Konukman**

B.S. in Ch.E., İstanbul Teknik Üniversitesi, 1985

M.S. in Ch.E., Boğaziçi University, 1989

Submitted to the Institute for Graduate Studies in  
Science and Engineering in partial fulfillment of  
the requirements for the degree of

**Doctor**

of

**Philosophy**

Bogazici University Library



39001100023731

**Boğaziçi University**

1996

## ACKNOWLEDGMENTS

I would like to express my deepest appreciation to my major advisor Doç. Dr. Uğur Akman and my co-advisor Doç. Dr. Mehmet C. Çamurdan for their supervision, invaluable guidance, everlasting support and encouragement throughout my study.

I am especially grateful to Prof. Dr. Aydın K. Sunol for his invaluable help, encouragement and suggestions.

I wish to thank to Prof. Dr. Ahmet Alp Sayar and Doç. Dr. Işıl Bozma for the time they devoted in reading and commenting on my dissertation.

Financial support provided by the Boğaziçi University Research Fund (Project No. 94A0525) is also acknowledged.

Finally, this dissertation is dedicated to my family.

## ABSTRACT

This study addresses optimal resilient retrofit design of heat-exchanger networks for predetermined structures.

A new index, called the Design Resiliency Index, which numerically indicates the size of feasible region in terms of uncertain source-temperature or flowrates for the fixed design parameters of a network structure, is proposed. Design Resiliency Index provides the opportunity to compare the effects of alternative placement of control variables on the feasible operating range of a pre-designed heat-exchanger network and it is also easily applicable for analyzing the retrofit alternatives of installed networks to make them resilient and controllable.

A new retrofit-design approach for given HEN structures, towards resilient and controllable designs at minimum cost is also proposed in this study. The task of designing a heat-exchanger network for a predetermined structure (retrofit design), which is not only economically at minimum cost but also has the ability to reject the disturbances predefined for all possible source streams and in all directions (increasing or decreasing), is introduced as a single nonlinear programming problem. The objective of this constrained nonlinear optimization problem is to find the individual exchanger areas, nominal utility consumptions, and nominal bypass fractions which minimize the total annualized cost (or the total area) of the given HEN structure and, at the same time, to satisfy the target-temperature constraints for set of disturbances predefined in all possible directions. For the definition of the expected disturbances for all possible directions in source streams, a new index, called the Retrofit Design Resiliency Index, is also proposed.

It is shown in this study that designing a control system using conventional approaches which offer the placement of control variables after the design stage, not only

limits the resiliency and hence the controllability range of a HEN, but also could be more expensive than the solutions generated by the optimal-resilient-retrofit-design method proposed in this study which incorporates the design and control variables in the retrofit stage. It is also shown on the demonstrated examples that the resilient HENs do not necessarily have more total heat-exchange area than the networks originally designed for nominal conditions, as commonly thought.

## ÖZET

Bu çalışma, yapısı önceden belirlenmiş ısı deęiřtirici aęlarının eniyi esnek yeniden-tasarımı üzerinedir.

Tasarım parametreleri belirli bir aę yapısı için olurluluk bölgesinin büyüklüğünü kaynak akımların sıcaklık ve debilerindeki belirsizlikler cinsinden sayısal olarak veren ve Tasarım Esneklik İndeksi olarak adlandırılan yeni bir indeks önerilmiştir. Tasarım Esneklik İndeksi, denetim deęişkenlerinin alternatif yerleşimlerinin, öntasarımı yapılmış bir aęın olurlu çalışma bölgesi üzerindeki etkilerini deęerlendirme olanağı sağlamakta ve ayrıca kurulu aęların esneklik ve denetlenebilirliklerini saęlıyabilecek yeniden-tasarım alternatiflerinin analizinde kolaylıkla kullanılabilir.

Ayrıca bu çalışmada, yapısı belirlenmiş aęları esnek ve denetlenebilir olacak şekilde enaz maliyetle yeniden-tasarımlayan bir yaklaşım da önerilmiştir. Yapısı belirlenmiş ısı deęiřtirici aęları için tasarım problemi (yeniden-tasarım), aęın hem enaz maliyeli hem de tüm kaynak akımların olası tüm yönlerindeki (artış veya azalış) bozucu etkileri karşılayabilecek yetide olmasını saęlayacak şekilde, tek bir doğrusal olmayan programlama problemi olarak sunulmuştur. Bu doğrusal olmayan eniyileme probleminin amacı, toplam yıllık maliyeti enazlıyacak bireysel ısı deęiřtirici alanlarını, nominal ek ısı alış-veriş miktarlarını ve yangeçit fraksiyonların bulmaktır. Formülasyonda kullanılacak, kaynak akımların tüm yönlerinde beklenen bozucu etki miktarını tanımlamak amacıyla, Yeniden-Tasarım Esneklik İndeksi olarak adlandırılan yeni bir indeks önerilmiştir.

Bu çalışmada, denetim deęişkenlerini tasarım aşamasından sonra yerleřtiren geleneksel yaklaşımların, bir ısı deęiřtirici aęı için sadece aęın esnekliğini sınırlamakla kalmayıp aynı zamanda bu çalışmada önerilen ve tasarım ve denetim deęişkenlerini tasarım aşamasında birlikte deęerlendiren eniyi esnek yeniden-tasarım yönteminden daha pahalıya

sonuçlandığı gösterilmiştir. Ayrıca, esnek ağların, sanıldığı gibi aksine, nominal koşullar için tasarlanan ağlardan daha fazla toplam ısı iletim alanına sahip olmasının gerekli olmadığı örnekler üzerinde gösterilmiştir.

## TABLE OF CONTENTS

	Page
ACKNOWLEDGMENT	iii
ABSTRACT	iv
ÖZET	vi
TABLE OF CONTENTS	viii
LIST OF FIGURES	xi
LIST OF TABLES	xx
LIST OF SYMBOLS	xxiii
1. INTRODUCTION	1
2. A BRIEF HISTORICAL OVERVIEW TO HEAT-EXCHANGER NETWORK PROBLEM	4
3. FLEXIBILITY OF HEAT-EXCHANGER NETWORKS	11
3.1. Downstream paths	11
3.2. Flexibility Index	14

4. EFFECTS OF BYPASS-STREAM MANIPULATIONS ON DISTURBANCE-PROPAGATION PATHS	21
4.1. Optimization Formulation	22
5. RETROFIT DESIGN OF RESILIENT HEAT-EXCHANGER NETWORKS	29
5.1. Design-Resiliency Index	29
5.2. Modeling and Formulation	44
5.2.1. Retrofit Design Resiliency Index	45
5.2.2. Formulation of Optimal Resilient Retrofit Design	42
6. DEMONSTRATION OF THE OPTIMAL RESILIENT RETROFIT DESIGN FORMULATION ON EXAMPLE PROBLEMS	55
6.1. Case Study A	64
6.2. Case Study B	78
6.3. Comparison of the Conventional Approaches for Controllable Design of of HENs with the RDRI-Based Optimal Resilient Retrofit Design	88
6.4. Heat-Capacity-Flowrate-Based RDRI	90
7. EFFECT OF SOME CONTROL VARIABLES AND DESIGN PARAMETERS ON OPTIMAL RESILIENT RETROFIT DESIGN	94

7.1. The Effect of Split-Fraction on the Retrofit Design	94
7.2. The Effect of Split-Mixing-Point Temperature on the Retrofit Design	98
7.3. The Effect of Target Specifications on the Retrofit Design	101
7.3.1. Case-Study for Hard Targets, (Case-C)	104
7.3.2. Case-Study for Soft Targets, (Case-D)	109
7.4. The Effect of Capital-Recovery Factor on the Retrofit Design	113
8. CONCLUSIONS AND RECOMMENDATIONS	115
APPENDICES	121
APPENDIX A The GAMS code for the evaluation of the Flexibility Index via linear programming formulation of the example heat-exchanger network given in Chapter 3 (Figure 3.1)	122
APPENDIX B The GAMS code for the solution of the optimization problem defined in Chapter 4	124
APPENDIX C The GAMS code for the solution of the optimization problem defined in Chapter 6	129
REFERENCES	136
REFERENCES NOT CITED	142

## LIST OF FIGURES

	Page
FIGURE 3.1. Pinch solution of the example problem.	12
FIGURE 3.2. Two paths between source of hot-stream 1 and target of cold-stream 1.	12
FIGURE 3.3. Two downstream paths between the source of cold-stream-2 and the target of cold-stream-1.	13
FIGURE 3.4. Structure modified by removing exchanger 3.	13
FIGURE 3.5. Structure modified by changing the placement of exchangers 2 and 4.	14
FIGURE 3.6. Notation for flexibility formulation of the example.	16
FIGURE 4.1. Nominal operating conditions of the example network. (Konukman et. al., 1995a)	23
FIGURE 4.2. Notation for a single exchanger.	23
FIGURE 5.1. Feasibility margins of the example network structure in terms of source-stream temperatures.	30
FIGURE 5.2. Procedure for finding DRI of a HEN.	33
FIGURE 5.3. Notation for the formulation.	34

FIGURE 5.4.	Network modified by introducing cold-side bypass on exchanger 3.	38
FIGURE 5.5.	Network modified by introducing cold-side bypasses on exchangers 1 and 3.	41
FIGURE 5.6.	Network modified by introducing cold-side bypasses on exchangers 1 and 3 and hot-side bypass on exchanger 4.	42
FIGURE 5.7.	Network modified by introducing double bypasses for all the exchangers.	43
FIGURE 5.8.	Notation for general formulation.	51
FIGURE 6.1.	Pinch-solution structure of the example 4SP1 problem.	56
FIGURE 6.2.	Notation for the pinch solution of the 4SP1 problem.	57
FIGURE 6.3.	Procedure for finding the MRDRI and BRDRI of a HEN.	67
FIGURE 6.4.	Variations in areas of heat exchangers and HEN with RDRI for Case-A1.	68
FIGURE 6.5.	Variations in areas of heat exchangers and HEN with RDRI for Case-A2.	68
FIGURE 6.6.	Variations in areas of heat exchangers and HEN with RDRI for Case-A3.	68
FIGURE 6.7.	Variations in areas of heat exchangers and HEN with RDRI for Case-A4.	69

FIGURE 6.8. Variations in areas of heat exchangers and HEN with RDRI for Case-A5.	69
FIGURE 6.9. Variations in areas of heat exchangers and HEN with RDRI for Case-A6.	69
FIGURE 6.10. Variations in areas of heat exchangers and HEN with RDRI for Case-A7.	70
FIGURE 6.11. Variations in areas of heat exchangers and HEN with RDRI for Case-A8.	70
FIGURE 6.12. Variations in areas of heat exchangers and HEN with RDRI for Case-A9.	70
FIGURE 6.13. Variations in areas of heat exchangers and HEN with RDRI for Case-A10.	71
FIGURE 6.14. Variations in areas of heat exchangers and HEN with RDRI for Case-A11.	71
FIGURE 6.15. Variations in areas of heat exchangers and HEN with RDRI for Case-A12.	71
FIGURE 6.16. Variations in areas of heat exchangers and HEN with RDRI for Case-A13.	72
FIGURE 6.17. Variations in areas of heat exchangers and HEN with RDRI for Case-A14.	72
FIGURE 6.18. Variations in areas of heat exchangers and HEN with RDRI for Case-A15.	72

FIGURE 6.19. Variations in areas of heat exchangers and HEN with RDRI for Case-A16.	73
FIGURE 6.20. Variations in areas of heat exchangers and HEN with RDRI for Case-A17.	73
FIGURE 6.21. Variations in areas of heat exchangers and HEN with RDRI for Case-A18.	73
FIGURE 6.22. Variations in areas of heat exchangers and HEN with RDRI for Case-A19.	74
FIGURE 6.23. Variations in areas of heat exchangers and HEN with RDRI for Case-A20.	74
FIGURE 6.24. Variations in areas of heat exchangers and HEN with RDRI for Case-A21.	74
FIGURE 6.25. Variations in areas of heat exchangers and HEN with RDRI for Case-A22.	75
FIGURE 6.26. Variations in areas of heat exchangers and HEN with RDRI for Case-A23.	75
FIGURE 6.27. Variations in areas of heat exchangers and HEN with RDRI for Case-A24.	75
FIGURE 6.28. Variations in areas of heat exchangers and HEN with RDRI for Case-A25.	76
FIGURE 6.29. Variations in areas of heat exchangers and HEN with RDRI for Case-A26.	76

FIGURE 6.30. Example network structure with a cold-side bypass on exchanger 2 (Structure-B1).	79
FIGURE 6.31. Example network structure with a hot-side bypass on exchanger 1 and a cold-side bypass on exchanger 3 (Structure-B2).	79
FIGURE 6.32. Changes in areas of heat exchangers and HEN for Case-B1.	81
FIGURE 6.33. Changes in utility costs for Case-B1.	82
FIGURE 6.34. Changes in costs for Case-B1.	82
FIGURE 6.35. Changes in areas of heat exchangers and HEN for Case-B2.	83
FIGURE 6.36. Changes in utility costs for Case-B2.	83
FIGURE 6.37. Changes in costs for Case-B2.	84
FIGURE 6.38. Changes in the areas of heat exchangers and HEN without considering the areas of utility exchangers for Case-B1.	85
FIGURE 6.39. Changes in utilities without considering the areas of utility exchangers for Case-B1.	86
FIGURE 6.40. Changes in costs without considering the areas of utility exchangers for Case-B1.	86
FIGURE 6.41. Changes in the areas of heat exchangers and HEN without considering areas of utility exchangers for Case-B2.	87
FIGURE 6.42. Changes in utilities without considering the areas of utility exchangers for Case-B2.	87

FIGURE 6.43. Changes in costs without considering the areas of utility exchangers for Case-B2.	88
FIGURE 6.44. Example structure used for the HCF-based retrofit evaluation.	91
FIGURE 6.45. Increases in the areas of heat exchangers and HEN for the example structure.	93
FIGURE 7.1. The relationship between the split-ratio and the flexibility index for the example structure.	95
FIGURE 7.2. Example bypassed-structure studied to demonstrate the effect of selecting fixed-split-ratios ( $x$ ) on the optimal resilient design.	95
FIGURE 7.3. Zero-resiliency design costs with respect to split fraction for the example bypassed-structure (shown in Figure 7.2).	96
FIGURE 7.4. Design parameters with respect to resiliency for fixed-split-fraction 0.42.	96
FIGURE 7.5. Design parameters with respect to resiliency for fixed-split-fraction 0.545.	96
FIGURE 7.6. Design parameters with respect to resiliency for fixed-split-fraction 0.639.	97
FIGURE 7.7. Design parameters with respect to resiliency for fixed-split-fraction 0.661.	97
FIGURE 7.8. Design parameters with respect to resiliency for fixed-split-fraction 0.72.	97

- FIGURE 7.9. Example bypassed-structure studied to demonstrate the effect of temperature difference in the split branches on the resilient design. 99
- FIGURE 7.10. Increases in the areas of heat exchangers and HEN for unconstrained  $\Delta T_{\text{mx}}$  (Case-A20). 100
- FIGURE 7.11. Increases in the areas of exchangers and HEN for  $\max \Delta T_{\text{mx}} = 30 \text{ K}$ . 100
- FIGURE 7.12. Increases in the areas of exchangers and HEN for  $\max \Delta T_{\text{mx}} = 15 \text{ K}$ . 100
- FIGURE 7.13. Increases in the areas of exchangers and HEN for  $\max \Delta T_{\text{mx}} = 0 \text{ K}$ . 101
- FIGURE 7.14. Example network with soft and hard target-temperature constraints. 102
- FIGURE 7.15. Temperature-based feasibility region of the example structure for Case-C. 103
- FIGURE 7.16. Temperature-based feasibility region of the example structure for Case-D. 104
- FIGURE 7.17. Changes in the areas and capital cost for the example network structure with a hot-side bypass on HX-1 and a hot-side bypass on HX-2. 105
- FIGURE 7.18. Changes in the areas and capital cost for the example network structure with a hot-side bypass on HX-1 and a cold-side bypass on HX-2. 105

- FIGURE 7.19. Changes in the areas and capital cost for the example network structure with a cold-side bypass on HX-1 and a hot-side bypass on HX-2. 106
- FIGURE 7.20. Changes in the areas and capital cost for the example network structure with a cold-side bypass on HX-1 and a cold-side bypass on HX-2. 106
- FIGURE 7.21. Changes in the areas and capital cost for the example network structure with a hot- and cold-side bypass on HX-1 and a hot-side bypass on HX-2. 106
- FIGURE 7.22. Changes in the areas and capital cost for the example network structure with a hot- and cold-side bypass on HX-1 and a cold-side bypass on HX-2. 107
- FIGURE 7.23. Changes in the areas and capital cost for the example network structure with a hot-side bypass on HX-1 and a hot- and cold-side bypass on HX-2. 107
- FIGURE 7.24. Changes in the areas and capital cost for the example network structure with a cold-side bypass on HX-1 and a hot- and cold-side bypass on HX-2. 107
- FIGURE 7.25. Changes in the areas and capital cost for the example network structure when all exchangers has double (hot-/cold-side) bypasses. 108
- FIGURE 7.26. Relationship between the areas of the exchangers for the example structure when the targets of the HEN are treated as soft. 110

FIGURE 7.27. Relationship between the areas of the exchangers for different DRI values.	110
FIGURE 7.28. Changes in areas and costs for the example network structure for the soft-target case when exchangers have no bypasses.	111
FIGURE 7.29. Changes in areas costs for the example network structure for the soft-target case when exchanger 2 has a hot-side bypass.	111
FIGURE 7.30. Changes in the total area of HEN for the example network structure for the soft-target case when exchanger 2 has a hot-side bypass or when exchangers have no bypasses. (#s indicate the DRI values).	112
FIGURE 7.31. Changes in the areas costs for the example network structure for the soft-target case when exchanger 1 has a cold-side bypass and exchanger 2 has a hot side bypass.	113
FIGURE 7.32. Total area for different values of rate-of-return.	114
FIGURE 7.33. Operating cost for different values of rate-of-return.	114
FIGURE 7.34. Total cost for different values of rate-of-return.	114

## LIST OF TABLES

	Page
TABLE 3.1. Definition of the example problem.	11
TABLE 3.2. Maximum disturbance magnitudes ( $\delta$ ) for the two alternative structure for all possible disturbance directions.	20
TABLE 3.3. Maximum disturbance magnitudes ( $\delta$ ) for the two alternative structures obtained by assuming cold-stream-2 as the source of disturbance.	20
TABLE 4.1. Optimal heat-capacity-flow-rate values of the bypass streams and the target temperatures.	26
TABLE 4.2. Nonuniqueness of the optimal heat-capacity-flow-rate values of the bypass streams and the target temperatures.	27
TABLE 5.1. Maximum disturbance magnitudes for the example design for all possible disturbance directions (with a cold-side bypass on exchanger 3).	40
TABLE 5.2. Maximum disturbance magnitudes for the example design for all possible disturbance directions (with a cold-side bypasses on exchangers 1 and 3).	41
TABLE 5.3. Maximum disturbance magnitudes for the example design for all possible disturbance directions (with a cold-side bypasses on exchangers 1 and 3, and hot side bypass on exchanger 4).	42

TABLE 5.4. Maximum disturbance magnitudes for the example design for all possible disturbance directions (with hot and cold bypasses on all the exchangers).	43
TABLE 6.1. Definition of the example problem.	55
TABLE 6.2. Source-temperature values for each disturbance direction for 5 K RDRI value.	63
TABLE 6.3. Bypass configurations analyzed. (H1 indicates a bypass around the hot-side of exchanger 1, C1 indicates a bypass around the cold-side of exchanger ... so on.)	66
TABLE 6.4. BRDRI and MRDRI values for different bypass configurations for Case-A.	77
TABLE 6.5. Economic parameters used for the evaluation of the example structure.	80
TABLE 6.6. Initial design (zero-resiliency) values of the example structure.	80
TABLE 6.7. Initial design (zero-resiliency) values for the example structure without considering areas of utility exchangers.	85
TABLE 6.8. Design parameters obtained by different design criterion.	90
TABLE 6.9. Maximum disturbance magnitudes for each disturbance direction based on HCF.	92
TABLE 6.10. Economic parameters and initial (nominal) design costs.	92
TABLE 7.1. Different fixed-split-fraction vs. MRDRI.	98

TABLE 7.2. Total annualized cost (\$) of the designs for different fixed-split-fraction values and for different RDRI values.	98
TABLE 7.3. Maximum disturbance magnitudes for each disturbance direction for Case-C (hard targets).	102
TABLE 7.4. Maximum disturbance magnitudes for each disturbance direction for Case D (soft targets).	103
TABLE 7.5. Economic parameters and zero-resiliency-design costs.	105
TABLE 7.6. Bypass placements vs. maximum RDRI values.	108
TABLE 7.7. Costs of zero-resiliency (initial) design.	111

## LIST OF SYMBOLS

$A_j$	Area of $j^{\text{th}}$ exchanger
$A_{j0}$	Area of $j^{\text{th}}$ exchanger for zero-disturbance design
$A_k$	Area of $k^{\text{th}}$ cooler
$A_l$	Area of $l^{\text{th}}$ heater
BRDRI	Break-point Retrofit Design Resiliency Index
$C_C$	Investment cost coefficient for coolers
$C_{CU}$	Cost coefficient for cooling utility
$C_E$	Investment cost coefficient for exchangers
$C_H$	Investment cost coefficient for heaters
$C_{HU}$	Cost coefficient for heating utility
DRI	Design Resiliency Index
FI	Flexibility Index
HCF	Heat Capacity Flowrate
HEN	Heat-Exchanger Network
HX	Heat exchanger
$h_{c,j}$	Individual heat-transfer coefficient of cold stream entering $j^{\text{th}}$ exchanger
$h_{h,j}$	Individual heat-transfer coefficient of hot stream entering $j^{\text{th}}$ exchanger
$h_{\text{ind}}$	Individual heat-transfer coefficients for streams
LP	Linear Programming
MER	Maximum Energy Recovery
MINLP	Mixed-Integer Nonlinear Programming
NLP	Nonlinear Programming
RDRI	Retrofit Design Resiliency Index

NC	Number of coolers in the network
NCB	Number of cold-side bypasses
NCS	Number of cold streams in the network
NE	Number of exchangers in the network
NH	Number of heaters in the network
NHB	Number of hot-side bypasses
NHS	Number of hot streams in the network
NHT	Number of hard targets
NS	Number of source streams entering the network
NST	Number of soft targets
NX	Number of split streams
MRDRI	Maximum Retrofit Design Resiliency Index
$Q_{c,k}^0$	Heat load of $k^{\text{th}}$ cooler for zero-disturbance direction
$Q_{h,l}^0$	Heat load of $l^{\text{th}}$ heater for zero-disturbance direction
TAC	Total Annualized Cost
$T_{c,l}^{t,p}$	Target temperature of cold stream leaving $l^{\text{th}}$ heater for $p^{\text{th}}$ period
$T_{ce,j}^{i,p}$	Temperature of cold output of $j^{\text{th}}$ exchanger for $i^{\text{th}}$ disturbance direction for $p^{\text{th}}$ period
$T_{ci,j}^{i,p}$	Temperature of cold input of $j^{\text{th}}$ exchanger for $i^{\text{th}}$ disturbance direction for $p^{\text{th}}$ period
$T_{cf,j}^{i,p}$	Temperature of cold stream leaving $j^{\text{th}}$ exchanger after mixing point for $i^{\text{th}}$ disturbance direction for $p^{\text{th}}$ period
$T_{cle,k}^{i,p}$	Outlet temperature of cooling fluid leaving $k^{\text{th}}$ cooler for $i^{\text{th}}$ disturbance direction for $p^{\text{th}}$ period
$T_{cli,k}^{i,p}$	Inlet temperature of cooling fluid entering $k^{\text{th}}$ cooler for $i^{\text{th}}$ disturbance direction for $p^{\text{th}}$ period
$T_{h,k}^{t,p}$	Target temperature of hot stream leaving $k^{\text{th}}$ cooler for $p^{\text{th}}$ period
$T_{he,j}^{i,p}$	Temperature of hot output of $j^{\text{th}}$ exchanger for $i^{\text{th}}$ disturbance direction

	for $p^{\text{th}}$ period
$T_{hi,j}^{i,p}$	Temperature of hot input of $j^{\text{th}}$ exchanger for $i^{\text{th}}$ disturbance direction for $p^{\text{th}}$ period
$T_{hf,j}^{i,p}$	Temperature of hot stream leaving $j^{\text{th}}$ exchanger after mixing point for $i^{\text{th}}$ disturbance direction for $p^{\text{th}}$ period
$T_{hte,l}^{i,p}$	Outlet temperature of heating fluid leaving $l^{\text{th}}$ heater for $i^{\text{th}}$ disturbance direction for $p^{\text{th}}$ period
$T_{hti,l}^{i,p}$	Inlet temperature of heating fluid entering $l^{\text{th}}$ heater for $i^{\text{th}}$ disturbance direction for $p^{\text{th}}$ period
$T_{in}$	Stream inlet temperature to network
$\Delta T_{lm,j}^i$	Logarithmic-mean-temperature difference of $j^{\text{th}}$ exchanger for $i^{\text{th}}$ disturbance direction
$\Delta T_{min}$	Minimum approach temperature
$\Delta T_{mx}$	Difference in temperatures in the split branches
$T_n^s$	Temperature of source stream $n$
$T_{out}$	Stream outlet temperature from network
$t_p$	Period time for operation
$U_j$	Overall heat-transfer coefficient for exchanger $j$
$u_{c,j}^{i,p}$	Cold-side bypass fraction for $j^{\text{th}}$ exchanger for $i^{\text{th}}$ disturbance direction for $p^{\text{th}}$ period
$u_{h,j}^{i,p}$	Hot-side bypass fraction for $j^{\text{th}}$ exchanger for $i^{\text{th}}$ disturbance direction for $p^{\text{th}}$ period
$u_{c,j}^{max}$	Maximum permissible bypass fraction for cold-side bypass on exchanger $j$
$u_{c,j}^{min}$	Minimum permissible bypass fraction for cold-side bypass on exchanger $j$
$u_{h,j}^{max}$	Maximum permissible bypass fraction for hot-side bypass on exchanger $j$
$u_{h,j}^{min}$	Minimum permissible bypass fraction for hot-side bypass on exchanger $j$
$x^i$	Split fraction for $i^{\text{th}}$ disturbance direction

$w_{c,j}^{i,p}$	Heat-capacity-flowrate of cold stream entering $j^{\text{th}}$ exchanger (leaving $j^{\text{th}}$ exchanger after mixing point) for $i^{\text{th}}$ disturbance direction for $p^{\text{th}}$ period
$w_{h,j}^{i,p}$	Heat-capacity-flowrate of hot stream entering $j^{\text{th}}$ exchanger (leaving $j^{\text{th}}$ exchanger after mixing point) for $i^{\text{th}}$ disturbance direction for $p^{\text{th}}$ period
$w_n^s$	Heat-capacity-flowrate of source stream n
$\alpha$	Investment cost coefficient for exchangers
$\beta$	Investment cost coefficient for exchangers
$\delta$	Disturbance magnitude
$\delta^*$	Maximum disturbance magnitude
$\gamma$	Capital-recovery factor

## 1. INTRODUCTION

Heat-Exchanger Networks (HENs) are one of the major components of large-scale chemical processes since they provide great amount of energy savings. In a HEN, hot and cold process streams are integrated (matched) in order to reduce the amount of utility consumption (i.e., external heating and/or cooling requirement) and/or total cost. Techniques of integration of heat exchangers with process units applied to industry in the late 70's. Linnhoff (1982) reported that application of HEN techniques in ICI (especially pinch technology) resulted in energy savings ranged from 6 - 60 per cent and capital savings as high as 30 per cent between 1977 and 1981.

Solution techniques offered for the heat-integration problem of chemical processes up to now, evaluated the design problem of HENs for the fixed environmental conditions. However, in a real process, many flows and temperatures are variable and even it may be requested to change the process conditions. These situations may cause not only a decrease in the efficiency of heat-recovery process hence of the overall process but also risk the operability of other process units integrated to heat-recovery system. Hence, a HEN is to be flexible so that it must cope with variations in its inlet streams. Although the synthesis and design task of a HEN processing under different operating modes are studied by some authors, the design tasks of processing under disturbances are not well investigated. Only very limited number of studies have been observed addressing simultaneously the evaluation of the synthesis and the safety of operation under disturbances in source-streams of HENs. Furthermore, these studies, that may be useful in the synthesis or evolutionary steps of conventional HEN-generating algorithms, evaluate the control problem of HENs with respect to structural controllability.

Although the concept of numerical evaluation of the flexibility (resiliency) of chemical processes was developed in the mid 80's, the evaluation of flexibility of HENs is

still thought as an auxiliary tool in the synthesis step for the selection of alternative structures/designs among those similar in economic characteristics. The 'flexibility index' defined for HENs determines the thermodynamic limits of HEN structures in terms of expected disturbances in its source streams, and hence, gives the information about a HEN structure without considering the design and control variables.

In this study, a new index is introduced which evaluates the flexibility (resiliency) of designed HENs. With this new index, it is possible to see the effects of selection of alternative manipulated variables on resiliency of alternative HEN designs with given structure.

The major problem when designing a control system to a HEN generated by the conventional algorithms, is the lack of degrees of freedom after the design. Assigning manipulated variables after the design stage restricts the control objectives, hence the resiliency of the designed network. Therefore, the design and control objectives must be considered simultaneously in the design stage.

In this study, a new approach which may also be applicable in the evolutionary stage of conventional HEN-generating algorithms, is presented. The proposed approach aims to get a resilient/controllable network at minimum cost for the specified HEN structure. The networks designed by the proposed method are resilient and controllable under the specified set of expected disturbances in temperatures or flowrates of all source-streams of the HENs.

The following is the brief layout of the contents of each chapter in this dissertation.

In Chapter 2, the standard definition of the HEN problem, general solution-approaches to heat recovery problems in chemical processes and approaches for synthesis of flexible/resilient/controllable HENs are briefly given.

In Chapter 3, a classical approach for obtaining flexible/controllable HENs that begins with a pinch structure (i.e., energy optimal), offered by Linnhoff and Kotjabasakis

and the 'flexibility index' concept proposed by Swaney and Grossmann are presented and comparatively discussed on an example problem.

In Chapter 4, the possibility of creation of alternative disturbance-propagation paths in a pre-designed HEN is demonstrated by presenting the disturbance-propagation problem as a constrained nonlinear optimization problem.

In Chapter 5, a new index, termed the Design Resiliency Index (DRI), for evaluating the HEN resiliency of a given HEN structure with given design parameters and control variables, is proposed. Also, in this chapter, a new approach for resilient/controllable retrofit design of HENs, which may be used as an evolutionary stage tool for a HEN problem, is presented.

In Chapter 6, the application of the proposed formulation for the optimal resilient retrofit designs of HENs is demonstrated on example HEN problems and the results of the method is compared with the conventional approaches for obtaining resilient/controllable HENs.

In Chapter 7, the results of investigating of the effects of some common control variables and design parameters on the optimal resilient designs are discussed.

Finally, Chapter 8 is devoted to conclusions drawn from this work.

## 2. A BRIEF HISTORICAL OVERVIEW TO HEAT-EXCHANGER NETWORK PROBLEM

The standard definition of the Heat-Exchanger Network (HEN) problem was given in 1969. Masso and Ruud (1969) stated the problem as: "Given  $n_h$  hot streams to be cooled and  $n_c$  cold streams to be heated from specified supply temperatures to specified target temperatures, design the network of heat exchangers, heaters and coolers accomplishing this task at the least cost". Over the past two decades, many heuristic/evolutionary/algorithmic approaches for the solution of the problem were developed. Most of these methods (Hohmann, 1971; Raghavan, 1977; Nishida et al., 1977 ; Linnhoff and Flowers, 1978a, 1978b; Linnhoff et. al., 1982; Linnhoff and Hindmarsh, 1983) decompose the problem into mainly three stages: i) *targeting* of minimum utility consumption (or minimum heat-transfer area) and minimum number of units (exchangers, heaters, and coolers), ii) *synthesis* of a HEN structure with minimum utility consumption and with minimum or close to minimum number of units, iii) *evolution* of the synthesized structure using heuristics or optimization techniques to get a cheaper network design or to get a network design that provides specific requirements such as operability, flexibility, and safety at the same time.

Up to now, two most popular *synthesis* approaches have been the 'minimum area' algorithm (Nishida et al., 1977) targeting minimum total heat-exchange area and Linnhoff's algorithm (Linnhoff et al. 1978a, 1978b, 1982; Linnhoff and Hindmarsh, 1983) based on the thermodynamic pinch concept targeting maximum energy recovery (minimum utility (external heating/cooling) consumption).

Also, since the mid 80's, mathematical programming techniques were applied to the HEN problem. Papoulias and Grossmann (1983a, b, c) first applied these techniques for the optimal *synthesis* of HENs. They used linear-programming technique for predicting the

minimum utility cost, while also handling restricted matches and multiple utilities. They also applied mixed-integer programming techniques using transshipment models to the HEN problems that yield minimum utility cost networks in which the number of units is minimized, while allowing stream splitting and selection of most-preferred matches.

Floudas et. al. (1986) extended the study of Papoulias and Grossmann (1983a, b, c) by formulating the final design as a nonlinear-programming problem and optimizing the heat-exchanger areas. They proposed a full automatic generation of heat-exchanger network configurations that feature minimum investment cost *subject to* minimum utility cost and fewest number of units. Their method bases on linear-programming and mixed-integer linear-programming transshipment models for heat integration and a superstructure that includes options for series and parallel matching, as well as stream splitting, mixing and bypassing. They implemented their method in computer code MAGNETS, and concluded that the development of high-quality automatic synthesis tools for HENs are indeed feasible.

Floudas and Ciric (1989) also proposed an approach, based on a match-network hyperstructure, that contains all possible matches and network configurations embedded within it. The hyperstructure is used to derive a mixed-integer nonlinear-programming formulation that models simultaneously both the selection of process-stream matches and the derivation of a HEN configuration for a *fixed level of energy recovery*. Optimization of their model determines the stream matches that minimize the total investment cost for a predefined level of energy recovery.

Yee and Grossmann (1990) and Yee et. al. (1990a, b) presented a general superstructure for heat-integration problems. The superstructure is a stage-wise representation where, within each stage, exchanges of heat can occur between each hot and cold stream. Their model can *simultaneously* target for *area* and *energy cost* while accounting for the differences in heat-transfer coefficients between the streams. Constraints on matches can also be easily handled. Furthermore, if a fixed utility consumption is specified, the model reduces to an area-targeting model. Yee and Grossmann (1990) formulated the proposed model as mixed-integer nonlinear-programming problem for the

synthesis/design of HENs. Their model simultaneously evaluates annual cost, comprising utility cost, area cost as well as fixed charges for heat-exchanger units.

Dolan et. al. (1989, 1990) also proposed an interesting solution procedure based on simulated-annealing technique developed by Kirkpatrick et. al. (1983). They proved that simulated annealing as a multivariable-optimization technique is effective useable for the generation of low-cost HENs.

Popular approaches that have been briefly mentioned above evaluate the HEN problem as given in its standard definition. That is, they generate HENs for fixed (nominal) values of stream supply temperatures, flowrates and target temperatures. In practice, however, stream supply temperatures and flowrates can vary and this affects the targets which may be important for operations of downstream process units. A HEN must cope with *desired* or *undesired* variations in operating conditions. In other words, a HEN should be *flexible* so that the effects of uncertainties in operating conditions on the targets should be minimum or preferably none. First necessary condition for this is that the synthesized *HEN structure* must provide steady-state operability (thermodynamical feasibility conditions) under disturbances in sources or under alternative desired operating modes. The concepts of being operable under disturbances and being operable under different operating modes should be differentiated from each other. Although the former concept covers the latter, the latter concept, which is cited as *multi-period operation* in the literature, does not cover the former.

Swaney and Grossmann (1985) proposed an index to quantitatively characterize the flexibility of chemical processes. The *flexibility index (FI)* gives a measure of the size of the region of feasible operation in the space of deviations of the uncertain parameters (generally source-temperatures) from their nominal values. Calculation of FI is a min-max problem which requires  $2^N$  (non)linear-programming problem to be maximized where N is the number of uncertain variables and solution of each of these (N)LPs determine the maximum deviation permitted by the structure from nominal design parameters (vertices of feasible space). In case of linear (in)equality constraints, the space formed by the vertices is a convex region, and the index value defines the hypercube with the maximum size within the

convex region. Due to convexity, feasible operation can be guaranteed by proper manipulation of control variables, in the space defined by FI. Later, Grossmann and Floudas (1987) proposed an optimization algorithm, based on an active-constraint strategy, for the calculation of flexibility index which reduces the problem size. However, Floudas and Grossmann (1987a) showed that active constraint-strategy has a single local optimum only if the areas of exchangers are not taken into account.

Saboo et. al. (1985) also defined a different index to quantify the ability of a HEN to cope with inlet- and target-temperatures changes. *Resilience Index (RI)* considers uncertainties in each stream individually and gives maximum total permissible deviation from nominal design parameters, instead of considering uncertainties in all streams simultaneously. The advantage of RI is that it defines the feasible region geometrically as a polytope and hence the number of N(LP)s to be solved for the determination of feasible region reduces to  $2*N$ .

These index based approaches mentioned above are useful in the analysis of synthesis of *alternative HEN structures*, when choosing the most resilient one among the networks having similar economic characteristics. Konukman et. al. (1994, 1995b) also proposed an index which also indicate the size of feasible region in terms of external uncertainties (source-temperatures or flowrates) for the *fixed design parameters* of a HEN. The main advantage of this index called the *Design Resiliency Index (DRI)* is that it provides the opportunity to compare alternative placement of control variables for a *pre-designed HEN*. It is also easily applicable for analyzing the retrofit alternatives of installed HENs for the purpose of developing resilient/controllable retrofit HENs.

Linnhoff and Kotjabasakis (1986) offered a qualitative procedure, for obtaining flexible HENs, that can be applicable in the evolutionary stage. In their terminology, if the disturbance in one source stream affects one target that should be controlled, the path in the grid diagram between these two is defined as 'downstream path', if not 'upstream path'. Their method proposes structural modifications in the base structure (preferably the structure synthesized by the pinch method) by breaking downstream paths, inserting upstream elements and also inserting bypasses that results in a flexible HEN. They also

proposed a quick reference manual, called '*sensitivity tables*', to evaluate the trade-offs between the capital and energy costs in order to find the best choice among the alternatives created by modifications in the steps of procedure (Kotjabasakis and Linnhoff, 1986). Although their approach provides a good physical insight to the flexibility/controllability problem of HENs, as indicated by Colberg and Morari (1988), has some disadvantages such that they do not consider: i) the interactions between two simultaneously varying supply temperatures, ii) interactions between two paths connecting the same supply and target temperatures, and iii) the nonlinearity of the area (capital cost) as a function of the varying supply temperatures and flowrates.

Floudas and Grossmann (1986) formulated the HEN problem for *multi-period operation* case. Their formulation is based on multi-period mixed-integer linear-programming transshipment model that determines the fewest stream matches that should take place over all the periods of operation. Model also determines the heat that is exchanged in each match in each period of operation. They also proposed a systematic procedure for the synthesis of multi-period energy-recovery configurations that feature minimum utility cost for each time period and the fewest number of units. They extended their study in automatic generation of HENs (for the multi-period case) where the sizing of heat exchangers and the assignment of bypasses are also performed (Floudas and Grossmann, 1987b). They showed that automatic synthesis of HENs for multi-period cases can be performed by a nonlinear-programming formulation that is based on a superstructure representation including all possible structural options for a given set of matches that are predicted for different time periods. They also proposed a graph representation for that superstructure to account for the changes in pinch points and to reduce the size of the nonlinear program. The solution of the nonlinear-programming model of the proposed superstructure provides a feasible network structure that features minimum investment cost, minimum number of units, and minimum utility cost for each time period.

Papalexandri and Pistikopoulos (1993) also proposed a mixed-integer nonlinear-programming model for the *retrofit* of HENs in order to improve their ability to operate feasibly over a specified set of operating conditions at minimum cost. Their model is based on a multi-period match-network hyperstructure representation and includes all possible

retrofit alternatives for all periods. The solution of the proposed problem provides a retrofit structure that is energy efficient and flexible to operate over a specified set of discrete operating conditions.

Controllability issues of HENs have been looked at by few authors. Mathisen et. al. (1991) reviewed different controllability measures and showed how these measures might be used to select bypasses and appropriate pairings among controlled and manipulated variables. They concluded that structural designs and bypass selections where all critical targets are controlled by either utility streams or bypasses with a direct effect should be preferred. Mathisen et. al. (1992), Mathisen and Skogestad (1992), and Mathisen (1994) suggested operability and control-related heuristics which may be applied in the evolutionary stage of traditional HEN-generating algorithms. They also suggested several optimization problems and proposed to take controllability into account by adding control-related constraints to the problem formulation.

Georgiou and Floudas (1989b) addressed the problem of simultaneous process *synthesis* and *control* of heat-recovery systems (HENs). In their study, they assembled the *structural controllability* aspects of a system proposed by Georgiou and Floudas (1989a) with the HEN-synthesis methodology based on the process super/hyper-structure approach developed by Floudas et. al. (1986) and Floudas and Ciric (1989). Their approach was formulated within the context of mixed-integer nonlinear-programming techniques. In their approach, the source of disturbances and the control outputs are certain for a HEN problem, and the objective of their iterative approach is to find the optimal heat exchanger configuration from the economic point of view featuring minimum disturbance effect on the control outputs. Their methodology offers, at the final stage, an analysis of the trade-off between the minimization of the disturbance effect and the total cost for the alternative final designs.

Huang and Fan (1992) also applied a knowledge-engineering (fuzzy-logic) approach to incorporate controllability issues into synthesis of HEN structures by expressing the effect of disturbance propagation on *structural controllability* in a controllability-assessment table that reveals fuzzy relations between the disturbance sources and control

variables. They also offered a structural-based *controllability index* which may be used as a criterion when selecting alternative structures.

As can be understood from this brief overview, the synthesis, flexibility, resiliency, retrofit design, and control of HENs are being studied profusely. Some studies concentrate solely on developing or testing various mathematical/optimization techniques using this difficult non-linear/non-convex problem with integer decision variables, without paying too much attention to ease of applicability of the results to real-life problems. Some studies, on the other hand, provide valuable but simple heuristic rules without too much mathematical complexity and can be easily applied to real-life problems by the engineers. The results of some of these studies can be applied, directly or with minor modifications, to various chemical processes such as the synthesis, flexibility, resiliency, retrofit design, and control of separation or reactor networks or even complete plants.

### 3. FLEXIBILITY OF HEAT-EXCHANGER NETWORKS

In this chapter, the general concepts developed for the evaluation of flexibility of HENs are discussed.

#### 3.1. Downstream paths

For obtaining flexible HENs, Linnhoff and Kotjabasakis (1986) proposed a qualitative procedure which can be applied in the evolutionary stage of synthesis. They introduced the concept of 'downstream paths' which is a very useful tool for understanding the HEN flexibility.

In the approach of Linnhoff and Kotjabasakis (1986), the initial structure is the pinch solution and the procedure can be illustrated with the following example problem defined in Table 3.1. The pinch solution of the problem is given in Figure 3.1. For this solution structure, two questions can be asked; (1) Will any disturbance in a source stream affect a target temperature? (2) What design changes can be made to eliminate these effects?

TABLE 3.1. Definition of the example problem.

Stream	HCF (kW/K)	T <sub>in</sub> (K)	T <sub>out</sub> (K)
Hot 1	30	573	353
Hot 2	45	473	313
Cold 1	40	313	453
Cold 2	60	413	513

As can be seen in Figure 3.1 the target temperatures of hot-stream 1, hot-stream 2 and cold-stream 2 can be controlled by varying the heater and cooler loads. Therefore, one must be concentrated on target temperature of cold-stream 1. Considering the disturbance in hot-stream 1, it can be seen that there are two paths (path: an unbroken connection between two points in a grid diagram) between the source of hot-stream 1 and the target of cold-stream 2 (Figure 3.2). A disturbance coming from the source of hot-stream-1 travels along Path 1 and reaches the target of cold-stream-1. It can be said that Path 1 is "completely downstream". On the other hand, a disturbance coming from the source of hot-stream-1 cannot pass through along Path 2, because the path between exchanger 1 and exchanger 2 is an upstream path. Therefore, Path 2 is "partially upstream". Hence, it is obvious that a disturbance can affect a target only if there is a "completely-downstream path" between the source and the target.

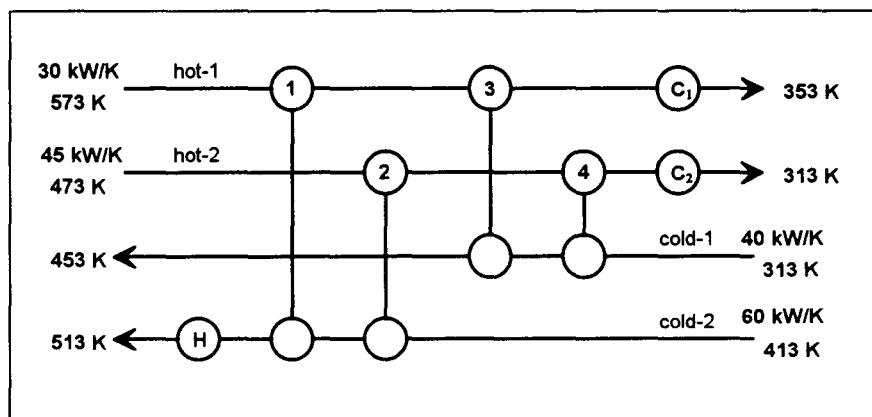


FIGURE 3.1. Pinch solution of the example problem.

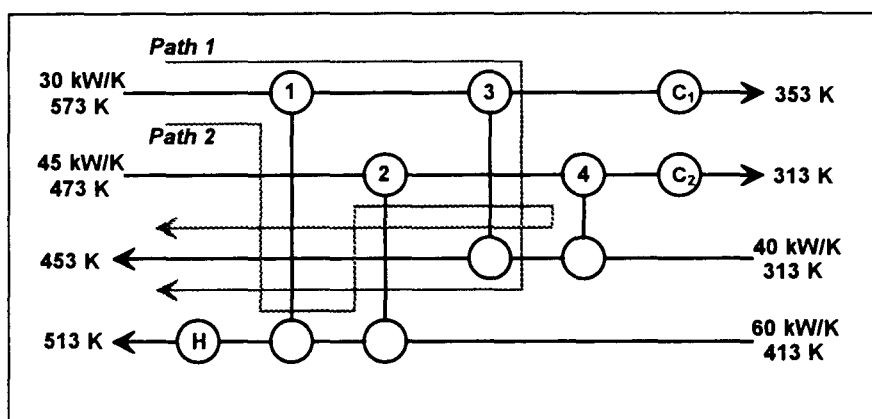


FIGURE 3.2. Two paths between source of hot-stream 1 and target of cold-stream 1.

The procedure for obtaining flexible HEN of Linnhoff and Kotjabasakis (1986) involves three steps.

(1) Breaking the downstream path(s) if the constraints ( $\Delta T_{\min}$ , area, load) permit:

When it is considered that a disturbance comes from the cold-stream-2, there are two completely-downstream paths (Figure 3.3). Removing Exchanger 3 will break Path 1 (Figure 3.4).

(2) Inserting the upstream element(s) if the constraints ( $\Delta T_{\min}$ , area, load) permit:

Upon interchanging the exchangers 2 and 4, the path between exchangers 2 and 4 will be upstream path. (Figure 3.5). (This structure is thermodynamically infeasible.)

(3) Applying the manipulation: If constraints do not permit the changes in the earlier steps, introduction of by-pass(es) to the network might be used to counteract the effects of changing conditions of cold-stream-2 on the target of cold-stream-1. In this situation, the manipulation effects of by-pass(es) to other targets must be considered.

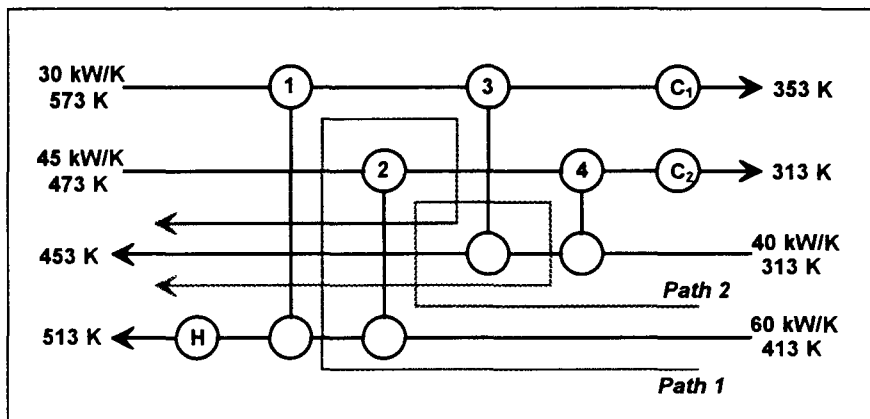


FIGURE 3.3. Two downstream paths between the source of cold-stream-2 and the target of cold-stream-1.

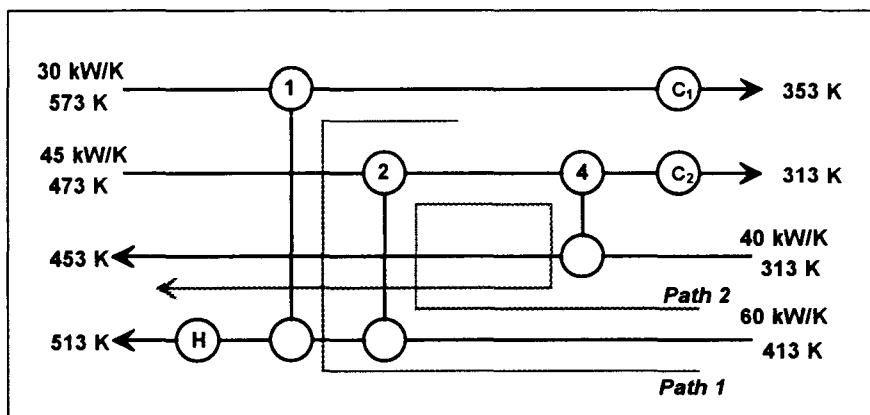


FIGURE 3.4. Structure modified by removing exchanger 3.

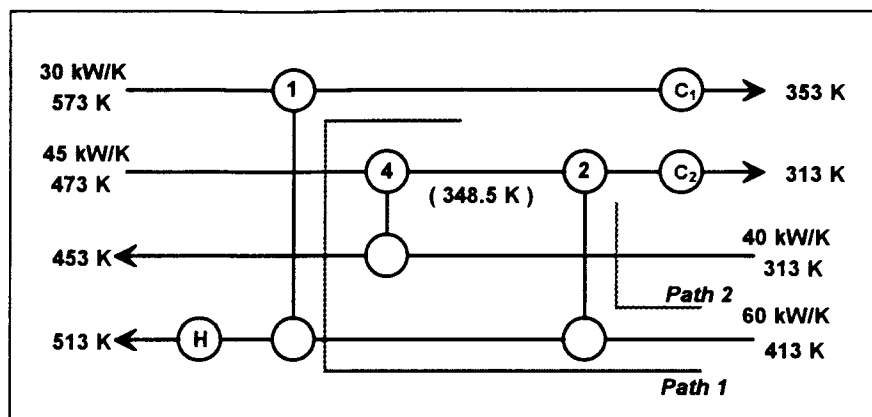


FIGURE 3.5. Structure modified by changing the placement of exchangers 2 and 4.

Linnhoff and Kotjabasakis' procedure offers several design changes which will change the cost of a network. Removing an exchanger, changing the position of two exchangers or installing bypasses to the network may increase the total heat-transfer area of the network and/or the utility consumption. Kotjabasakis and Linnhoff (1986) also presented the sensitivity tables for evaluating the trade-offs between capital and energy costs in order to find the best choice. Although sensitivity tables are quick references, Colberg and Morari (1988) indicate following disadvantages of them: they do not consider i) the nonlinearity of area (capital cost) as a function of the uncertain supply temperatures and flowrates, ii) interactions between two simultaneously-varying supply temperatures and iii) interactions between two paths connecting the same supply and target temperatures.

### 3.2. Flexibility Index

Swaney and Grossmann (1985), offered a procedure for the numerical computation of an index for flexibility of chemical processes. Flexibility index (FI) was expressed as:

$$FI = \min_{\theta \in T} \delta^*(\bar{\theta}) \quad (3.1)$$

$$\bar{T} = \left\{ \bar{\theta} - \Delta\theta^- \leq \bar{\theta} \leq +\Delta\theta^+ \right\} \quad (3.2)$$

where  $\delta^*$  was given by the nonlinear programming

$$\delta^*(\bar{\theta}) = \max_{\delta, z} \delta \quad (3.3)$$

$$\text{subject to } f(d, z, \theta) \leq 0 \quad (3.4)$$

$$\theta = \theta^N + \delta\bar{\theta} \quad (3.5)$$

where  $\delta$  is the parameter deviation,  $f(d, z, \theta)$  are the reduced inequality constraints of the process given in terms of the design variables  $d$ , the control variables  $z$ , and the uncertain variables  $\theta$ ;  $\bar{\theta}$  is a displacement vector from the nominal point  $\theta^N$ , and is bounded by the expected deviations  $\Delta\theta^-$ ,  $\Delta\theta^+$ .

Proposed formulation was demonstrated for the pinch solution of the example problem defined in the previous section (Table 3.1, Figure 3.1, Figure 3.6) (Konukman et al., 1992)

$$FI = \min_{\theta \in \bar{T}} \delta^*(\bar{\theta}) \quad (3.6)$$

$$\delta^*(\bar{\theta}) = \max_{\delta, z} \delta \quad (3.7)$$

subject to ;

energy balances :

$$\text{HX - 1 : } 30(T_1^s - T_1) + 60(T_4 - T_2) = 0 \quad (3.8.a)$$

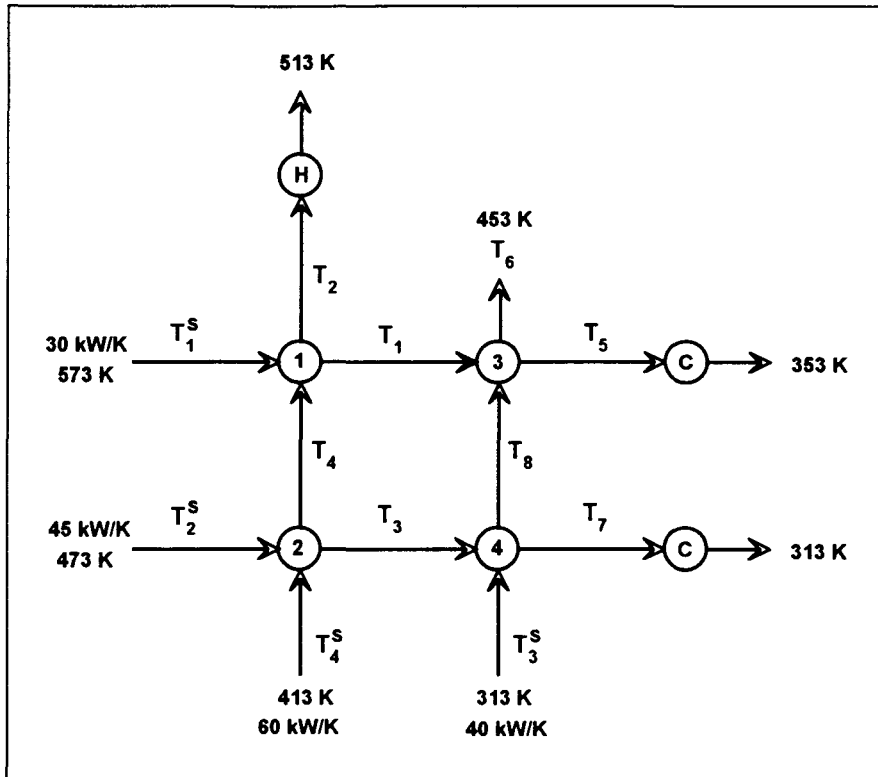


FIGURE 3.6. Notation for flexibility formulation of the example.

or in open form  $30 T_1^s - 30 T_1 - 60 T_2 + 60 T_4 = 0$  (3.8.b)

HX - 2 :  $45 T_2^s + 60 T_3^s - 45 T_3 - 60 T_4 = 0$  (3.9)

HX - 3 :  $30 T_1 - 30 T_5 - 40 T_6 + 40 T_8 = 0$  (3.10)

HX - 4 :  $40 T_4^s + 45 T_3 - 45 T_7 - 40 T_8 = 0$  (3.11)

heat-load constraints :

HX - 1 :  $T_1 - T_1^s \leq 0 \quad T_4 - T_2 \leq 0$  (3.12)

HX - 2 :  $T_3 - T_2^s \leq 0 \quad T_4^s - T_4 \leq 0$  (3.13)

$$\text{HX - 3 :} \quad T_5 - T_1 \leq 0 \quad T_8 - T_6 \leq 0 \quad (3.14)$$

$$\text{HX - 4 :} \quad T_7 - T_3 \leq 0 \quad T_3^s - T_8 \leq 0 \quad (3.15)$$

$$\text{cooler (1}^{\text{st}}) \quad T_5 \geq 353 \quad (3.16)$$

$$\text{cooler (2}^{\text{nd}}) \quad T_7 \geq 313 \quad (3.17)$$

$$\text{heater} \quad T_2 \leq 513 \quad (3.18)$$

approach-temperature constraints :

$$\text{HX - 1 :} \quad T_4 - T_1 \leq 0 \quad T_2 - T_1^s \leq 0 \quad (3.19)$$

$$\text{HX - 2 :} \quad T_4^s - T_3 \leq 0 \quad T_4 - T_2^s \leq 0 \quad (3.20)$$

$$\text{HX - 3 :} \quad T_8 - T_5 \leq 0 \quad T_6 - T_1 \leq 0 \quad (3.21)$$

$$\text{HX - 4 :} \quad T_3^s - T_7 \leq 0 \quad T_8 - T_3 \leq 0 \quad (3.22)$$

$$\begin{bmatrix} T_1^s \\ T_2^s \\ T_3^s \\ T_4^s \end{bmatrix} = \begin{bmatrix} 573 \\ 473 \\ 313 \\ 413 \end{bmatrix} + \delta \bar{\theta} \quad (3.23)$$

$$\bar{T} = \left\{ \bar{\theta} \mid \begin{bmatrix} -1 \\ -1 \\ -1 \\ -1 \end{bmatrix}, \begin{bmatrix} +1 \\ -1 \\ -1 \\ -1 \end{bmatrix}, \begin{bmatrix} -1 \\ +1 \\ -1 \\ -1 \end{bmatrix}, \dots, \begin{bmatrix} +1 \\ +1 \\ +1 \\ +1 \end{bmatrix} \right\} \quad (3.24)$$

As can be seen from the demonstrated formulation, finding flexibility index for a HEN requires solving  $2^{\text{NS}}$  linear programming problems. Every problem includes energy-balance constraints, minimum-approach-temperature constraints for exchangers, and heat-load constraints for exchangers and utilities for specified disturbance direction ( $\theta$ ). Flexibility index is the minimum of maximum value of disturbance magnitudes (i.e. deviations from nominal values of temperatures) found from  $2^{\text{NS}}$  LPs. Disturbance magnitudes are the corner points of a hyper-trapezium in  $2^{\text{NS}}$  dimensional space of uncertain variables. If the problem is LP, due to the property of LP, this region is convex. The flexibility index geometrically is a hyper-cube in the inner side of the hyper-trapezium defining feasibility region and at least one of the corner points of the hyper-cube is the corner point of the hyper-trapezium (critical vertice determining the flexibility index). This means that, for every value of deviation in the range of  $\pm \text{FI}$  from nominal value(s) of uncertain variable(s), the HEN structure will always be feasible. A three dimensional representation of feasibility region of a HEN in the space of uncertain variables can be seen in Section 3 of Chapter 7.

It should be noted that, in the example presented, it is assumed that the source of uncertainty is the temperatures of source-streams (i.e. source of disturbances are the temperatures of source streams). This renders the problem linear. In cases of evaluating uncertain flowrates or in cases of evaluating the structures including steam split(s), problem will be nonlinear unless the split ratio(s) are taken as constant.

For the above example, LP contains 7 equality constraints, 19 inequality constraints and 8 independent variables for every disturbance direction. Maximum values of the disturbance magnitudes for each disturbance direction are tabulated in Table 3.2 under the second column (Structure 1). Flexibility Index of the structure is 30 K. This means that the particular *structure* tolerates the changes in the source streams in the range of  $\pm 30$  K.

For comparison, the maximum disturbance magnitudes for the solution structure resulting from the second step of Linnhoff and Kotjabasakis's procedure for the example (Figure 3.4) are also given in Table 3.2 under the third column (Structure 2). It can be seen

that 'flexibility index' (minimum of the maximum disturbance magnitudes) of original structure (FI = 30 K) is greater than that of the modified structure (FI = 18.8 K).

Here, it should be remembered that, the source of disturbance was taken as cold-stream-2, when "Linnhoff-Kotjabasakis approach" was applied to the problem. Therefore, flexibility of the two alternative structures were also evaluated by considering that cold-stream-2 is the only source of disturbance. Results are tabulated in Table 3.3. Both of the structures limit flexibility in the increasing direction of stream temperature with a maximum flexibility of 60 K. Hence, there is no difference between these structures with regard to their flexibilities.

As can be seen from the example, the steps of Linnhoff and Kotjabasakis's procedure may not definitely generate more flexible structures from the base structure (pinch structure). Therefore, before going into economic evaluation of all alternative structures, a numeric measure, like the 'flexibility index' offered by Swaney and Grossmann, which indicates the feasibility region of the structure will guide in eliminating structures which are inadequate for the purpose. This measure may also be a base for the evaluation of trade-offs between the flexibility and the cost (energy, capital, or total) in the design step. Flexibility over cost ratio ( $\Delta FI/\Delta Cost$ ) ratio may help the selection of the most suitable structure.

The LP problems of this chapter were solved by the software package GAMS (on PC platform), and an example input file is given in Appendix A.

TABLE 3.2. Maximum disturbance magnitudes ( $\delta$ ) for the two alternative structure for all possible disturbance directions.

Disturbance direction $T_1^s T_2^s T_3^s T_4^s$	(Structure 1) (Figure 3.1) $\delta^*$ (K)	(Structure 2) (Figure 3.4) $\delta^*$ (K)
+ + + +	100.0	100.0
+ + + -	140.0	140.0
+ + - +	100.0	100.0
+ + - -	unbounded	unbounded
+ - + +	<b>30.0</b>	20.0
+ - + -	80.0	20.0
+ - - +	<b>30.0</b>	<b>18.8</b>
+ - - -	149.1	<b>18.8</b>
- + + +	80.0	80.0
- + + -	120.0	140.0
- + - +	80.0	80.0
- + - -	120.0	220.0
- - + +	<b>30.0</b>	20.0
- - + -	80.0	20.0
- - - +	<b>30.0</b>	<b>18.8</b>
- - - -	71.3	<b>18.8</b>
<b>FI</b>	<b>30.0</b>	<b>18.8</b>

TABLE 3.3. Maximum disturbance magnitudes ( $\delta$ ) for the two alternative structures obtained by assuming cold-stream-2 as the source of disturbance.

Disturbance direction $T_1^s T_2^s T_3^s T_4^s$	(Structure 1) (Figure 3.1) $\delta^*$ (K)	(Structure 2) (Figure 3.4) $\delta^*$ (K)
0 0 0 +	<b>60.0</b>	<b>60.0</b>
0 0 0 -	unbounded	unbounded
<b>min <math>\delta^*</math></b>	<b>60.0</b>	<b>60.0</b>

#### 4. EFFECTS OF BYPASS-STREAM MANIPULATIONS ON DISTURBANCE-PROPAGATION PATHS

The control objective of a HEN is to satisfy target-temperature constraints for the safety of downstream process units. For this propose, target temperatures of the network may be introduced as hard (exact:  $\pm$  zero deviation) or soft (range: deviation within  $\pm$  range) targets. As indicated earlier, traditional HEN-synthesis methods do not necessarily accommodate utility exchangers for each of the target streams. Therefore, the control objectives can be achieved by manipulated variables that may exist in the network. The only manipulated variables that can be generated by the traditional HEN-synthesis methods are split streams. However, the number of splits generated may not be adequate for the satisfaction of a desired operability range. Therefore, the major problem in control of HENs produced by the traditional HEN-synthesis methods is the lack of degrees of freedom. In these situations, the required number of degrees of freedom may be provided only by introducing bypass streams to the network.

In this chapter, the effects of bypass streams on disturbance propagation paths are investigated for a *designed* network. The optimization problem presented for a pre-designed HEN is the minimization of target-temperature deviations subject to target-temperature constraints (soft or hard). Different range constraints on the hot and cold targets are imposed in order to demonstrate the possibility of creation of alternate disturbance-propagation (disturbance-rejection) paths via bypass streams and their manipulations. Nonuniqueness of the optimal solution and nonconvexity problems for this type of constrained, nonlinear optimization of HENs are also discussed.

#### 4.1. Optimization Formulation

The example network which will be used in this chapter is shown in Figure 4.1 (adapted from Colberg and Morari (1988)) (Konukman et. al, 1995a). Network has three exchangers and has no utility exchanger and no split streams. It is obvious that, if all the targets of the network are wanted to be hard targets, there is no possibility of meeting all the targets after disturbances in source streams, since the overall enthalpy balance around the HEN cannot be satisfied, and thus, no new feasible steady-state point can be found. The nominal flowrates, and the nominal values of the source and target temperatures are as given in Figure 4.1. The overall heat-transfer coefficients were taken as 1000 W/m<sup>2</sup>K for all the exchangers. All possible single-bypass (bypass over only one exchanger) configurations were taken into consideration in the modeling. Nominal values of bypasses (when no disturbance comes to the HEN) are zero.

The formulation of the optimization problem, referring to the nomenclature depicted in Figure 4.2, is as follows:

objective function:

$$\underset{u_{h,j}, u_{c,j}, T_{he,j}, T_{ce,j}}{\text{minimize}} \left\{ \sum_j^{\text{NHS}} |\Delta T_{hf,j}^t| + \sum_j^{\text{NCS}} |\Delta T_{cf,j}^t| \right\} \quad (4.1)$$

subject to:

equality constraints (energy balances):

$$w_{h,j} (T_{hi,j} - T_{hf,j}) + w_{c,j} (T_{ci,j} - T_{cf,j}) = 0 \quad (4.2)$$

$$w_{h,j} (1 - u_{h,j}) (T_{hi,i} - T_{he,i}) - U_j A_j \Delta T_{lm,j} = 0 \quad (4.3)$$

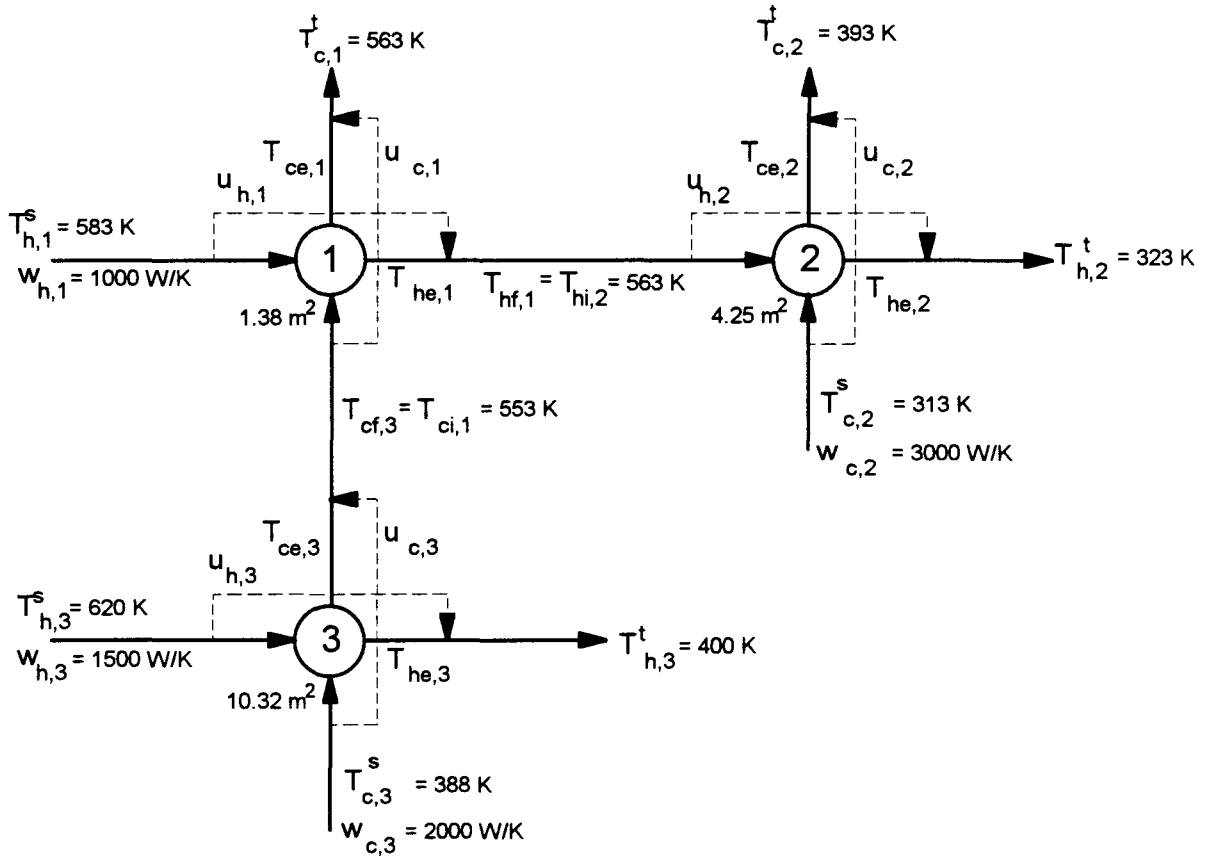


FIGURE 4.1. Nominal operating conditions of the example network. (Konukman et. al., 1995a)

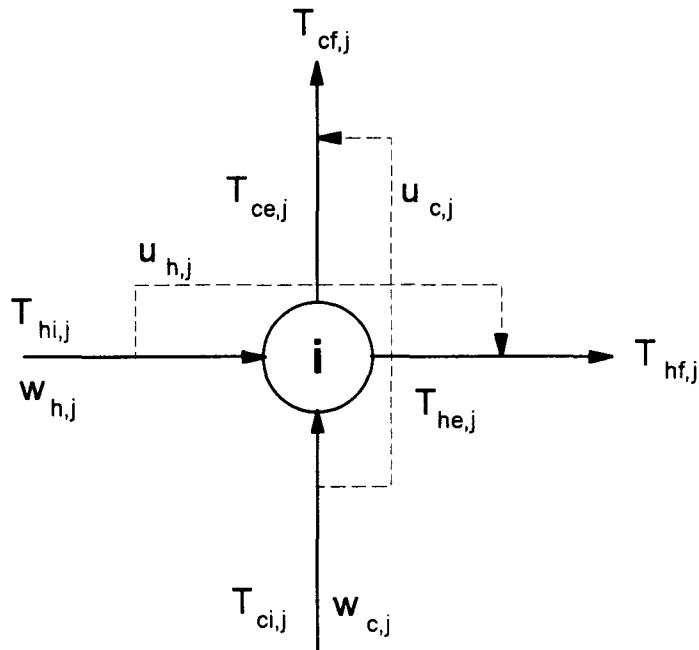


FIGURE 4.2. Notation for a single exchanger.

inequality constraints (minimum-approach-temperature constraints):

$$T_{ce,j} - T_{hi,j} \leq \Delta T_{\min} \quad (4.4)$$

$$T_{ci,j} - T_{he,j} \leq \Delta T_{\min} \quad (4.5)$$

where  $\Delta T_{\min} = 0$

inequality constraints (target-temperature range constraints):

$$\left( T_{hf,j}^t - \Delta T_{hf,j}^t \right) \leq T_{hf,j} \leq \left( T_{hf,j}^t + \Delta T_{hf,j}^t \right) \quad (4.6)$$

$$\left( T_{cf,j}^t - \Delta T_{cf,j}^t \right) \leq T_{cf,j} \leq \left( T_{cf,j}^t + \Delta T_{cf,j}^t \right) \quad (4.7)$$

inequality constraints (manipulated-variable range constraints):

$$u_{h,j}^{\min} \leq u_{h,j} < u_{h,j}^{\max} \quad (4.8)$$

$$u_{c,j}^{\min} \leq u_{c,j} < u_{c,j}^{\max} \quad (4.9)$$

where;

$$\Delta T_{lm,j} = \frac{\left( T_{hi,j} - T_{ce,j} \right) - \left( T_{he,j} - T_{ci,j} \right)}{\ln \left[ \left( T_{hi,j} - T_{ce,j} \right) / \left( T_{he,j} - T_{ci,j} \right) \right]} \quad (4.10)$$

$$\Delta T_{hf,j}^t = T_{hf,j} - T_{hf,j}^t \quad (4.11)$$

$$\Delta T_{cf,j}^t = T_{cf,j} - T_{cf,j}^t \quad (4.12)$$

The energy balances for the mixing points of the bypass streams are as follows:

$$T_{hf,j} = u_{h,j} T_{hi,j} + (1 - u_{h,j}) T_{he,j} \quad (4.13)$$

$$T_{cf,j} = u_{c,j} T_{ci,j} + (1 - u_{c,j}) T_{ce,j} \quad (4.14)$$

For the HEN shown in Figure 4.2 the following identities are valid:

$$\begin{array}{ll}
 w_{h,1} = w_{h,2} = 1000 \text{ W / K} & w_{h,3} = 1500 \text{ W / K} \\
 w_{c,1} = w_{c,3} = 2000 \text{ W / K} & w_{c,2} = 3000 \text{ W / K} \\
 T_{hi,1}^s = 583 \text{ K} & T_{hi,3}^s = 620 \text{ K} \\
 T_{ci,3}^s = 388 \text{ K} & T_{ci,2}^s = 313 \text{ K} \\
 T_{hf,2}^t = 323 \text{ K} & T_{hf,4}^t = 400 \text{ K} \\
 T_{cf,1}^t = 563 \text{ K} & T_{cf,2}^t = 393 \text{ K} \\
 T_{hf,2} = T_{hi,3} & T_{cf,3} = T_{ci,1}
 \end{array}$$

For the HEN shown in Figure 4.1, there are  $4 \cdot NE = 12$  decision variables (three  $u_{h,j}$ , three  $u_{c,j}$ , three  $T_{he,j}$ , three  $T_{ce,j}$ ), there are  $2 \cdot NE = 6$  equality constraints (Eq. 4.2, Eq. 4.3), there are  $2 \cdot NE = 6$ , minimum-approach-temperature constraints (Eq. 4.4, Eq. 4.5), there are  $NS = 4$  target-temperature range constraints (Eq. 4.6, Eq. 4.7), there are  $2 \cdot NE$  manipulated-variable range constraints (Eq. 4.8, Eq. 4.9), there are  $2 \cdot NE = 6$  energy balances for mixing points of bypass streams (Eq. 4.13, Eq. 4.14). The balances for mixing points should not be treated as additional equality constraints since the mixing balances are not independent of the equality constraints in this type of formulation. All equality constraints are nonlinear due to  $\Delta T_{lm,j}$  terms and bilinearities resulting from the product of the variables  $u_{h,j}$  and  $T_{he,j}$ , and,  $u_{c,j}$  and  $T_{ce,j}$ . Due to bilinearities in the energy balances for the mixing point of bypass streams, some of the inequality constraints are also nonlinear.

The nonlinear programming formulation given by Eqs. 4.1- 4.14 was solved by using the software package GAMS, and the coding of the formulation is given in Appendix B.

For the example HEN, three different scenarios of disturbance propagation are investigated. For all scenarios, the network was tested for the source-temperature disturbance of +5 K in both of the hot source streams and -5 K in both of the cold source streams. In the first scenario, the hot- and the cold-stream target temperatures were constrained within  $\pm 2$  K. In the second scenario, the hot-stream target temperatures were

constrained within  $\pm 4$  K and the cold ones within  $\pm 0.5$  K, i.e., propagation direction of disturbance was forced towards the hot end of the HEN. In the third scenario, the hot-stream target temperatures were constrained within  $\pm 0.5$  K and the cold ones within  $\pm 4$  K, i.e., propagation direction of disturbance was forced towards the cold end of the HEN.

Table 4.1 shows the heat-capacity-flowrate of the bypass streams and the target-temperature values for the three different scenarios mentioned above. In the first and third scenarios, the minimum-approach-temperature constraint of type Eq. 4.b is active for the first exchanger, but no minimum-approach-temperature constraint is active in the second scenario. In each scenario, some target constraints are active as well, as can be concluded from the table.

TABLE 4.1. Optimal heat-capacity-flow-rate values of the bypass streams and the target temperatures.

	$\Delta T_{h,j}^t = \pm 2 \text{ K}$	$\Delta T_{h,j}^t = \pm 4 \text{ K}$	$\Delta T_{h,j}^t = \pm 0.5 \text{ K}$
	$\Delta T_{c,j}^t = \pm 2 \text{ K}$	$\Delta T_{c,j}^t = \pm 0.5 \text{ K}$	$\Delta T_{c,j}^t = \pm 4 \text{ K}$
$w_{h,1} u_{h,1}$	359.9931	327.3805	142.8566
$w_{c,1} u_{c,1}$	1264.8895	1263.0901	63.8367
$w_{h,2} u_{h,2}$	17.8859	1.9692	16.6708
$w_{c,2} u_{c,2}$	17.4276	0.0000	211.0502
$w_{h,3} u_{h,3}$	18.2685	0.0059	29.6581
$w_{c,3} u_{c,3}$	40.6165	24.0836	61.1656
$T_{h,2}^t$	322.999	319.000	322.500
$T_{h,3}^t$	398.334	396.000	399.999
$T_{c,1}^t$	561.000	562.500	563.000
$T_{c,2}^t$	391.000	392.500	389.000

The results summarized were obtained when the optimization procedure was started using zero as the starting value for all bypass fractions. Initial-guess dependence of the optimal solution was demonstrated in Table 4.2 for the first scenario where the optimization

procedure was started using 0.5 as the initial guess for all bypass fractions. Although the values of the respective objective functions for the two cases considered in Table 4.1 and Table 4.2 are identical, bypass-fraction sets are quite different. This reveals the nonuniqueness of the optimal decision variables and initial-guess dependence of the solution. This is expected since, when the formulation includes two bypass streams per exchanger, there are  $2 \cdot NE$  equality constraints but  $4 \cdot NE$  variables. If the extra degrees of freedom are not consumed by various inequality constraints that may become active at the optimal solution, the hot- and cold-side bypass fractions are dependent on each other. When the problem is formulated by allowing only single bypass for each exchanger, then there are  $2 \cdot NE$  equality constraints and  $3 \cdot NE$  variables. Even though the use of single bypass per exchanger eliminates the interdependence of the bypass variables, the problem of nonuniqueness of the optimal decision variables may still be present depending on activities of the inequality constraints at the optimal solution. During optimization, multiple-solution, infeasible-solution, and local-minima problems may also be encountered due to nonlinearities and (possible) nonconvexity of the solution space.

TABLE 4.2. Nonuniqueness of the optimal heat-capacity-flow-rate values of the bypass streams and the target temperatures.

	$\Delta T_{h,j}^t = \pm 2 \text{ K}$ $\Delta T_{c,j}^t = \pm 2 \text{ K}$
$w_{h,1} u_{h,1}$	47.4431
$w_{c,1} u_{c,1}$	1269.3317
$w_{h,2} u_{h,2}$	11.8866
$w_{c,2} u_{c,2}$	0.0000
$w_{h,3} u_{h,3}$	13.2680
$w_{c,3} u_{c,3}$	51.0338
$T_{h,2}^t$	321.000
$T_{h,3}^t$	398.000
$T_{c,1}^t$	562.250
$T_{c,2}^t$	391.000

Even though there may be multiple (or, in some cases infinite) solutions to the HEN problem presented here, the results demonstrate that propagation direction of a disturbance vector can be forced towards either the hot or the cold end of a pre-designed HEN with minimum target-temperature deviations using different sets of bypass fractions.

## 5. RETROFIT DESIGN OF RESILIENT HEAT-EXCHANGER NETWORKS

In this chapter, a new index for evaluating the HEN resiliency is introduced. A new retrofit-design approach for predetermined HEN structures to obtain resilient and controllable designs at minimum cost is also presented.

### 5.1. Design-Resiliency Index

As mentioned in Chapter 3, ‘flexibility index’ (FI) of a HEN indicates the largest allowable deviation in external uncertain variables (usually the source temperatures), in all possible disturbance directions with the same magnitude, such that the HEN remains feasible. The value of this index, obtained by considering only the deviations in external variables, gives information about the feasibility of the *structure* but not the *design*. More explicitly this means that, using a HEN structure as the solution of a HEN problem and introducing *suitable* control variables to this structure, a design can be obtained such that it may have feasible paths in order to satisfy all energy constraints of the problem within the deviation-range of  $\pm$  FI from the nominal values of source temperatures or flowrates. Obviously, this concluding remark obtained by the concept of FI, does not answer these questions: i) does the *original structure* really have adequate number of control variables ?, ii) if not, what are the *suitable* control variables that must be introduced to the structure so that they will provide a flexibility/resiliency with a value of FI ?

For instance, for the pinch solution of example HEN problem given in Chapter 3 (Figure 3.1), the ‘flexibility index’ of the structure is calculated as 30 K. Here, flexibility



proposed in this dissertation. This index is termed as '*Design Resiliency Index*' (*DRI*), and its explicit definition is given as follows:

**Definition :** For a designed network, *DRI* is the maximum permissible simultaneous deviation of identical magnitude for all combinations of the increasing or decreasing directions (multidirectional) in all disturbances (deviations from nominal design values of the stream supply temperatures or flowrates) (Konukman et. al., 1994; Konukman et. al., 1995b).

Therefore, finding the *DRI* value of a designed network mathematically is a min-max problem which includes  $2^{NS}$  nonlinear-programming problems (NLP). The object is to find the minimum magnitude among the set of maximum permissible disturbance (in source-stream temperatures or flowrates) magnitudes of the individual disturbance directions. The formulation of this optimization problem for each disturbance direction can be described with the following standard form:

$$\text{objective function:} \quad \begin{array}{l} \text{maximize } \delta \\ (\delta, \mathbf{u}_h, \mathbf{u}_c \\ \mathbf{x}, \mathbf{T}_{he}, \mathbf{T}_{ce}) \end{array} \quad (5.1)$$

subject to:

$$\text{equality constraints:} \quad \mathbf{h}(\delta, \mathbf{u}_h, \mathbf{u}_c, \mathbf{x}, \mathbf{T}_{he}, \mathbf{T}_{ce}) = \mathbf{0} \quad 2 \times \text{NE} + \text{NHT} \quad (5.2)$$

$$\text{inequality constraints:} \quad \mathbf{g}(\delta, \mathbf{u}_h, \mathbf{u}_c, \mathbf{x}, \mathbf{T}_{he}, \mathbf{T}_{ce}) \leq \mathbf{0} \quad 4 \times \text{NE} + \text{NC} + \text{NH} + \text{NST} \quad (5.3)$$

$$\text{side constraints:} \quad \mathbf{0} \leq \mathbf{u}_h < \mathbf{1} \quad \text{NHB} \quad (5.4)$$

$$\mathbf{0} \leq \mathbf{u}_c < \mathbf{1} \quad \text{NCB} \quad (5.5)$$

$$\mathbf{0} < \mathbf{x} < \mathbf{1} \quad \text{NX} \quad (5.6)$$

where,

$$\mathbf{u}_h = \begin{bmatrix} u_{h,1} \\ \vdots \\ \vdots \\ \vdots \\ \vdots \\ u_{h,NE} \end{bmatrix}_{NHB \times 1} \quad \mathbf{u}_c = \begin{bmatrix} u_{h,1} \\ \vdots \\ \vdots \\ \vdots \\ \vdots \\ u_{h,NE} \end{bmatrix}_{NCB \times 1} \quad \mathbf{x} = \begin{bmatrix} x_1 \\ \vdots \\ \vdots \\ \vdots \\ \vdots \\ x_{NX} \end{bmatrix}_{NX \times 1} \quad (5.7)$$

$$\mathbf{T}_{he} = \begin{bmatrix} T_{he,1} \\ \vdots \\ \vdots \\ \vdots \\ \vdots \\ T_{he,NE} \end{bmatrix}_{NE \times 1} \quad \mathbf{T}_{ce} = \begin{bmatrix} T_{ce,1} \\ \vdots \\ \vdots \\ \vdots \\ \vdots \\ T_{ce,NE} \end{bmatrix}_{NE \times 1} \quad (5.8)$$

In this formulation, the decision variables are  $\delta$  (maximum disturbance magnitude),  $\mathbf{u}_h$  (vector of hot-side bypass fractions),  $\mathbf{u}_c$  (vector of cold-side bypass fractions),  $\mathbf{x}$  (vector of split fractions),  $\mathbf{T}_{he}$  (vector of hot-side outlet temperatures of exchangers), and  $\mathbf{T}_{ce}$  (vector of cold-side outlet temperatures of exchangers). The total number of the decision variables is  $1+NHB+NCB+2 \times NE+NX$ . The vector of equality constraints,  $\mathbf{h}$ , is formed by the energy balance equations (two per exchangers) and the hard-target constraints (if present). The total number of such equality constraints is  $2 \times NE+NHT$ . The vector of inequality constraints,  $\mathbf{g}$ , is formed by the heat-load constraints for exchangers, heat-load constraints for heaters and/or coolers (if present), approach temperature constraints, and by the soft-target (range) constraints (if present). The total number of such inequality constraints is  $4 \times NE+NH+NC+NST$ .

The NLP problem generalized by Equations 5.1 to 5.6 must be solved for all possible disturbance directions in all source streams, i.e., the number of such NLP problems is  $2^{NS}$  since there are two directions (+ or -) and  $NS = NHS + NCS$  source streams. Figure 5.2 summarizes the procedure for finding the DRI of a HEN.

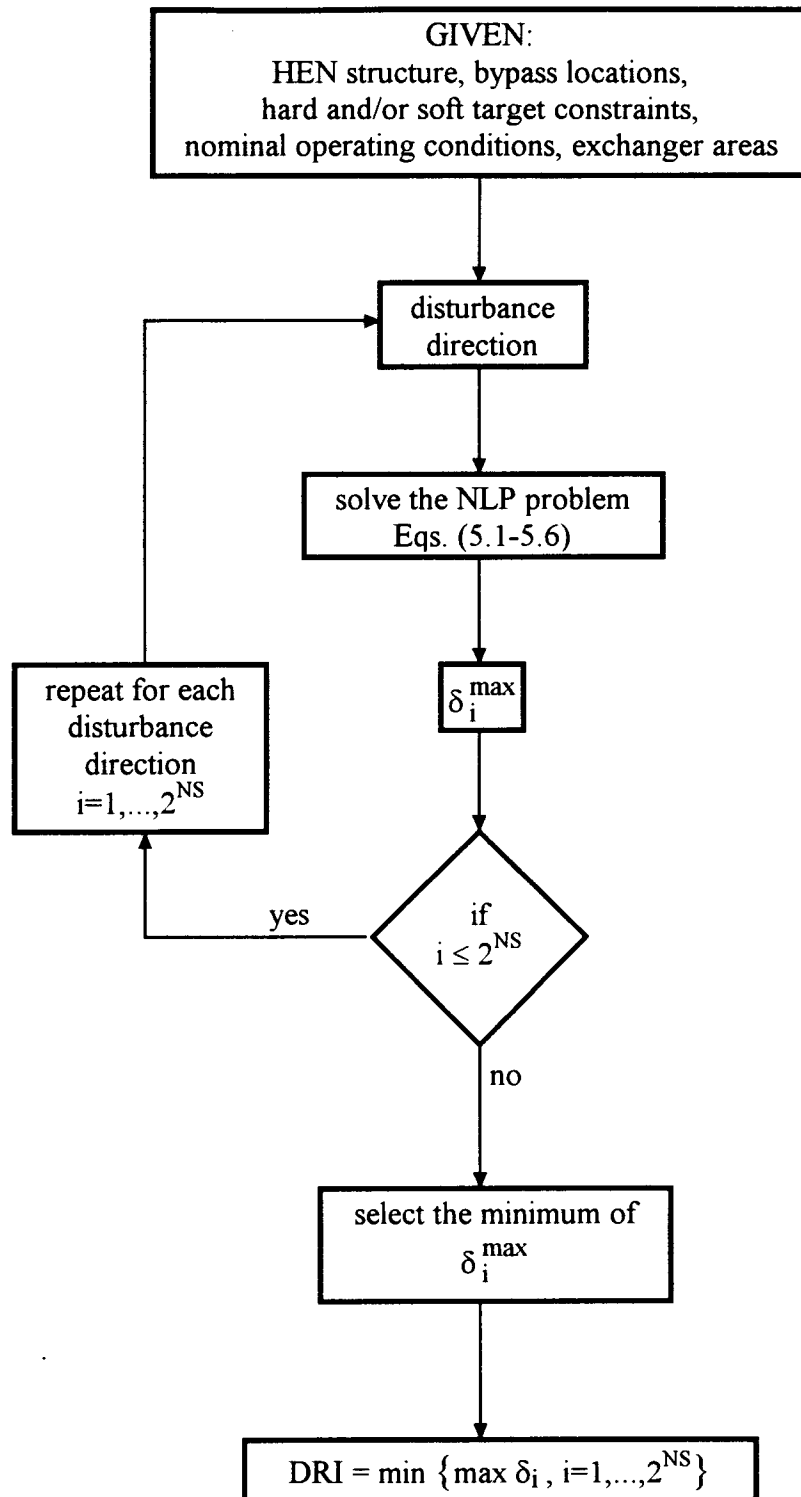


FIGURE 5.2. Procedure for finding the DRI of a HEN.

Mathematical formulation of the NLP for positive disturbance directions (increasing directions for all disturbances in source temperatures) to find the DRI is given for the particular example shown in Figure 5.3. In the design, overall heat-transfer coefficients are considered constant and as  $1 \text{ kW/m}^2\text{K}$  for all the exchangers in the network. The resulting exchanger areas for these coefficients and for the nominal source-stream temperatures indicated in Figure 5.3 are  $A_1 = 63.3 \text{ m}^2$ ,  $A_2 = 146.0 \text{ m}^2$ ,  $A_3 = 101.7 \text{ m}^2$ ,  $A_4 = 269.0 \text{ m}^2$ . (It is assumed that all the exchangers are single-pass counter-current exchangers.)

The objective function is 
$$\text{maximize } \delta \quad (5.9)$$

$$\begin{pmatrix} T_1, T_2, T_3, T_4 \\ T_5, T_6, T_7, \delta \end{pmatrix}$$

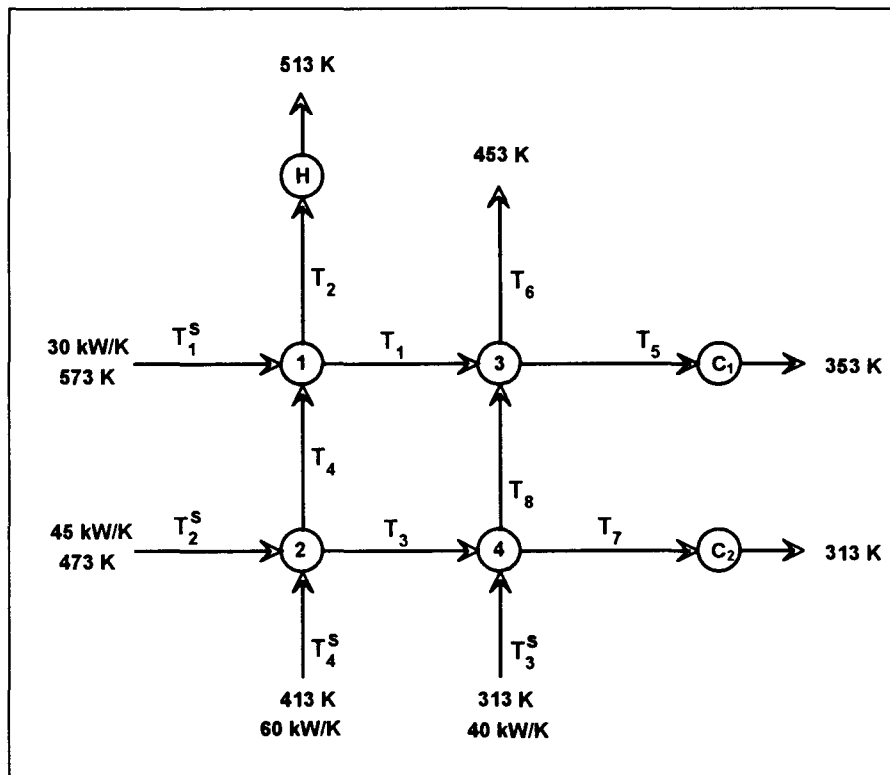


FIGURE 5.3. Notation for the formulation.

subject to:

energy balances (equality constraints):

$$\text{HX - 1 :} \quad 30(T_1^s - T_1) + 60(T_4 - T_2) = 0 \quad (5.10)$$

$$30(T_1^s - T_1) - 63.3 \frac{[(T_1^s - T_2) - (T_1 - T_4)]}{\ln[(T_1^s - T_2)/(T_1 - T_4)]} = 0 \quad (5.11.a)$$

or

$$60(T_4 - T_2) + 63.3 \frac{[(T_1^s - T_2) - (T_1 - T_4)]}{\ln[(T_1^s - T_2)/(T_1 - T_4)]} = 0 \quad (5.11.b)$$

$$\text{HX - 2 :} \quad 45(T_2^s - T_3) + 60(T_4^s - T_4) = 0 \quad (5.12)$$

$$45(T_2^s - T_3) - 146.0 \frac{(T_2^s - T_4) - (T_3 - T_4^s)}{\ln[(T_2^s - T_4)/(T_3 - T_4^s)]} = 0 \quad (5.13.a)$$

or

$$45(T_4^s - T_4) + 146.0 \frac{(T_2^s - T_4) - (T_3 - T_4^s)}{\ln[(T_2^s - T_4)/(T_3 - T_4^s)]} = 0 \quad (5.13.b)$$

$$\text{HX - 3 :} \quad 30(T_1 - T_5) + 40(T_8 - T_6) = 0 \quad (5.14)$$

$$30(T_1 - T_5) - 101.7 \frac{(T_1 - T_6) - (T_5 - T_8)}{\ln[(T_1 - T_6)/(T_5 - T_8)]} = 0 \quad (5.15.a)$$

or

$$40(T_8 - T_6) + 101.7 \frac{(T_1 - T_6) - (T_5 - T_8)}{\ln[(T_1 - T_6)/(T_5 - T_8)]} = 0 \quad (5.15.b)$$

$$\text{HX - 4 :} \quad 45(T_3 - T_7) + 40(T_3^s - T_8) = 0 \quad (5.16)$$

$$45(T_3 - T_7) - 269.0 \frac{[(T_3 - T_8) - (T_7 - T_3^s)]}{\ln[(T_3 - T_8)/(T_7 - T_3^s)]} = 0 \quad (5.17.a)$$

or

$$40(T_3^s - T_8) - 269.0 \frac{[(T_3 - T_8) - (T_7 - T_3^s)]}{\ln[(T_3 - T_8)/(T_7 - T_3^s)]} = 0 \quad (5.17.b)$$

heat-load constraints (inequality constraints):

$$\text{HX - 1 :} \quad T_1 - T_1^s \leq 0 \quad T_4 - T_2 \leq 0 \quad (5.18)$$

$$\text{HX - 2 :} \quad T_3 - T_2^s \leq 0 \quad T_4^s - T_4 \leq 0 \quad (5.19)$$

$$\text{HX - 3 :} \quad T_5 - T_1 \leq 0 \quad T_8 - T_6 \leq 0 \quad (5.20)$$

$$\text{HX - 4 :} \quad T_7 - T_3 \leq 0 \quad T_3^s - T_8 \leq 0 \quad (5.21)$$

$$\text{cooler (1<sup>st</sup>) :} \quad T_5 \geq 353 \quad (5.22)$$

$$\text{cooler (2<sup>nd</sup>) :} \quad T_7 \geq 313 \quad (5.23)$$

$$\text{heater :} \quad T_2 \leq 513 \quad (5.24)$$

approach-temperature constraints (inequality constraints):

$$\text{HX - 1 :} \quad T_4 - T_1 \leq 0 \quad T_2 - T_1^s \leq 0 \quad (5.25)$$

$$\text{HX - 2 :} \quad T_4^s - T_3 \leq 0 \quad T_4 - T_2^s \leq 0 \quad (5.26)$$

$$\text{HX - 3 :} \quad T_8 - T_5 \leq 0 \quad T_6 - 453 = 0 \quad (5.27)$$

$$\text{HX - 4 :} \quad T_3^s - T_7 \leq 0 \quad T_8 - T_3 \leq 0 \quad (5.28)$$

for increasing direction of source temperatures :

$$T_1^s = 573 + \delta \quad (5.29)$$

$$T_2^s = 473 + \delta \quad (5.30)$$

$$T_3^s = 313 + \delta \quad (5.31)$$

$$T_4^s = 413 + \delta \quad (5.32)$$

hard-target constraint (equality constraint):

$$T_6 - 453 = 0 \quad (5.33)$$

In the above formulation the reason why the target of cold-stream-1 will never be satisfied after a disturbance can be seen mathematically. For one disturbance direction, NLP includes 9 independent variables ( $T_1, T_2, T_3, T_4, T_5, T_6, T_7, T_8, \delta$ ) and 9 equality constraints (Eqs. 5.10, 5.11.a, 5.12, 5.13.a, 5.14, 5.15.a, 5.16, 5.17.a, 5.33), therefore the degrees of freedom is zero for each disturbance direction. Hence, there is no adequate number of manipulated variables to get resiliency for the designed network and it is impossible to provide a control action for this network during operation. In other words, the resiliency of the designed network is zero (DRI = 0 K). Introducing bypass(es) (i.e., control variables) over exchangers will increase the degrees of freedom. For example, as shown in Figure 5.4, in case of placing a cold-side bypass to exchanger-3, energy balances for exchanger-3 have

to be modified, and a mixing-balance equation for bypass-mixing-point has to be added as follows:

energy-balance equations for HX - 3 (equality constraints):

$$30(T_1 - T_5) + 40(1 - u_{c,3})(T_8 - T_9) = 0 \quad (5.34)$$

$$30(T_1 - T_5) - 101.7 \frac{(T_1 - T_9) - (T_5 - T_8)}{\ln[(T_1 - T_9)/(T_5 - T_8)]} = 0 \quad (5.35.a)$$

or

$$40(1 - u_{c,3})(T_8 - T_9) + 101.7 \frac{(T_1 - T_9) - (T_5 - T_8)}{\ln[(T_1 - T_9)/(T_5 - T_8)]} = 0 \quad (5.35.b)$$

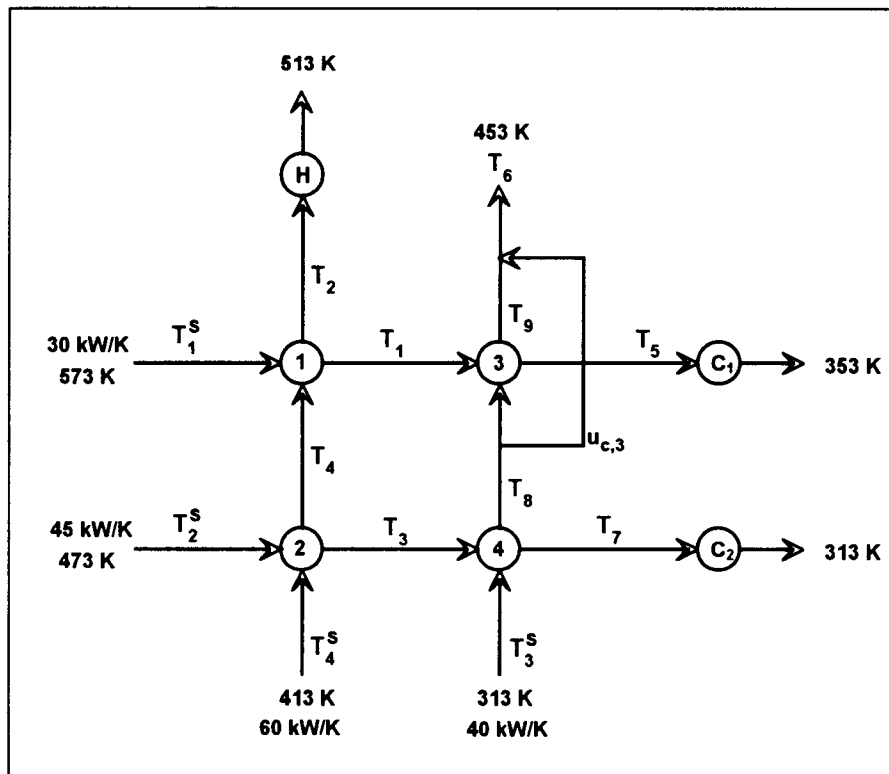


FIGURE 5.4. Network modified by introducing cold-side bypass on exchanger 3.

energy-balance equation for mixing point after HX-3:

$$T_6 = u_{c,3} T_8 + (1 - u_{c,3}) T_9 \quad (5.36)$$

hard-target constraint (equality constraint):

$$T_6 - 453 = 0 \quad (5.37)$$

bypass-limit constraint (side constraint):

$$0 \leq u_{c,3} < 1 \quad (5.38)$$

Placing a bypass to the designed network has increased the number of independent variables to 10 ( $T_1, T_2, T_3, T_4, T_5, T_7, T_8, T_9, \delta, u_{c,3}$ ) and the number of equality constraints to 9 (Eqs. 5.10, 5.11.a, 5.12, 5.13.a, 5.34, 5.35.a, 5.16, 5.17.a, 5.37). That is, placing a bypass to an exchanger in this network increases the degrees of freedom by one. For the presented network structure, Figure 5.4, which was designed for the nominal values of source-stream conditions and *then* to which a hot-side bypass was added on exchanger-3, the values of the maximum disturbance magnitudes for each disturbance direction are shown in Table 5.1. It is to be noted that placing a bypass made the network resilient only for some disturbance directions. For some of the disturbance directions, the network is still nonresilient. At those directions, there are no feasible path(s) for directing the disturbances to the utilities. Therefore, for the HEN shown in Figure 5.4, the minimum value of the maximum disturbance magnitudes, i.e. DRI, is zero.

The results of the three different bypass placement cases for the example network are tabulated in Tables 5.2, 5.3, and 5.4. As can be seen from Table 5.2, placing one more bypass (cold-side bypass on exchanger-1, Figure 5.5), has increased the DRI value from zero to 21.1 K. In Table 5.3, the network has three bypasses (cold-side bypass on

exchanger-1 and exchanger-3, and hot-side bypass on exchanger-4, Figure 5.6), and in this case DRI value is 30 K. When all the exchangers of the network have double bypasses (on hot- and cold-sides, Figure 5.7), the DRI value is 30 K, as can be seen in Table 5.4, which is also the flexibility index (FI) value of the network.

TABLE 5.1. Maximum disturbance magnitudes for the example design for all possible disturbance directions (with a cold-side bypass on exchanger 3).

Disturbance Direction $T_1^s$ $T_2^s$ $T_3^s$ $T_4^s$	Maximum Disturbance Magnitude, $\delta$ (K)
+ + + +	14.17
+ + + -	25.95
+ + - +	14.17
+ + - -	22.55
+ - + +	30.00
+ - + -	<b>0.00</b>
+ - - +	30.00
+ - - -	<b>0.00</b>
- + + +	33.26
- + + -	<b>0.00</b>
- + - +	34.26
- + - -	<b>0.00</b>
- - + +	<b>0.00</b>
- - + -	<b>0.00</b>
- - - +	<b>0.00</b>
- - - -	<b>0.00</b>
<b>DRI</b>	<b>0.00</b>

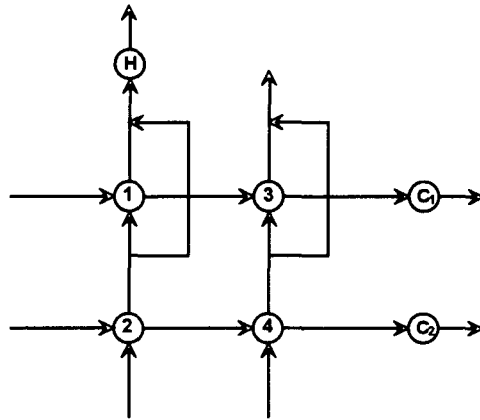


FIGURE 5.5. Network modified by introducing cold-side bypasses on exchangers 1 and 3.

TABLE 5.2. Maximum disturbance magnitudes for the example design for all possible disturbance directions (with a cold-side bypasses on exchangers 1 and 3).

Disturbance Direction	Maximum Disturbance Magnitude, $\delta$ (K)
$T_1^s$ $T_2^s$ $T_3^s$ $T_4^s$	
+ + + +	27.97
+ + + -	66.00
+ + - +	32.05
+ + - -	22.55
+ - + +	30.00
+ - + -	55.00
+ - - +	30.00
+ - - -	<b>21.11</b>
- + + +	33.26
- + + -	66.00
- + - +	34.26
- + - -	22.55
- - + +	30.00
- - + -	55.00
- - - +	30.00
- - - -	<b>21.11</b>
<b>DRI</b>	<b>21.11</b>

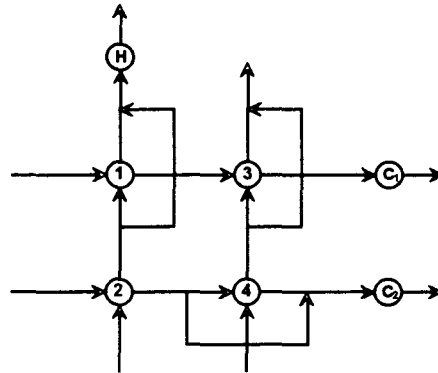


FIGURE 5.6. Network modified by introducing cold-side bypasses on exchangers 1 and 3 and hot-side bypass on exchanger 4.

TABLE 5.3. Maximum disturbance magnitudes for the example design for all possible disturbance directions (with a cold-side bypasses on exchangers 1 and 3, and hot side bypass on exchanger 4).

Disturbance Direction	Maximum Disturbance
$T_1^s$ $T_2^s$ $T_3^s$ $T_4^s$	Magnitude, $\delta$ (K)
+ + + +	55.44
+ + + -	66.00
+ + - +	55.44
+ + - -	107.79
+ - + +	<b>30.00</b>
+ - + -	55.00
+ - - +	<b>30.00</b>
+ - - -	80.89
- + + +	61.25
- + + -	66.00
- + - +	61.25
- + - -	51.21
- - + +	<b>30.00</b>
- - + -	55.00
- - - +	<b>30.00</b>
- - - -	43.04
<b>DRI</b>	<b>30.00</b>

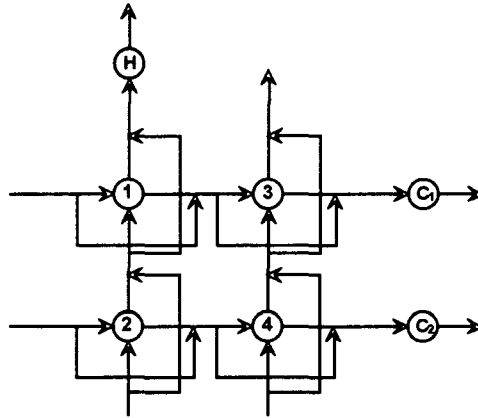


FIGURE 5.7. Network modified by introducing double bypasses for all the exchangers.

TABLE 5.4. Maximum disturbance magnitudes for the example design for all possible disturbance directions (with hot and cold bypasses on all the exchangers).

Disturbance Direction	Maximum Disturbance Magnitude, $\delta$ (K)
$T_1^s$ $T_2^s$ $T_3^s$ $T_4^s$	
+ + + +	100.00
+ + + -	140.00
+ + - +	100.0
+ + - -	unbounded
+ - + +	<b>30.00</b>
+ - + -	80.00
+ - - +	<b>30.00</b>
+ - - -	160.00
- + + +	80.00
- + + -	120.00
- + - +	80.00
- + - -	120.00
- - + +	<b>30.00</b>
- - + -	80.00
- - - +	<b>30.00</b>
- - - -	105.71
<b>DRI</b>	<b>30.00</b>

## 5.2. Modeling and Formulation

In the previous section, an index value has been defined that evaluates the resiliency of a HEN together with the design parameters and the control variables and provides the advantage of analyzing the effects of different placements of control variables for a predesigned HEN. It has been demonstrated on an example that the number and placement of control variables determine the feasibility margins of the design. These feasibility margins (indicated by Design Resiliency Index - DRI) also determine the controllability range of the HEN during operation by providing feasible paths for disturbance rejection. It has been seen in the example that inserting double bypass to all the exchangers in the network *after* the design, the resiliency of the network (DRI) reached the value indicated by the flexibility index (FI). On the other hand, this value of resiliency is also obtained by using only three bypasses (with a cold-side bypasses on exchangers 1 and 3, and hot side bypass on exchanger 4). It is obvious that selecting less bypasses is a more cheaper solution to the resiliency problem. Also using two bypasses (with a cold-side bypasses on exchangers 1 and 3), network gains a resiliency degree somewhat lower than FI (21.1 K). The questions that must be asked now are: i) is it really necessary to get a degree of resiliency which is also the structure limit indicated by FI ? ii) if so then, is it possible to get a less expensive solution for that resiliency value (changing the areas of exchangers or utility consumption levels) using the same configuration of control variables ? iii) is it possible to get the *lowest cost* solution for a resiliency value *specified by the designer (optimal resiliency)* retrofitting the specified structure using the same configuration of control variables ?

In this section, an approach to resilient and controllable design of HENs is presented. The design problem of HEN is formulated as constrained nonlinear optimization problem whose solution generates a HEN which is not only flexible/resilient/controllable in the range of expected disturbances but also economically optimal. The objective is to find the individual exchanger areas, utility consumptions, and nominal bypass fractions which minimize the total annualized cost (or the total area) of the given HEN structure and, at the

same time, to satisfy the target-temperature constraints for set of disturbances predefined in all possible disturbance directions.

### 5.2.1. Retrofit Design Resiliency Index

A general numerical measure (index) to define the disturbance range of external variables in the design formulation is proposed. Proposed measure is called '*Retrofit Design Resiliency Index*' (*RDRI*). Its definition of disturbance range is the same as that of Design Resiliency Index (*DRI*). That is, for *RDRI*, the disturbance range is also defined as simultaneous deviations of equal magnitude for all combinations of the increasing or decreasing directions, from the nominal values of stream supply temperatures or flowrates. The use of a predefined *RDRI* value in the proposed formulation leads to the retrofit designs with a capacity of disturbance rejection that is *at least* *RDRI* for given set of economic parameters. From another point of view, as will be seen in the resulting designs of the following sections, *DRI* values of the retrofit designs obtained from the proposed formulation is at least the value defined by *RDRI* in the formulation of the retrofit design.

### 5.2.2. Formulation of Optimal Resilient Retrofit Design

The task of designing a HEN (retrofit design), which is not only economically at minimum cost but also has the ability to reject the disturbances predefined in *all* disturbance directions, can be introduced as a single nonlinear-programming problem. The equality constraints (energy balances for exchangers and mixing points) and the inequality constraints (heat loads for exchangers and utilities, minimum-approach temperatures for exchangers) for each disturbance direction can be evaluated in the same problem. The only common variables of each disturbance set are the heat-exchanger areas which must be valid

for all disturbance directions. The reason for evaluating all possible disturbances in a single nonlinear-programming problem is not only because it is time saving, but more importantly, evaluation of each disturbance direction independent of each other gives different design results (heat-exchanger areas) and there is no guarantee that any one of such designs (or a set of exchanger-areas independently selected from such designs) will provide the retrofit HEN with the desired RDRI in overall (i.e., for all disturbance directions). In the formulation, the zero-disturbance case (design for the nominal source-stream values) is also considered as a direction. As it will be explained later, the effect of the zero-disturbance direction on the overall cost of the resulting optimal retrofit design is profound since the utility consumptions are taken into account only in the zero-disturbance case. The formulation may also retrofit a HEN structure for multi-period operation scenarios if the structure permits (i.e., if it is feasible for each period). In this situation, the resulting network will be flexible/resilient/controllable (with the specified RDRI values) for each period of operation.

The formulation of the retrofit-design optimization problem for each operation period for a specified RDRI can be described with the following standard form:

objective function:

$$\begin{aligned} & \text{minimize } f(\mathbf{u}_h^i, \mathbf{u}_c^i, \mathbf{x}, \mathbf{T}_{he}^i, \mathbf{T}_{ce}^i, \mathbf{A}_j, \mathbf{A}_k, \mathbf{A}_l, \mathbf{Q}_h^0, \mathbf{Q}_c^0) \\ & \left( \begin{array}{l} \mathbf{u}_h^i, \mathbf{u}_c^i, \mathbf{x}^i, \mathbf{T}_{he}^i, \mathbf{T}_{ce}^i \\ \mathbf{A}_j, \mathbf{A}_k, \mathbf{A}_l, \mathbf{Q}_h^0, \mathbf{Q}_c^0 \end{array} \right) \end{aligned} \quad (5.39)$$

subject to:

equality constraints:

$$\mathbf{h}(\mathbf{u}_h^i, \mathbf{u}_c^i, \mathbf{x}^i, \mathbf{T}_{he}^i, \mathbf{T}_{ce}^i, \mathbf{A}_j, \mathbf{A}_k, \mathbf{A}_l, \mathbf{Q}_h^0, \mathbf{Q}_c^0) = \mathbf{0} \quad (2^{NS+1}) (2 \times NE + NHT) + 2 \times (NC + NH) \quad (5.40)$$

inequality constraints:

$$\mathbf{g}(\mathbf{u}_h^i, \mathbf{u}_c^i, \mathbf{x}^i, \mathbf{T}_{he}^i, \mathbf{T}_{ce}^i, \mathbf{A}_j, \mathbf{A}_k, \mathbf{A}_l, \mathbf{Q}_h^0, \mathbf{Q}_c^0) \leq \mathbf{0} \quad (2^{NS+1}) (4 \times NE + NC + NH + NST) \quad (5.41)$$



$$\mathbf{A}_j = \begin{bmatrix} \mathbf{A}_1 \\ \vdots \\ \vdots \\ \vdots \\ \mathbf{A}_{NE} \end{bmatrix}_{NE \times 1}, \quad \mathbf{A}_l = \begin{bmatrix} \mathbf{A}_1 \\ \vdots \\ \vdots \\ \vdots \\ \mathbf{A}_{NH} \end{bmatrix}_{NH \times 1}, \quad \mathbf{A}_k = \begin{bmatrix} \mathbf{A}_1 \\ \vdots \\ \vdots \\ \vdots \\ \mathbf{A}_{NC} \end{bmatrix}_{NC \times 1} \quad (5.46)$$

$$\mathbf{Q}_h^0 = \begin{bmatrix} Q_1^0 \\ \vdots \\ \vdots \\ \vdots \\ \vdots \\ Q_{NH}^0 \end{bmatrix}_{NH \times 1}, \quad \mathbf{Q}_c^0 = \begin{bmatrix} Q_1^0 \\ \vdots \\ \vdots \\ \vdots \\ \vdots \\ Q_{NC}^0 \end{bmatrix}_{NC \times 1} \quad (5.47)$$

$$\mathbf{T}_{\text{he}}^i = \begin{bmatrix} T_{\text{he},1}^0 \\ \vdots \\ T_{\text{he,NE}}^0 \\ T_{\text{he},1}^1 \\ \vdots \\ T_{\text{he,NE}}^1 \\ \vdots \\ T_{\text{he},1}^{2^{\text{NS}}} \\ \vdots \\ T_{\text{he,NE}}^{2^{\text{NS}}} \end{bmatrix}_{((2^{\text{NS}}+1)\text{NE}) \times 1}, \quad \mathbf{T}_{\text{ce}}^i = \begin{bmatrix} T_{\text{ce},1}^0 \\ \vdots \\ T_{\text{ce,NE}}^0 \\ T_{\text{ce},1}^1 \\ \vdots \\ T_{\text{ce,NE}}^1 \\ \vdots \\ T_{\text{ce},1}^{2^{\text{NS}}} \\ \vdots \\ T_{\text{ce,NE}}^{2^{\text{NS}}} \end{bmatrix}_{((2^{\text{NS}}+1)\text{NE}) \times 1} \quad (5.48)$$

In this formulation, the decision variables are  $\mathbf{u}_h^i$  (vector of hot-side bypass fractions for all disturbance directions),  $\mathbf{u}_c^i$  (vector of cold-side bypass fractions for all disturbance directions),  $\mathbf{x}^i$  (vector of split fractions, if present, for all disturbance directions),  $\mathbf{T}_{\text{he}}^i$  (vector of hot-side outlet temperatures for all disturbance directions),  $\mathbf{T}_{\text{ce}}^i$  (vector of cold-side outlet temperatures for all disturbance directions),  $\mathbf{A}_j$  (vector of heat-exchanger areas common for all disturbance directions),  $\mathbf{A}_1$  (vector of heater areas for zero-disturbance direction),  $\mathbf{A}_k$  (vector of cooler areas for zero-disturbance direction),  $\mathbf{Q}_h^0$  (vector of heater duties, if present, for zero disturbance direction),  $\mathbf{Q}_c^0$  (vector of cooler duties, if present, for

zero disturbance direction). The total number of decision variables is  $(2^{NS}+1)(NCB+NHB+NX+2\times NE) + NE + 2\times(NC+NH)$ . The vector of equality constraints,  $\mathbf{h}$ , is formed by the energy-balance equations (two per exchanger for all disturbance directions), hard-target constraints for all disturbance directions (if present), energy balance equation for each heater (two per heater), and energy balance equation for each cooler (two per cooler) for zero-disturbance direction. The total number of such equality constraints is  $(2^{NS}+1)(2\times NE+NHT) + 2\times(NC+NH)$ . The vector of inequality constraints,  $\mathbf{g}$ , is formed by the heat-load constraints for exchangers (two per exchanger), for all disturbance directions, approach-temperature constraints for exchangers (two per exchanger) for all disturbance directions, heat-load constraints for heaters and/or coolers (if present) for all disturbance directions, and by the soft-target (range) constraints (if present) for all disturbance directions: The total number of such inequality constraints is  $(2^{NS}+1)(4\times NE+NC+NH+NST)$ . The vector of side constraints is formed by the upper and lower bounds on the hot- and cold-side bypass fractions and on the split fractions for all disturbance directions. The total number of such side constraints is  $(2^{NS}+1)(NCB+NHB+NX)$ .

In the explicit formulation given below, exchangers are taken as counter-current single-pass exchangers. Heat capacities of fluids and heat-transfer coefficients are assumed to be constant. For the mean temperature difference, logarithmic-mean temperature difference is used. Although some authors (Paterson, 1984; Chen, 1987) suggest some different approximations in order to avoid numerical difficulties, examples evaluated in this study using the software package GAMS (with MINOS module for NLP) did not cause any problems with the logarithmic-mean temperature difference. Such numerical difficulties are avoided by using an extra constraint which prevented the approach temperatures of both sides of the exchangers becoming *exactly* equal.

General notation for the explicit formulation given below is shown in Figure 5.8, where indices  $j$ ,  $k$ , and  $l$  refer to network-exchanger, cooler, and heater, respectively.

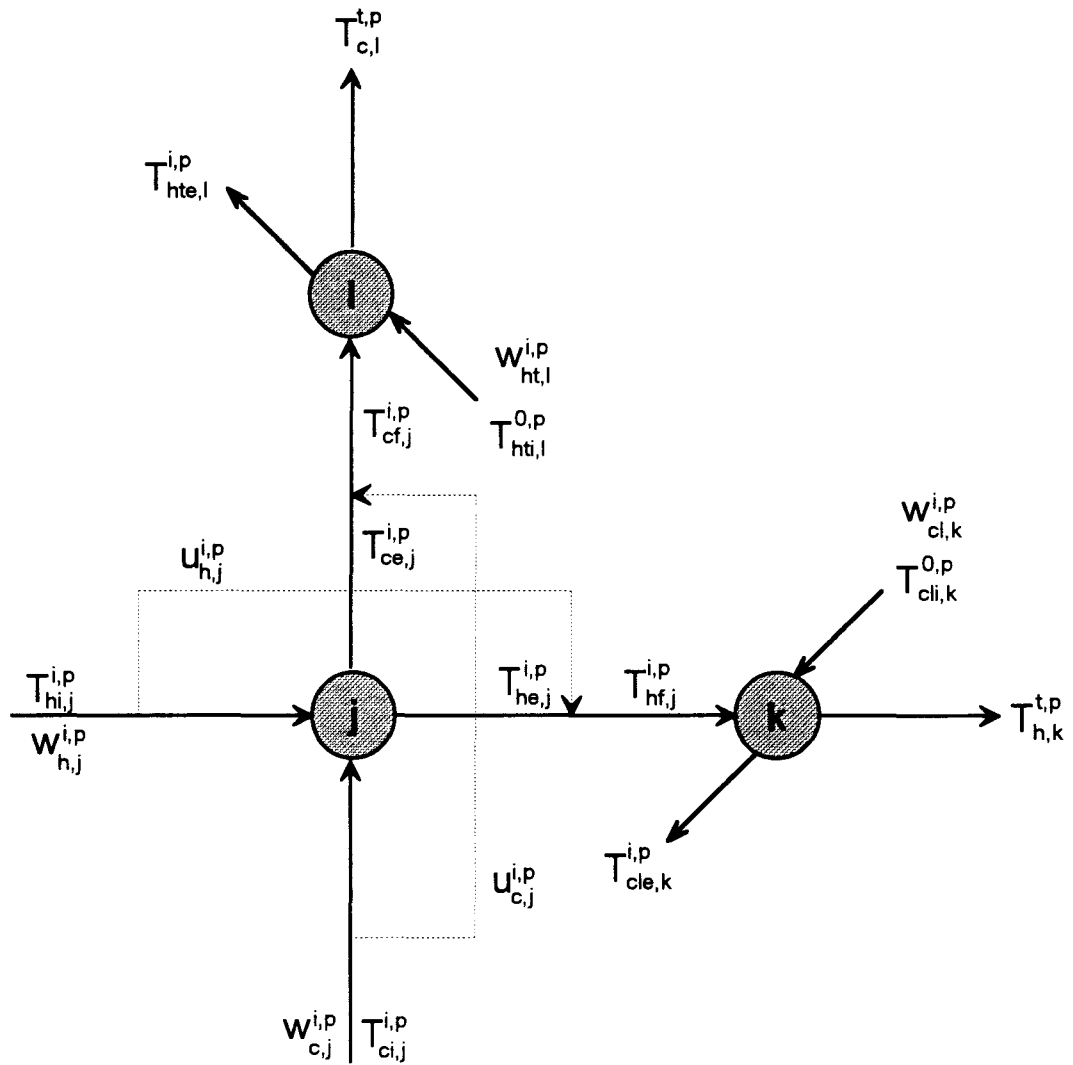


FIGURE 5.8. Notation for general formulation.

Objective function:

$$\begin{aligned}
 & \text{minimize} \left[ \gamma \left( \sum_{j=1}^{NE} (C_E + \alpha A_j^\beta) \right) + \sum_{k=1}^{NC} (C_C + \alpha A_k^\beta) + \sum_{l=1}^{NH} (C_H + \alpha A_l^\beta) \right) \\
 & \left( \begin{array}{c} u_{h,j}^{i,p}, u_{h,j}^{i,p}, x^{i,p} \\ T_{he,j}^{i,p}, T_{ce,j}^{i,p}, Q_h^{0,p}, Q_c^{0,p} \\ A_j, A_l, A_k \end{array} \right) \\
 & + \sum_{p=1}^{NP} t_p \left( \sum_{k=1}^{NP} C_{CU} Q_{c,k}^{0,p} + \sum_{l=1}^{NH} C_{HU} Q_{h,l}^{0,p} \right) \right] \quad (5.49)
 \end{aligned}$$

For every disturbance direction (i) in all the source streams and for every exchanger (j) in the network, equality and inequality constraints are:

for  $i = 0, \dots, 2^{NS}$ ,  $j = 1, \dots, NE$  and  $p=1, \dots, NP$

energy-balance equations (equality constraints):

$$w_{h,j}^{i,p} (1 - u_{h,j}^{i,p}) (T_{hi,j}^{i,p} - T_{he,j}^{i,p}) + w_{c,j}^{i,p} (1 - u_{c,j}^{i,p}) (T_{ci,j}^{i,p} - T_{ce,j}^{i,p}) = 0 \quad (5.50)$$

$$w_{h,j}^{i,p} (1 - u_{h,j}^{i,p}) (T_{hi,j}^{i,p} - T_{he,j}^{i,p}) + U_j A_j \Delta T_{lm,j}^{i,p} = 0 \quad (5.51.a)$$

or

$$w_{c,j}^{i,p} (1 - u_{c,j}^{i,p}) (T_{ci,j}^{i,p} - T_{ce,j}^{i,p}) - U_j A_j \Delta T_{lm,j}^{i,p} = 0 \quad (5.51.b)$$

where:

$$\Delta T_{lm,j}^{i,p} = \frac{(T_{hi,j}^{i,p} - T_{ce,j}^{i,p}) - (T_{he,j}^{i,p} - T_{ci,j}^{i,p})}{\ln \left[ \frac{(T_{hi,j}^{i,p} - T_{ce,j}^{i,p})}{(T_{he,j}^{i,p} - T_{ci,j}^{i,p})} \right]} \quad (5.52)$$

overall heat-transfer coefficients can be introduced as the property of streams:

$$U_j = \frac{1}{\left( \frac{1}{h_{h,j}} \right) + \left( \frac{1}{h_{c,j}} \right)} \quad (5.53)$$

for every mixing point after an exchanger, energy-balance equations if bypass exist:

$$u_{h,j}^{i,p} T_{hi,j}^{i,p} + (1 - u_{h,j}^{i,p}) T_{he,j}^{i,p} - T_{hf,j}^{i,p} = 0 \quad (5.54)$$

$$u_{c,j}^{i,p} T_{ci,j}^{i,p} + (1 - u_{c,j}^{i,p}) T_{ce,j}^{i,p} - T_{cf,j}^{i,p} = 0 \quad (5.55)$$

load constraints (inequality constraints):

$$T_{he,j}^{i,p} - T_{hi,j}^{i,p} \leq 0 \quad (5.56)$$

$$T_{ci,j}^{i,p} - T_{ce,j}^{i,p} \leq 0 \quad (5.57)$$

minimum approach-temperature constraints (inequality constraints):

$$T_{ce,j}^{i,p} - T_{hi,j}^{i,p} \leq 0 \quad (5.58)$$

$$T_{ci,j}^{i,p} - T_{he,j}^{i,p} \leq 0 \quad (5.59)$$

bypass-ratio constraints (if bypasses exist) (side constraints):

$$0 \leq u_{h,j}^{i,p} < 1 \quad (5.60)$$

$$0 \leq u_{c,j}^{i,p} < 1 \quad (5.61)$$

split-ratio constraints (if splits exist) (side constraints):

$$0 \leq x^{i,p} < 1 \quad (5.62)$$

heater load constraints (inequality constraints):

$$T_{cf,j}^{i,p} - T_{c,l}^{t,p} \leq 0 \quad (5.63)$$

cooler load constraints (inequality constraints):

$$T_{h,k}^{t,p} - T_{hf,j}^{i,p} \leq 0 \quad (5.64)$$

The heat loads of heaters for the zero-disturbance direction for each period (equality constraints):

for  $l=1, \dots, NH$

$$Q_{h,l}^{0,p} - w_{c,j}^{0,p} \left( T_{c,l}^{t,p} - T_{cf,j}^{0,p} \right) = 0 \quad (5.65)$$

$$Q_{h,l}^{0,p} - U_l A_l \Delta T_{lm,l}^{0,p} = 0 \quad (5.66)$$

where:

$$\Delta T_{lm,l}^{0,p} = \frac{\left(T_{cf,j}^{0,p} - T_{hte,l}^{0,p}\right) - \left(T_{c,j}^{t,p} - T_{hti,l}^{0,p}\right)}{\ln\left[\left(T_{cf,j}^{0,p} - T_{hte,l}^{0,p}\right) / \left(T_{c,j}^{t,p} - T_{hti,l}^{0,p}\right)\right]} \quad (5.67)$$

The heat loads of coolers for the zero-disturbance direction for each period (equality constraints):

for  $k=1, \dots, NC$

$$Q_{c,k}^{0,p} = w_{h,j}^{0,p} \left(T_{hf,j}^{0,p} - T_{h,k}^{t,p}\right) \quad (5.68)$$

$$Q_{c,k}^{0,p} - U_k A_k \Delta T_{lm,k}^{0,p} = 0 \quad (5.69)$$

where:

$$\Delta T_{lm,k}^{0,p} = \frac{\left(T_{hf,j}^{0,p} - T_{cle,k}^{0,p}\right) - \left(T_{h,k}^{t,p} - T_{cli,k}^{0,p}\right)}{\ln\left[\left(T_{hf,j}^{0,p} - T_{cle,k}^{0,p}\right) / \left(T_{h,k}^{t,p} - T_{cli,k}^{0,p}\right)\right]} \quad (5.70)$$

In order to complete the general formulation:

- 1- the connections between the exchangers should be defined for every disturbance direction (i) and for every period (p),
- 2- the target temperatures of the network should be defined as hard (equality) or soft (inequality/range) constraints,
- 3- the temperatures of all the source streams entering the exchangers should be defined in terms of desired RDRI values for each period.

## 6. DEMONSTRATION OF THE OPTIMAL RESILIENT RETROFIT DESIGN FORMULATION ON EXAMPLE PROBLEMS

Following is the demonstration of the proposed formulation for a standard HEN problem which is called as 4SP1 in the literature (Lee et. al., 1970). The definition of the HEN problem is given in Table 6.1 and one solution of the problem is shown in Figure 6.1. This solution structure has been obtained via the pinch method (taking  $\Delta T_{\min} = 10$  K) (Linnhoff and Flower, 1978a, 1978b; Linnhoff et. al., 1982; Linnhoff and Hindmarsh, 1983) by breaking a loop. It is still a maximum-energy-recovery solution and includes a split. In the following demonstration, split ratio is considered as a manipulated variable as well. It is also assumed that disturbances (temperatures in source streams) may come from all of the source streams in all directions simultaneously with the same magnitude (i.e., retrofit-design-resiliency-index) for single-period. The explicit notation for the optimal retrofit-design formulation of the example HEN is shown by Figure 6.2. For simplicity, superscript indicating the period number (Section 5.2.2) is ignored in the following formulation.

TABLE 6.1. Definition of the example problem.

Flow	HCF (kW/K)	$T_{in}$ (K)	$T_{out}$ (K)	$h_{ind}$ (kW/m <sup>2</sup> K)
Hot 1	10.55	522	411	2
Hot 2	8.792	433	366	2
Cold 1	6.082	389	533	2
Cold 2	7.623	333	433	2
Heating		680	680	5
Cooling		300	320	2

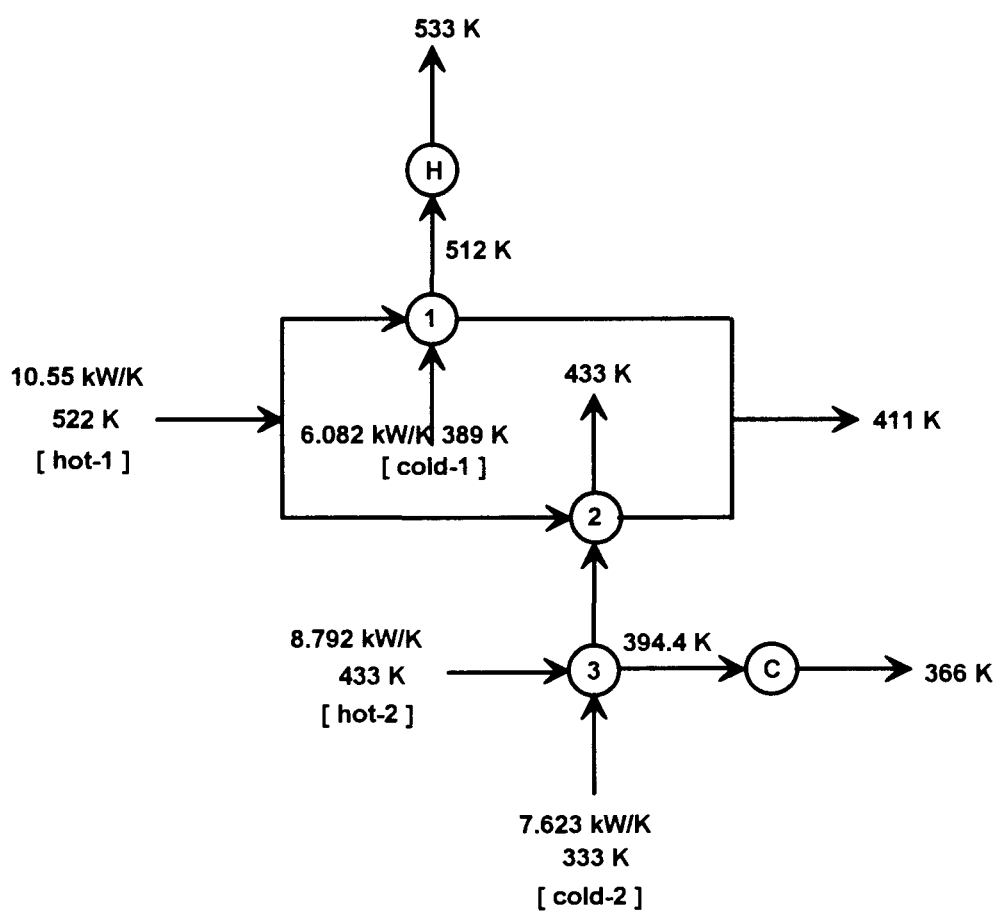


FIGURE 6.1. Pinch-solution structure of the example 4SP1 problem.

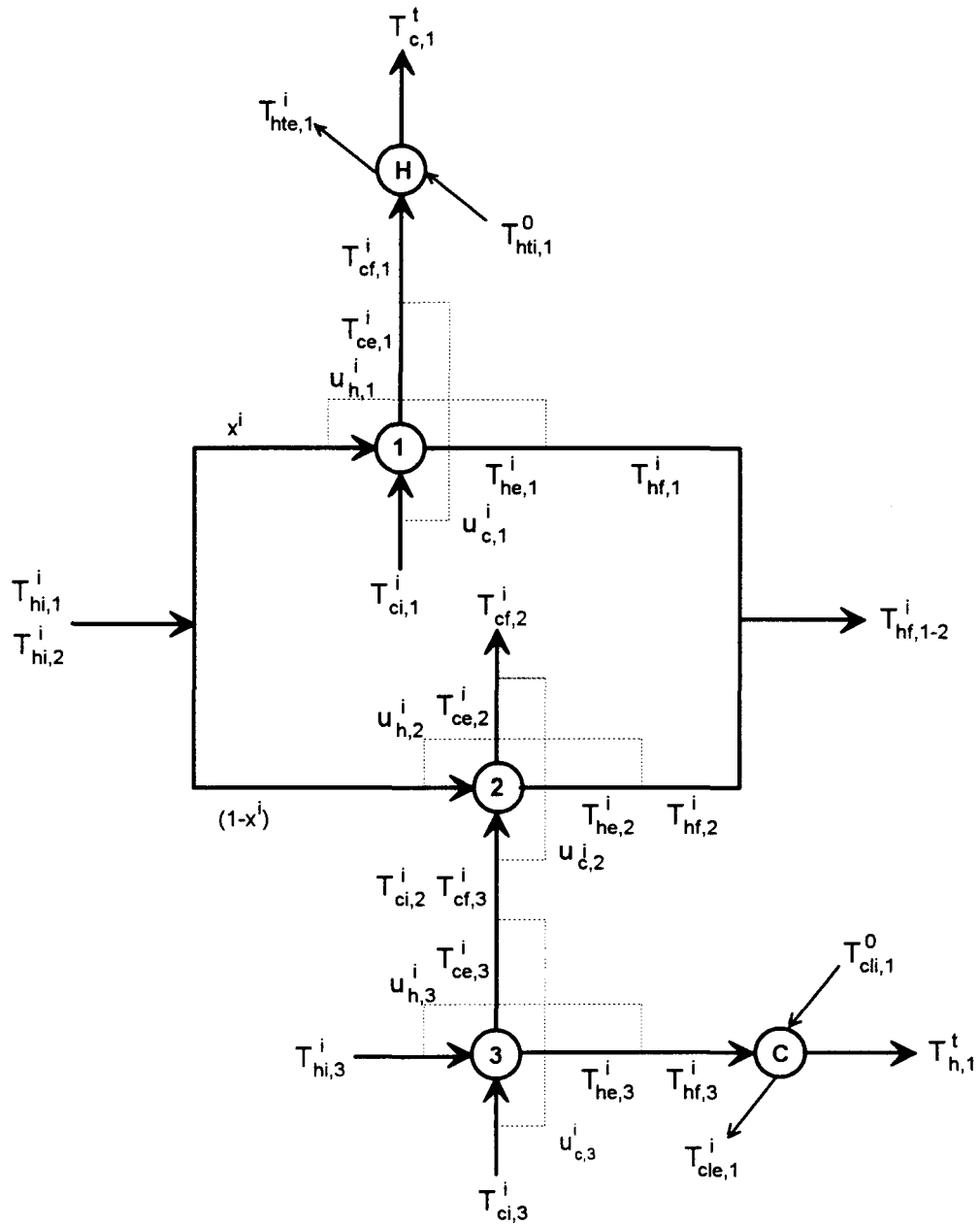


FIGURE 6.2. Notation for the pinch solution of the 4SP1 problem.

Objective function is the minimization of the total annualized cost:

$$\min \left[ 3\gamma C_E + \gamma C_C + \gamma C_H + \alpha \gamma \left( A_1^\beta + A_2^\beta + A_3^\beta + A_C^\beta + A_H^\beta \right) + C_{CU} Q_{c,1}^0 + C_{HU} Q_{h,1}^0 \right] \quad (6.1)$$

Equality constraints for every disturbance direction ( $i = 0, \dots, 2^{NS} = 2^4 = 16$ )

for exchanger 1

$$w_{h,1}^i x^i (1 - u_{h,1}^i) (T_{hi,1}^i - T_{he,1}^i) + w_{c,1}^i (1 - u_{c,1}^i) (T_{ci,1}^i - T_{ce,1}^i) = 0 \quad (6.2)$$

$$w_{h,1}^i x^i (1 - u_{h,1}^i) (T_{hi,1}^i - T_{he,1}^i) + U_1 A_1 \Delta T_{lm}^i = 0 \quad (6.3)$$

$$u_{h,1}^i T_{hi,1}^i + (1 - u_{hi,1}^i) T_{he,1}^i - T_{hf,1}^i = 0 \quad (6.4)$$

$$U_1 = \frac{1}{(1/h_{h,1}) + (1/h_{c,1})} \quad (6.5)$$

$$\Delta T_{lm,1}^i = \frac{(T_{hi,1}^i - T_{ce,1}^i) - (T_{he,1}^i - T_{ci,1}^i)}{\ln \left[ (T_{hi,1}^i - T_{ce,1}^i) / (T_{he,1}^i - T_{ci,1}^i) \right]} \quad (6.6)$$

for exchanger 2

$$w_{h,2}^i (1 - x^i) (1 - u_{h,2}^i) (T_{hi,2}^i - T_{he,2}^i) + w_{c,2}^i (1 - u_{c,2}^i) (T_{ci,2}^i - T_{ce,2}^i) = 0 \quad (6.7)$$

$$w_{h,2}^i (1 - x^i) (1 - u_{h,2}^i) (T_{hi,2}^i - T_{he,2}^i) + U_2 A_2 \Delta T_{lm,2}^i = 0 \quad (6.8)$$

$$u_{h,2}^i T_{hi,2}^i + (1 - u_{hi,2}^i) T_{he,2}^i - T_{hf,2}^i = 0 \quad (6.9)$$

$$U_2 = \frac{1}{(1/h_{h,2}) + (1/h_{c,2})} \quad (6.10)$$

$$\Delta T_{lm,2}^i = \frac{(T_{hi,2}^i - T_{ce,2}^i) - (T_{he,2}^i - T_{ci,2}^i)}{\ln \left[ (T_{hi,2}^i - T_{ce,2}^i) / (T_{he,2}^i - T_{ci,2}^i) \right]} \quad (6.11)$$

for exchanger 3

$$w_{h,3}^i (1 - u_{h,3}^i) (T_{hi,3}^i - T_{he,3}^i) + w_{c,3}^i (1 - u_{c,3}^i) (T_{ci,3}^i - T_{ce,3}^i) = 0 \quad (6.12)$$

$$w_{h,3}^i (1 - u_{h,3}^i) (T_{hi,3}^i - T_{he,3}^i) + U_3 A_3 \Delta T_{lm,3}^i = 0 \quad (6.13)$$

$$u_{h,3}^i T_{hi,3}^i + (1 - u_{hi,3}^i) T_{he,3}^i - T_{hf,3}^i = 0 \quad (6.14)$$

$$U_3 = \frac{1}{(1/h_{h,3}) + (1/h_{c,3})} \quad (6.15)$$

$$\Delta T_{lm,3}^i = \frac{(T_{hi,3}^i - T_{ce,3}^i) - (T_{he,3}^i - T_{ci,3}^i)}{\ln \left[ \frac{(T_{hi,3}^i - T_{ce,3}^i)}{(T_{he,3}^i - T_{ci,3}^i)} \right]} \quad (6.16)$$

for split mixing point

$$x^i T_{hf,1}^i + (1 - x^i) T_{hf,2}^i - T_{hf,1-2}^i = 0 \quad (6.17)$$

Inequality constraints for every disturbance direction ( $i = 0, \dots, 16$ )

for exchanger 1  $T_{he,1}^i - T_{hi,1}^i \leq 0$  (load constraint for hot-side) (6.18)

$$T_{ci,1}^i - T_{ce,1}^i \leq 0 \quad (\text{load constraint for cold-side}) \quad (6.19)$$

$$T_{ce,1}^i - T_{hi,1}^i \leq 0 \quad (\text{minimum-approach-temperature constraint}) \quad (6.20)$$

$$T_{ci,1}^i - T_{he,1}^i \leq 0 \quad (\text{minimum-approach-temperature constraint}) \quad (6.21)$$

$$0 \leq u_{hi,1}^i < 1 \quad (\text{bypass-ratio constraints}) \quad (6.22)$$

for exchanger 2  $T_{he,2}^i - T_{hi,2}^i \leq 0$  (load constraint for hot-side) (6.23)

$$T_{ci,2}^i - T_{ce,2}^i \leq 0 \quad (\text{load constraint for cold-side}) \quad (6.24)$$

$$T_{ce,2}^i - T_{hi,2}^i \leq 0 \quad (\text{minimum-approach-temperature constraint}) \quad (6.25)$$

$$T_{ci,2}^i - T_{he,2}^i \leq 0 \quad (\text{minimum-approach-temperature constraint}) \quad (6.26)$$

$$0 \leq u_{hi,2}^i < 1 \quad (\text{bypass-ratio constraints}) \quad (6.27)$$

for exchanger 3  $T_{he,3}^i - T_{hi,3}^i \leq 0$  (load constraint for hot-side) (6.28)

$$T_{ci,3}^i - T_{ce,3}^i \leq 0 \quad (\text{load constraint for cold-side}) \quad (6.29)$$

$$T_{ce,3}^i - T_{hi,3}^i \leq 0 \quad (\text{minimum-approach-temperature constraint}) \quad (6.30)$$

$$T_{ci,3}^i - T_{he,3}^i \leq 0 \quad (\text{minimum-approach-temperature constraint}) \quad (6.31)$$

$$0 \leq u_{hi,3}^i < 1 \quad (\text{bypass-ratio constraints}) \quad (6.32)$$

for split fraction  $0 < x^i < 1$  (6.33)

for heater  $T_{cf,1}^i - 533 \leq 0$  (6.34)

for cooler  $366 - T_{hf,3}^i \leq 0$  (6.35)

The heat load of the heater in zero-disturbance direction is

$$Q_{h,1}^0 = w_{c,1}^0 (T_{c,1}^t - T_{cf,1}^0) \quad (6.36)$$

$$Q_{h,1}^0 - U_h A_h \Delta T_{lm,h}^0 = 0 \quad (6.37)$$

The heat load of the cooler in zero-disturbance direction is

$$Q_{c,1}^0 = w_{h,3}^0 (T_{hf,3}^0 - T_{h,1}^t) \quad (6.38)$$

$$Q_{c,1}^0 - U_c A_c \Delta T_{lm,c}^0 = 0 \quad (6.39)$$

The connections between exchangers ( $i = 0, \dots, 16$ )

$$T_{cf,3}^i = T_{ci,2}^i \quad (6.40)$$

since only the deviations in source temperatures are evaluated, heat-capacity-flowrates are constant as defined in problem;

$$w_{h,1}^i = w_{h,2}^i = 10.550 \quad (6.41)$$

$$w_{h,3}^i = 8.790 \quad (6.42)$$

$$w_{c,1}^i = 6.082 \quad (6.43)$$

$$w_{c,2}^i = w_{c,3}^i = 7.62 \quad (6.44)$$

Target temperatures of the network ( $i = 0, \dots, 16$ )

$$T_{hf,1-2}^i = 411 \quad (\text{target of the hot stream 1 after split remix}) \quad (6.45)$$

$$T_{cf,2}^i = 433 \quad (6.46)$$

$$T_{h,1}^t = 533 \quad (6.47)$$

$$T_{c,1}^t = 366 \quad (6.48)$$

the temperatures of the source streams entering the exchangers according to disturbance directions are given in Table 6.2 (for a 5 K temperature disturbance for each direction, i.e. RDRI = 5 K).

Using the nonlinear-programming (NLP) problem defined above, the network structure is examined for two different main cases. In Case-A, the objective function is taken as the minimization of the total area of the exchangers of the network; ( $\min (A_1+A_2+A_3)$ ). In Case-B, objective function is taken as the minimization of the total annualized cost (Eq. 6.1).

TABLE 6.2. Source-temperature values for each disturbance direction for 5 K RDRI value.

$i$	$T_{hi,1}^i$	$T_{hi,2}^i$	$T_{hi,3}^i$	$T_{ci,1}^i$	$T_{ci,3}^i$
0	522	522	433	389	333
1	522+5	522+5	433+5	389+5	333+5
2	522+5	522+5	433+5	389+5	333-5
3	522+5	522+5	433+5	389-5	333+5
4	522+5	522+5	433+5	389-5	333-5
5	522+5	522+5	433-5	389+5	333+5
6	522+5	522+5	433-5	389+5	333-5
7	522+5	522+5	433-5	389-5	333+5
8	522+5	522+5	433-5	389-5	333-5
9	522-5	522-5	433+5	389+5	333+5
10	522-5	522-5	433+5	389+5	333-5
11	522-5	522-5	433+5	389-5	333+5
12	522-5	522-5	433+5	389-5	333-5
13	522-5	522-5	433-5	389+5	333+5
14	522-5	522-5	433-5	389+5	333-5
15	522-5	522-5	433-5	389-5	333+5
16	522-5	522-5	433-5	389-5	333-5

### 6.1. Case Study A

As mentioned above, the objective function of Case-A is taken as the minimization of total area of the exchangers for the desired value of RDRI subject to target-temperature constraints. In this situation, therefore, the terms related to heater and cooler in the objective function (Eq. 6.1) disappear. It is also desired for the solution design to preserve its maximum-energy-recovery (MER) property when operating at the nominal values of source streams which requires that  $T_{cf,1}^0=512$  K and  $T_{hf,3}^0=394.4$  K. Obviously, the zero-resiliency design (initial design) is the ‘minimum-area-design’ of the structure for the MER condition (for  $\Delta T_{\min} = 10$  K). ( $A_1 = 40.5$  m<sup>2</sup>,  $A_2 = 10.5$  m<sup>2</sup>,  $A_3 = 5.8$  m<sup>2</sup>).

The total possible number of single-bypass (bypass over only one exchanger) configurations for a HEN is

$$\sum_{i=0}^{2 \text{ NE}} \binom{2 \text{ NE}}{i} = \sum_{i=0}^{2 \text{ NE}} \frac{(2 * \text{NE})!}{i! (2 * \text{NE} - i)!} = 2^{2 * \text{NE}} \quad (6.49)$$

The structure was analyzed for some of the single-bypass configurations given in Table 6.3. When these bypass configurations are implemented on the structure, the increases in the areas of the individual exchangers and the total area of the HEN, relative to those of the initial designs (zero-disturbance with no bypass stream), as a function of RDRI are given in Figure 6.4 through Figure 6.29. The generation of such figures requires considerable computation time since the optimization problem defined at the beginning of this chapter should be solved repeatedly for each RDRI value. Iterations continue till the *maximum RDRI* value, which is called as *MRDRI* (beyond which a feasible solution cannot be obtained), is reached. The solution to the NLP problems presented here were obtained using the software package GAMS (with MINOS module for NLP) and the GAMS code of the formulation is given in Appendix C.

Using the logarithmic-mean temperature in the constraint equations renders the feasible solution set nonconvex and hence the existence of local minima and the nonuniqueness of the optimal decision variables. Therefore, in this work, a practical solution has been sought to obtain the global minimum. For each of the bypass configurations given in Table 6.3, the problem was first solved for the zero RDRI value, and then RDRI value was increased by at most 0.1 K repeatedly until the maximum RDRI value is reached. In some iterations, the increment had to be reduced to 0.001 K in order to capture the feasible solution. Initial guess point used in the zero-resiliency design is the MER solution and hence the global minimum point for the zero RDRI. The next iteration then starts with a RDRI value equal to 0.1 K and finds the minimum. This is the global minimum for the given RDRI since the perturbed nominal inlet temperatures are very near to nominal ones. Starting from a point (current global minimum) very near to the next global minimum point also results in the global solution of the next iteration. In GAMS programming, the results (values of variables) of each step successively were used in the following steps as initial guesses. The solution obtained in the second iteration then becomes the initial guess point for the third iteration wherein RDRI now is increased to 0.2. Iterations advance in this manner till no feasible solution exists (thermodynamic violation) which is the end point of the curves (i.e., MRDRI) in Figure 6.4 - 6.29. It should also be noted that solution to only one NLP problem takes approximately 2.5 minutes on a 486-PC/50 MHz machine. This means that, for example, construction of Figure 6.4 (MRDRI = 20.6 K) requires at least 9 hours of computation time. Figure 6.3 summarizes the procedure for finding the MRDRI of a HEN.

The resulting area increase vs. RDRI curves are presented in Figures 6.4 - 6.29. It can be seen that for some bypass configurations, areas of individual exchangers and the total area of the network immediately increase with a small increase in RDRI from zero, and continues to increase until the MRDRI value is reached. For the other bypass configurations areas remain constant up to a certain RDRI value, and then increase towards their MRDRI value. Hereafter, the point that the areas begin to increase is referred to as '*break point*' (*BRDRI*). It should be noticed that, the DRI value of this type of designs are BRDRI up to BRDRI. This means that, networks designed for the nominal values of stream conditions can be rendered resilient/controllable by simply installing bypasses to appropriate heat exchangers in the network without installing additional exchanger areas.

TABLE 6.3. Bypass configurations analyzed. (H1 indicates a bypass around the hot-side of exchanger 1, C1 indicates a bypass around the cold-side of exchanger ... so on.)

#	H1	C1	H2	H3	C3
A1	✓	✓	✓	✓	✓
A2	✓	✓	✓	✓	
A3	✓	✓	✓		✓
A4	✓	✓		✓	✓
A5	✓		✓	✓	✓
A6		✓	✓	✓	✓
A7	✓	✓	✓		
A8	✓	✓		✓	
A9	✓	✓			✓
A10	✓		✓	✓	
A11	✓		✓		✓
A12	✓			✓	✓
A13		✓	✓	✓	
A14		✓	✓		✓
A15		✓		✓	✓
A16			✓	✓	✓
A17	✓	✓			
A18	✓		✓		
A19	✓			✓	
A20	✓				✓
A21		✓	✓		
A22		✓		✓	
A23		✓			✓
A24			✓	✓	
A25			✓		✓
A26				✓	✓
A27	✓				
A28		✓			
A29			✓		
A30				✓	
A31					✓
A32					

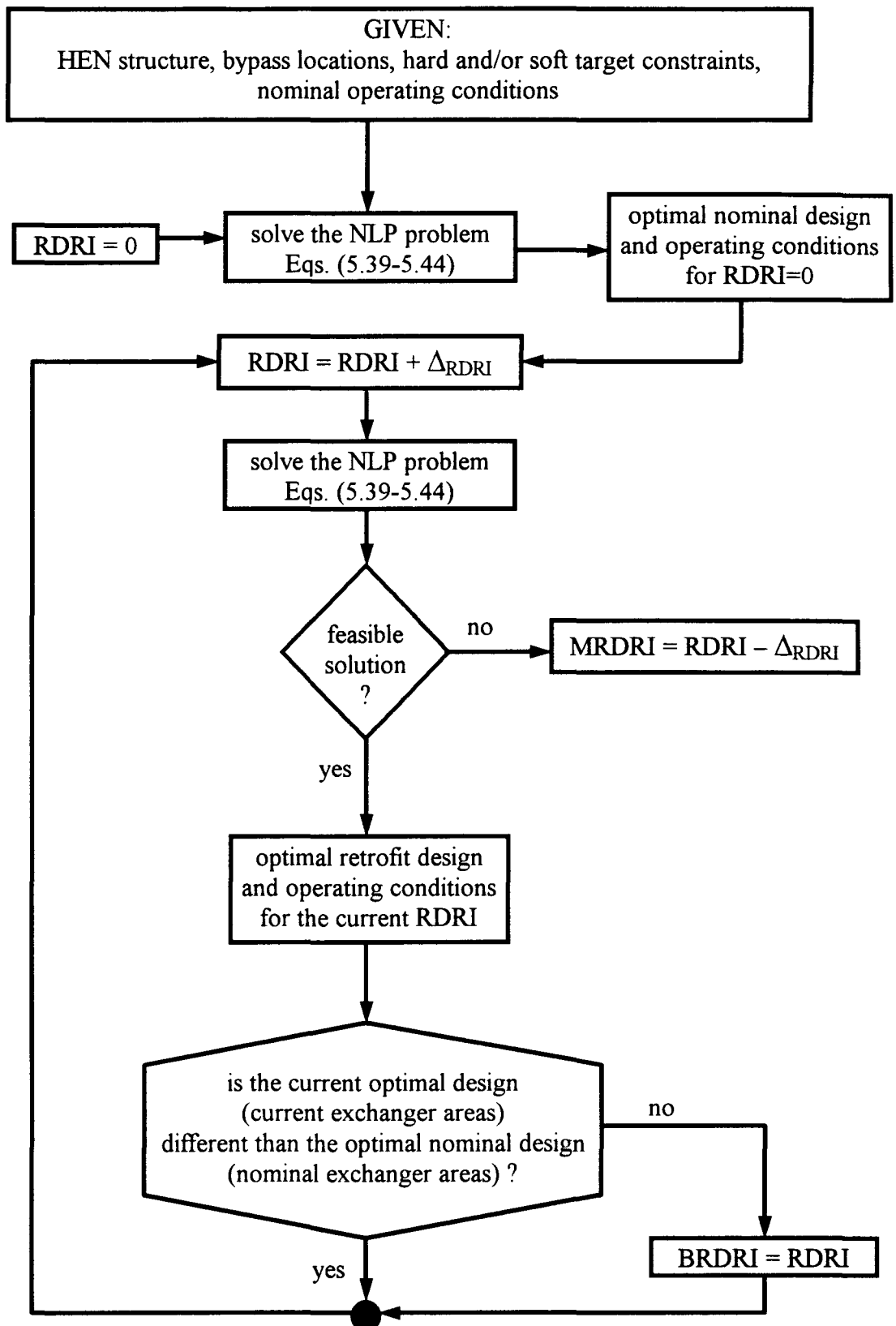


FIGURE 6.3. Procedure for finding the MRDRI and BRDRI of a HEN.

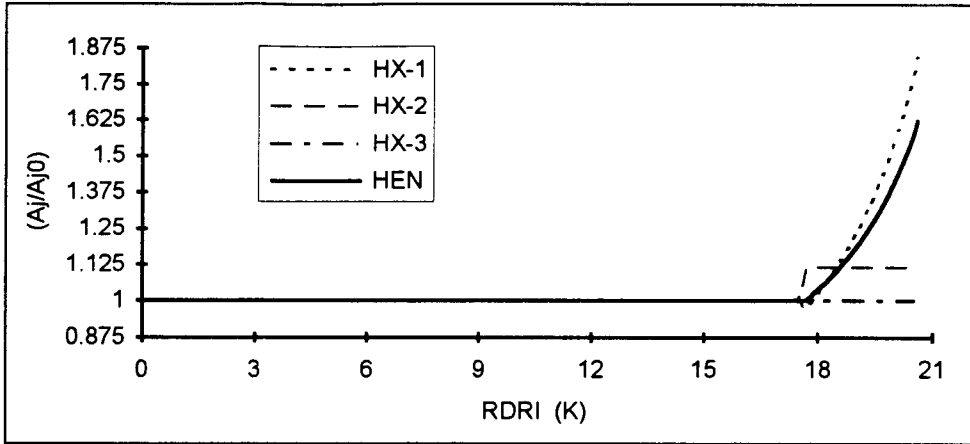


FIGURE 6.4. Variations in areas of heat exchangers and HEN with RDRI for Case-A1.

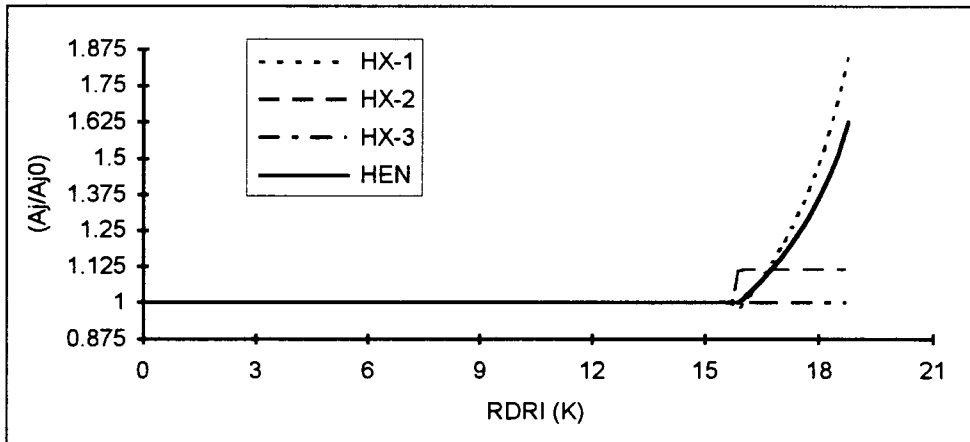


FIGURE 6.5. Variations in areas of heat exchangers and HEN with RDRI for Case-A2.

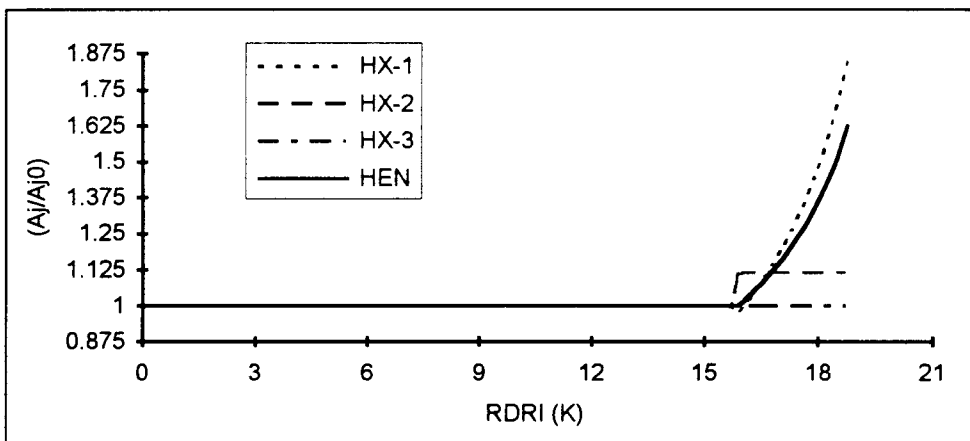


FIGURE 6.6. Variations in areas of heat exchangers and HEN with RDRI for Case-A3.

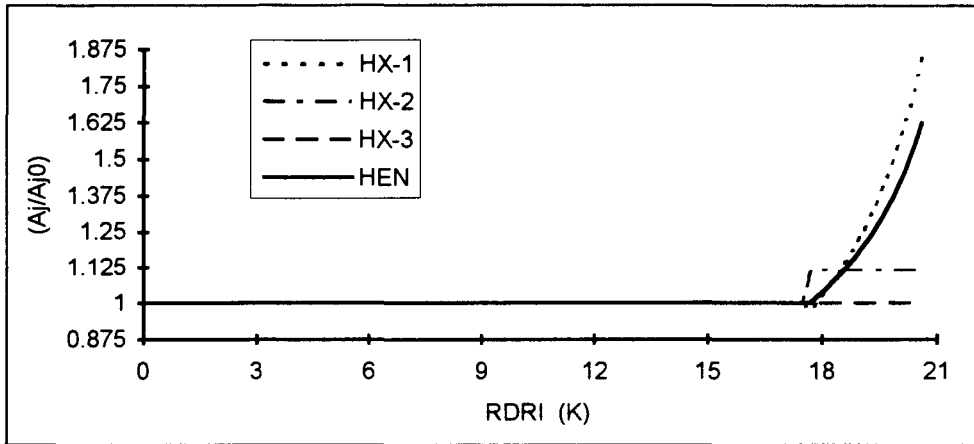


FIGURE 6.7. Variations in areas of heat exchangers and HEN with RDRI for Case-A4.

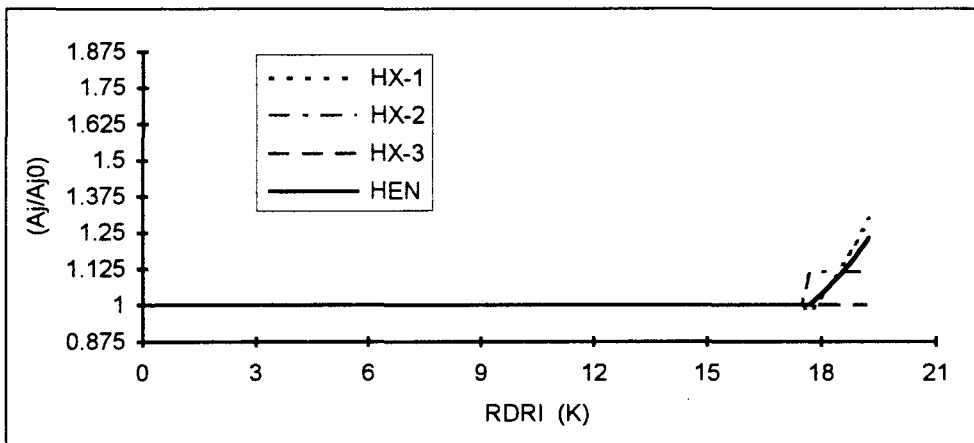


FIGURE 6.8. Variations in areas of heat exchangers and HEN with RDRI for Case-A5.

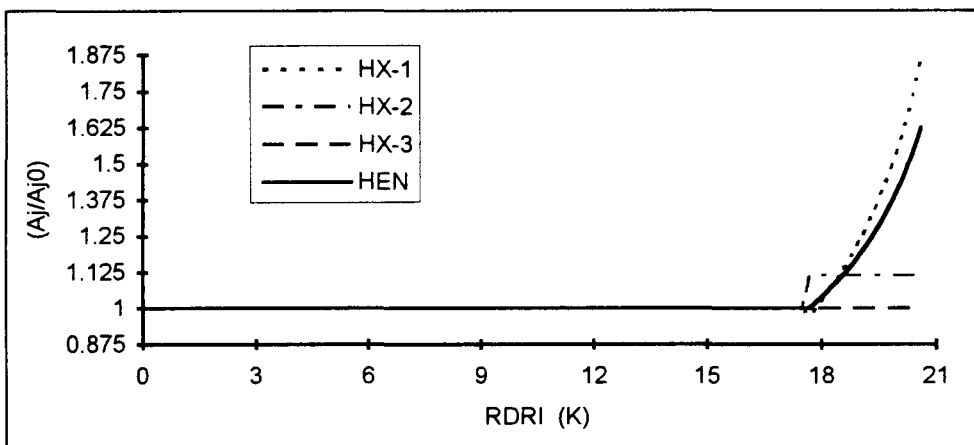


FIGURE 6.9. Variations in areas of heat exchangers and HEN with RDRI for Case-A6.

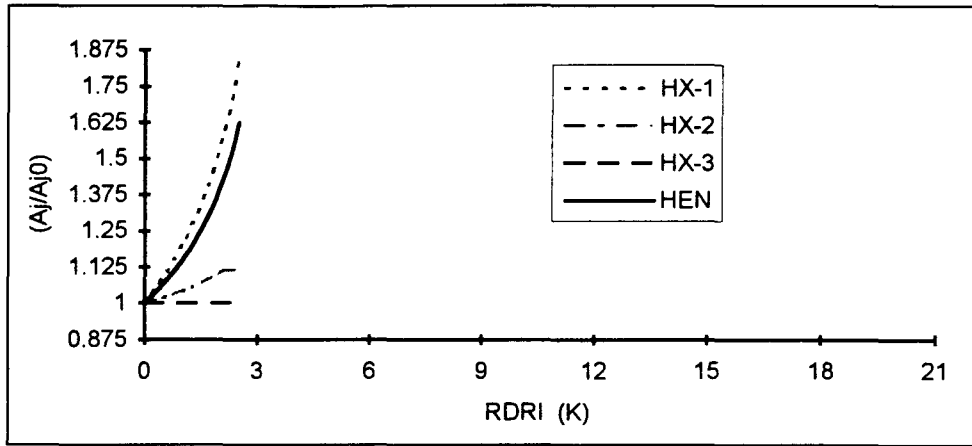


FIGURE 6.10. Variations in areas of heat exchangers and HEN with RDRI for Case-A7.

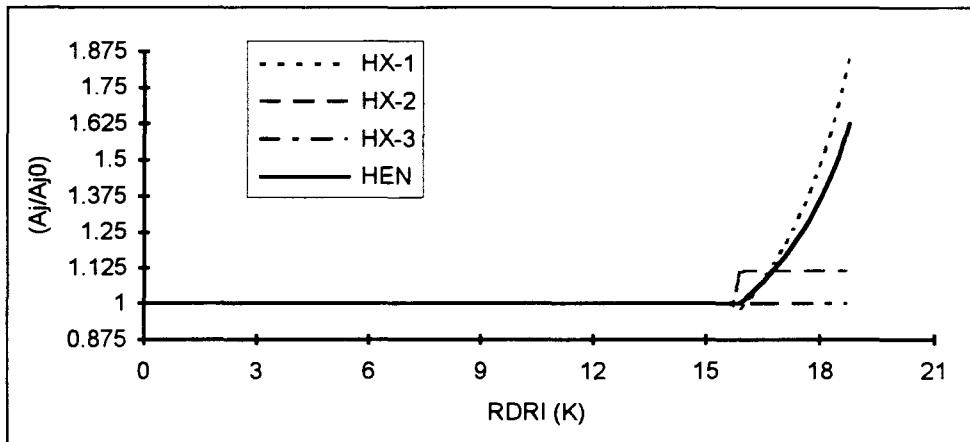


FIGURE 6.11. Variations in areas of heat exchangers and HEN with RDRI for Case-A8.

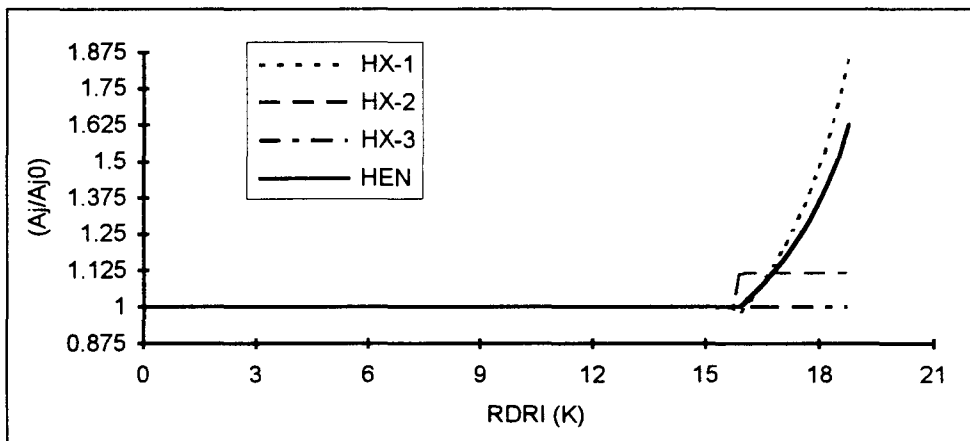


FIGURE 6.12. Variations in areas of heat exchangers and HEN with RDRI for Case-A9.

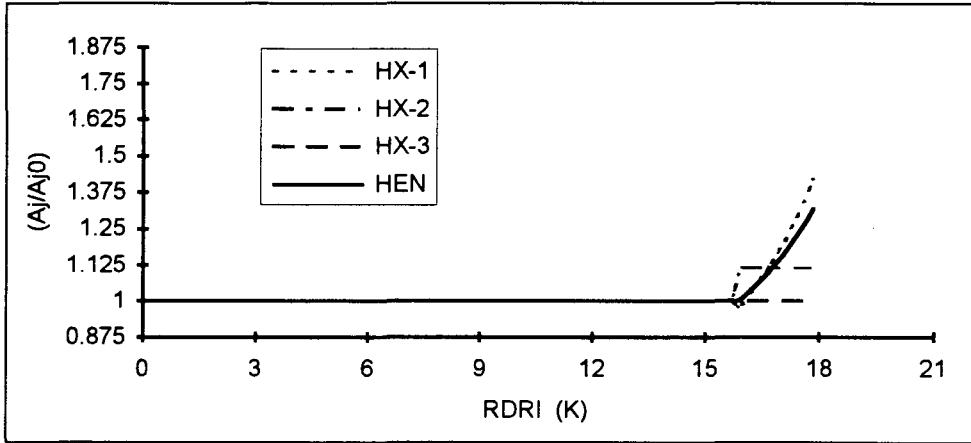


FIGURE 6.13. Variations in areas of heat exchangers and HEN with RDRI for Case-A10.

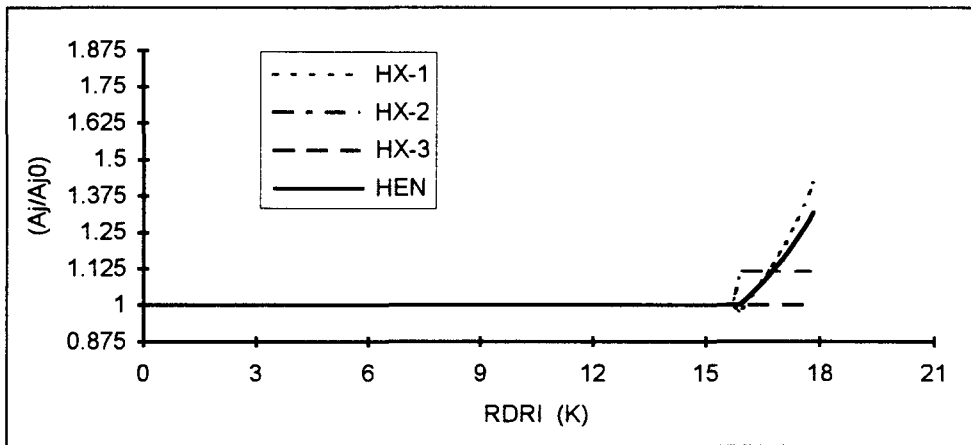


FIGURE 6.14. Variations in areas of heat exchangers and HEN with RDRI for Case-A11.

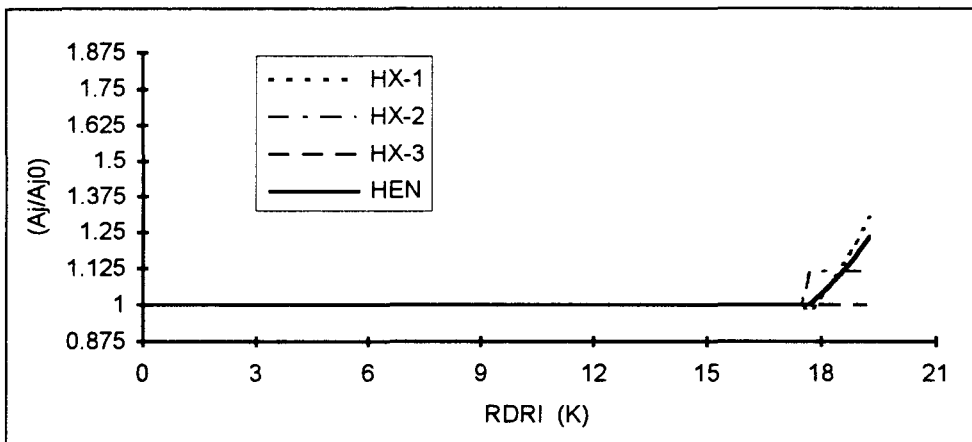


FIGURE 6.15. Variations in areas of heat exchangers and HEN with RDRI for Case-A12.

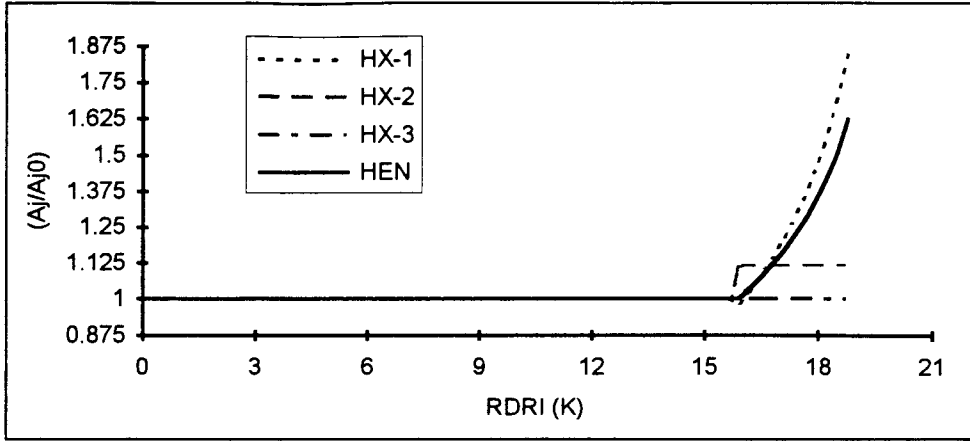


FIGURE 6.16. Variations in areas of heat exchangers and HEN with RDRI for Case-A13.

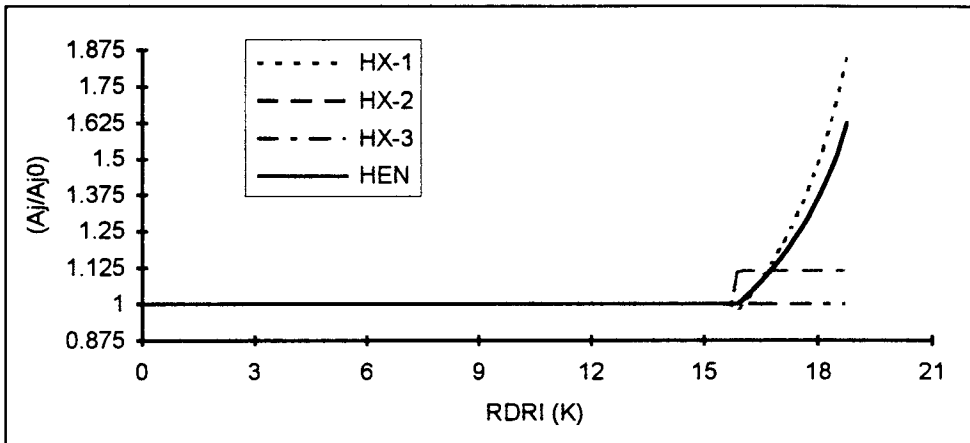


FIGURE 6.17. Variations in areas of heat exchangers and HEN with RDRI for Case-A14.

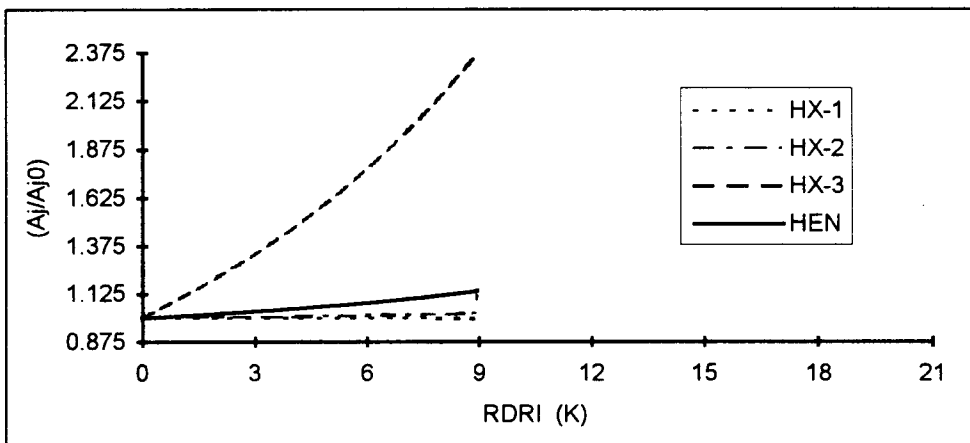


FIGURE 6.18. Variations in areas of heat exchangers and HEN with RDRI for Case-A15.

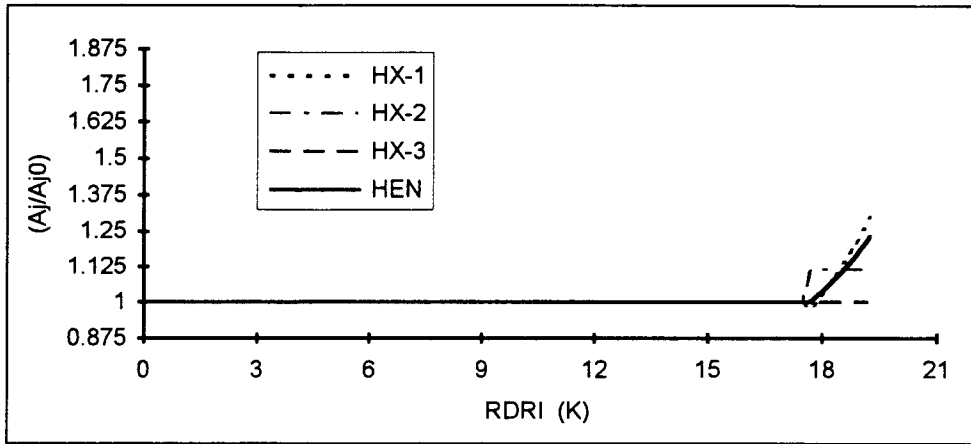


FIGURE 6.19. Variations in areas of heat exchangers and HEN with RDRI for Case-A16.

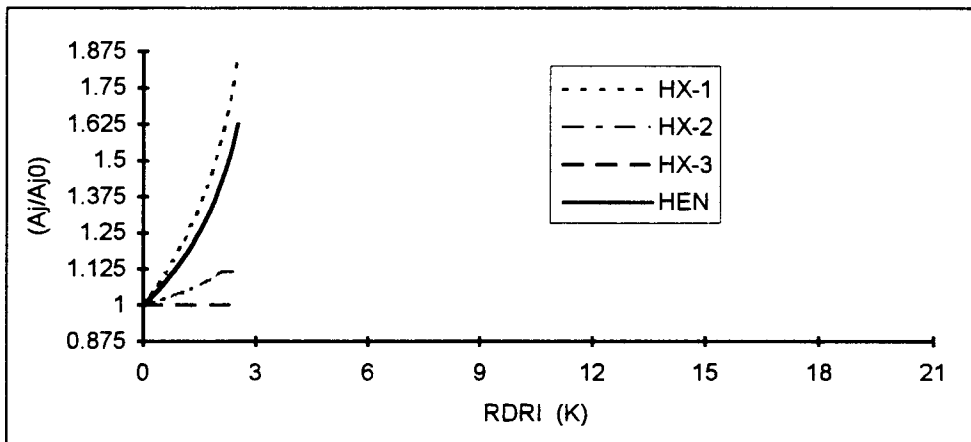


FIGURE 6.20. Variations in areas of heat exchangers and HEN with RDRI for Case-A17.

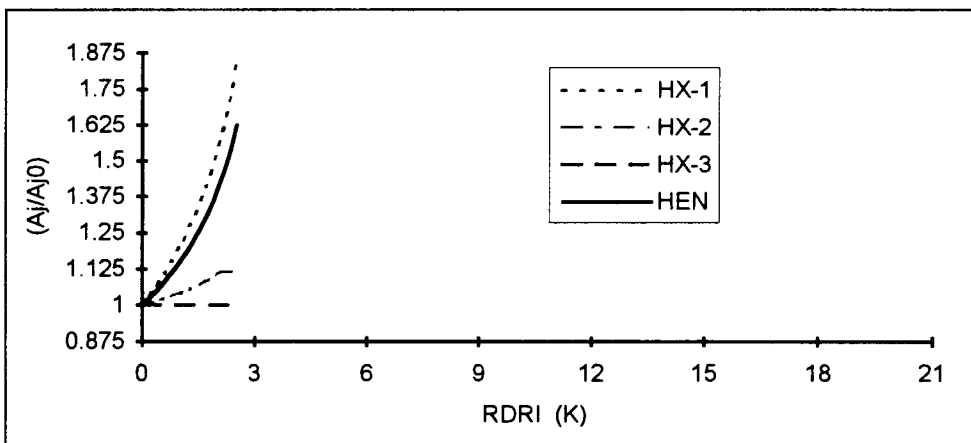


FIGURE 6.21. Variations in areas of heat exchangers and HEN with RDRI for Case-A18.

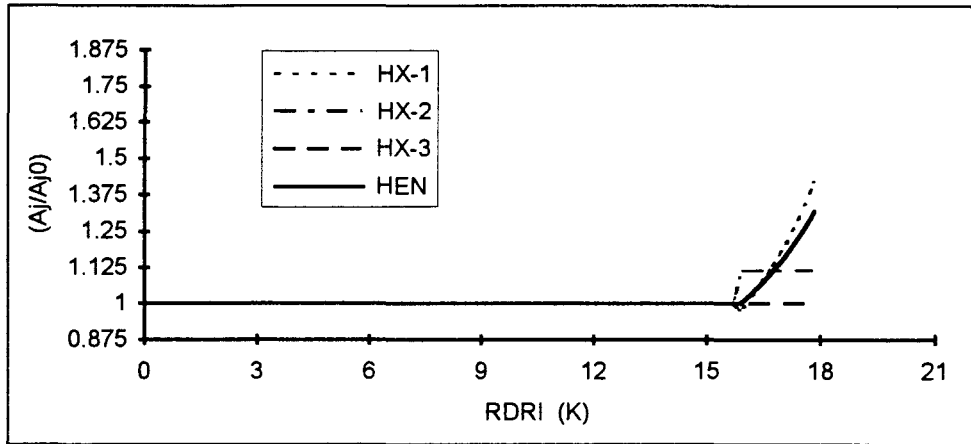


FIGURE 6.22. Variations in areas of heat exchangers and HEN with RDRI for Case-A19.

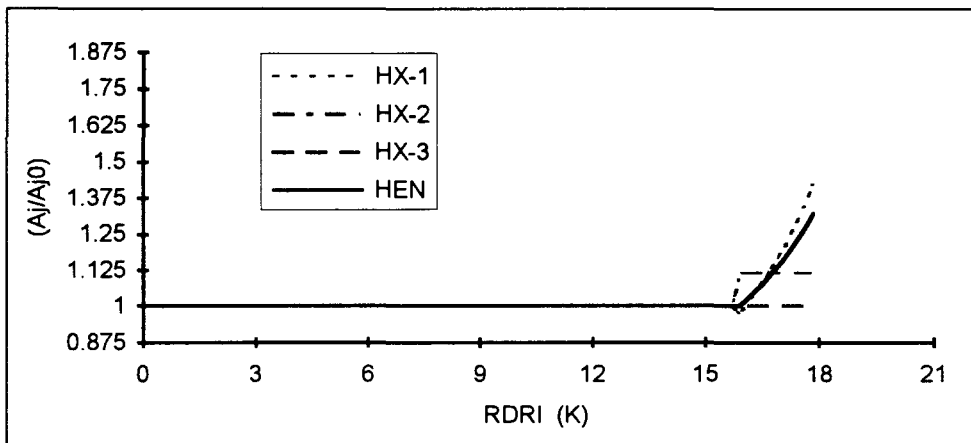


FIGURE 6.23. Variations in areas of heat exchangers and HEN with RDRI for Case-A20.

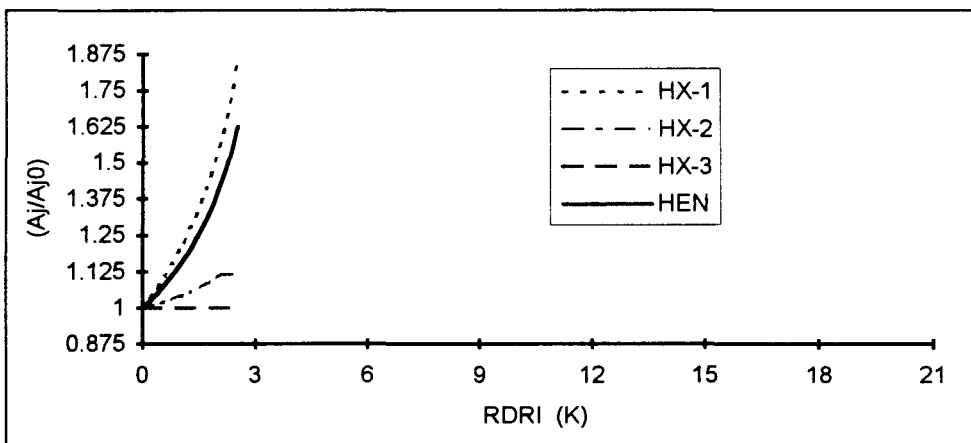


FIGURE 6.24. Variations in areas of heat exchangers and HEN with RDRI for Case-A21.

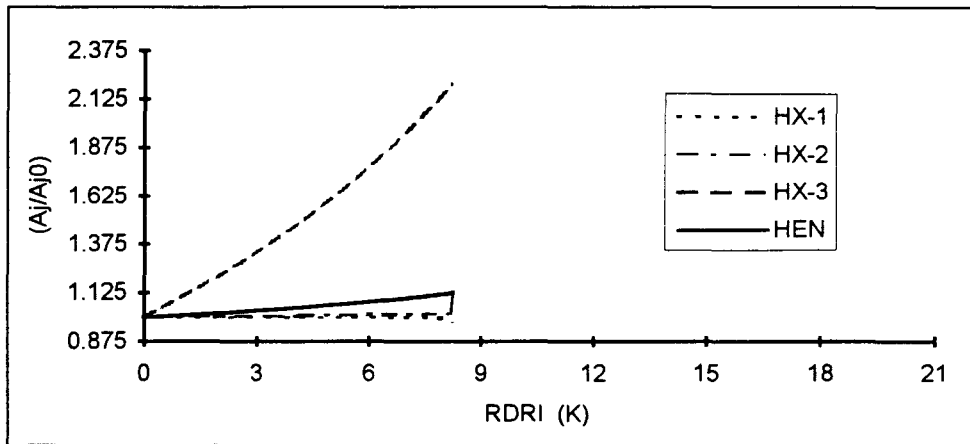


FIGURE 6.25. Variations in areas of heat exchangers and HEN with RDRI for Case-A22.

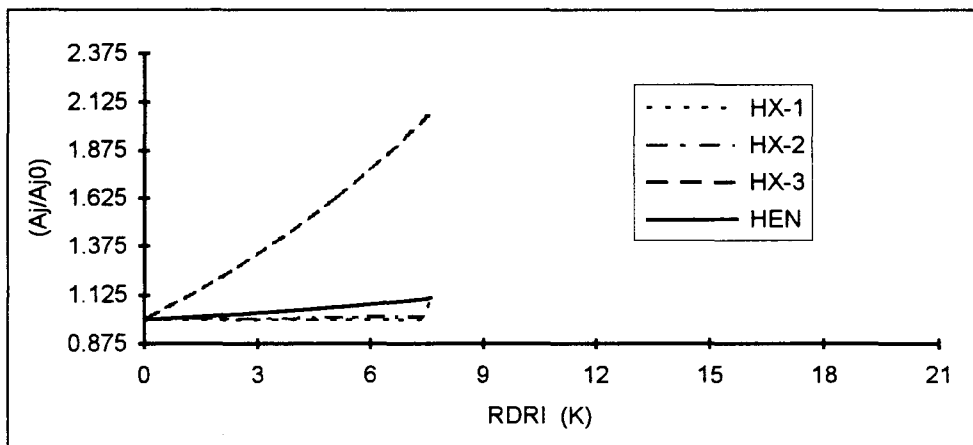


FIGURE 6.26. Variations in areas of heat exchangers and HEN with RDRI for Case-A23.

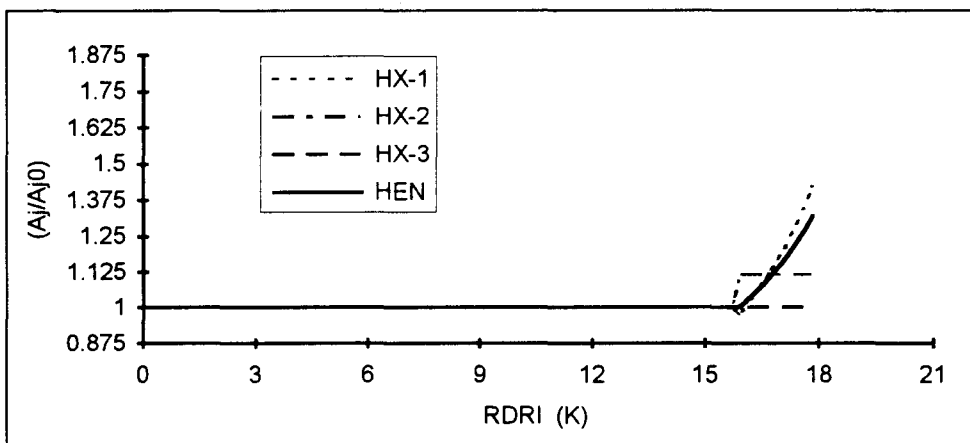


FIGURE 6.27. Variations in areas of heat exchangers and HEN with RDRI for Case-A24.

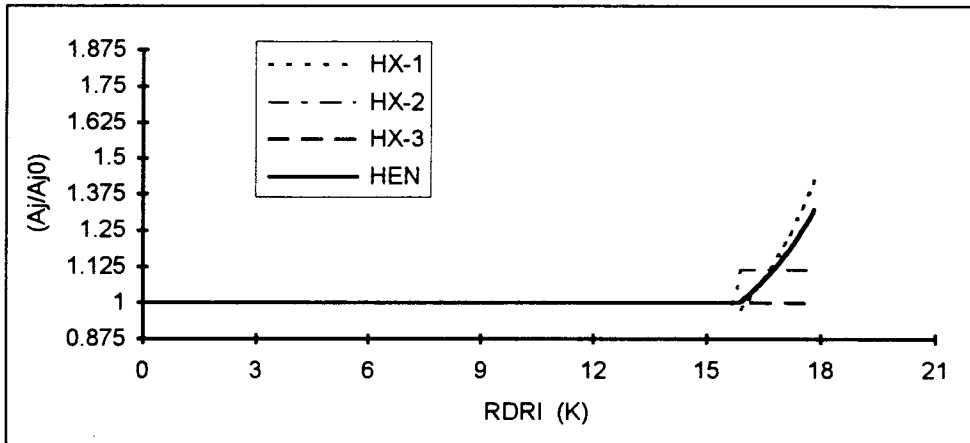


FIGURE 6.28. Variations in areas of heat exchangers and HEN with RDRI for Case-A25.

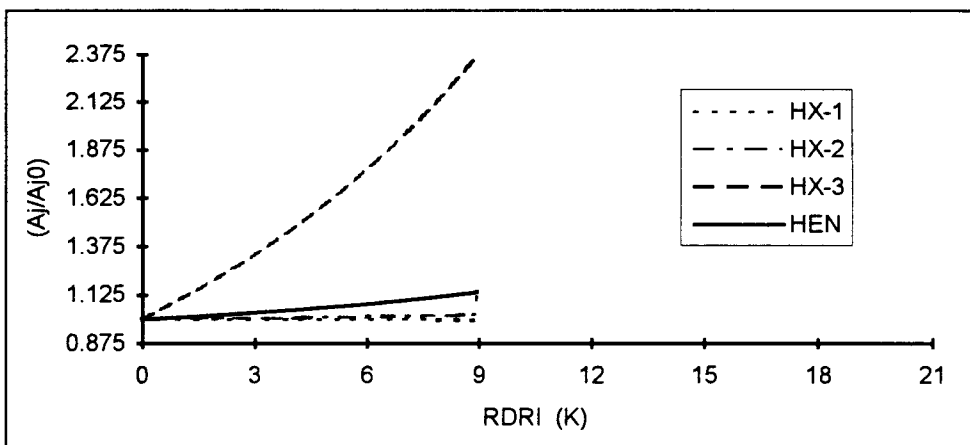


FIGURE 6.29. Variations in areas of heat exchangers and HEN with RDRI for Case-A26.

TABLE 6.4. BRDRI and MRDRI values for different bypass configurations for Case-A.

Case	# of bypasses	BRDRI (K)	MRDRI (K)
A4	4	17.5	20.6
A6	4	17.5	20.6
A1	5	17.5	20.6
A12	3	17.5	19.3
A16	3	17.5	19.3
A5	4	17.5	19.3
A8	3	15.7	18.8
A9	3	15.7	18.8
A13	3	15.7	18.8
A14	3	15.7	18.8
A2	4	15.7	18.8
A3	4	15.7	18.8
A19	2	15.7	17.8
A20	2	15.7	17.8
A24	2	15.7	17.8
A10	3	15.7	17.8
A11	3	15.7	17.8
A25	2	15.5	17.8
A26	2	0.0	8.9
A15	3	0.0	8.9
A22	2	0.0	8.3
A23	2	0.0	7.6
A17	2	0.0	2.5
A18	2	0.0	2.5
A21	2	0.0	2.5
A7	3	0.0	2.5
A32	0	0.0	0.0
A27	1	0.0	0.0
A28	1	0.0	0.0
A29	1	0.0	0.0
A30	1	0.0	0.0
A31	1	0.0	0.0

In Table 6.4, BRDRI and MRDRI values of different bypass configurations of the example structure are given. As can be seen in the table and figures, cases A1, A4 and A6 have the same value of BRDRI and MRDRI values and the same trajectories. The only difference is in the placement and the number of bypasses. While cases A4 and A6 have four bypasses, case A1 has five bypasses. The BRDRI and MRDRI values of these cases are the highest among the bypass configurations examined for this structure. Also, it can be seen that cases A7, A17, A18 and A21 has the same value of BRDRI and MRDRI values and same trajectories as well. While case A7 has three bypasses, cases A17, A18 and A21 have two bypasses. The increase in the total area of heat-exchangers for these cases are 62.5 per cent for 2.5 K DRI value. On the other hand, with the 62.5 per cent increase in the total area for cases A1, A4 and A6 the DRI value is 20.6 K. Furthermore, for a 2.5 K DRI value, cases A1, A4 and A6 does not need not any increase in total area (capital cost). Only by inserting bypasses to the base design, these cases automatically gains resiliency with the value of 17.5 K DRI.

The selection and the location of the bypasses has therefore, a great impact on the resiliency of the resulting HENs. At the design stage, designer must consider the trade-offs between the resiliency and the cost for different bypass configurations of the proposed structure.

## 6.2. Case Study B

Herein, the example problem studied in the previous section is analyzed for two bypass configurations, with the objective function being the total annualized cost (Eq. 6.1). One of the bypassed-structure, Structure-B1, (Figure 6.30, Case-B1) has one bypass on the cold-side of exchanger-2. It is decided to locate the bypass there in accordance with the controllability-heuristics outlined in Mathisen and Skogestad (1992) and Mathisen (1994). The heuristic offers to place bypasses so that the effect on the controlled target should be direct. In Case-B2 (Structure-B2, Figure 6.31), two bypasses are used and one is located on hot side of exchanger 1 and the other on the cold side of exchanger 3.

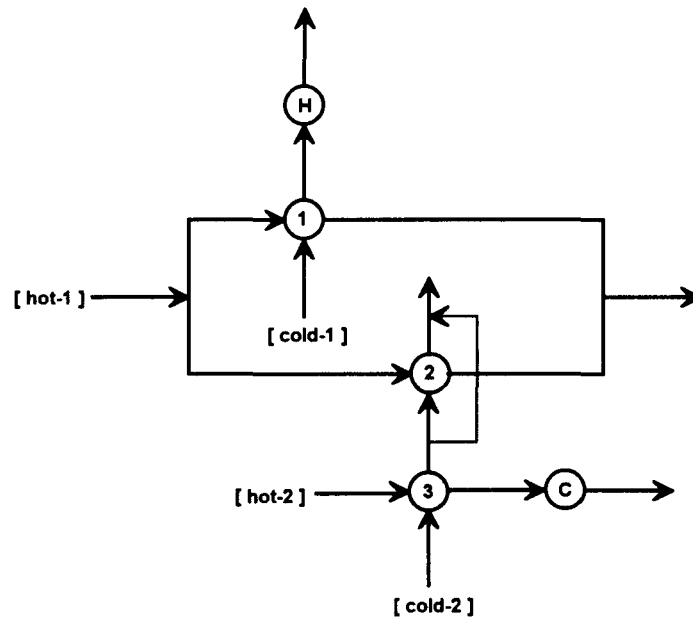


FIGURE 6.30. Example network structure with a cold-side bypass on exchanger 2 (Structure-B1).

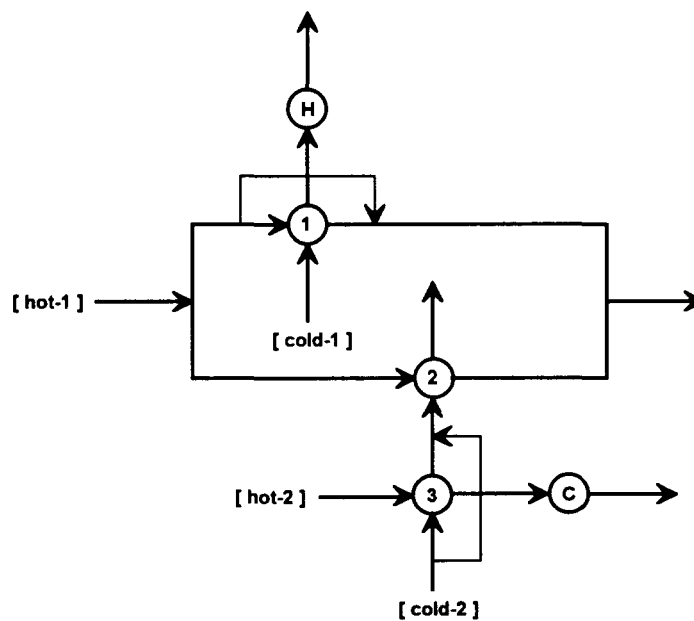


FIGURE 6.31. Example network structure with a hot-side bypass on exchanger 1 and a cold-side bypass on exchanger 3 (Structure-B2).

The economic parameters in the objective function are given in Table 6.5. Initial design (zero-disturbance) values are given in Table 6.6. These values are obtained by considering nominal source temperatures, flowrates and target specifications for the given economic parameters. Hence, the initial design is neither ‘the minimum-total-area design’ nor ‘the minimum-utility-cost design’ of the structure.

TABLE 6.5. Economic parameters used for the evaluation of the example structure.

$C_E, C_H, C_C$	5500 \$
$\alpha$	150 \$/m <sup>2</sup>
$\beta$	1
$\gamma$	0.125
$C_{CU}$	15 \$/kW-year
$C_{HU}$	80 \$/kW-year

TABLE 6.6. Initial design (nominal design) values of the example structure.

$A_1$ (m <sup>2</sup> )	99.1
$A_2$ (m <sup>2</sup> )	12.5
$A_3$ (m <sup>2</sup> )	7.7
$A_H$ (m <sup>2</sup> )	0.3
$A_C$ (m <sup>2</sup> )	2.9
$A_T$ (m <sup>2</sup> )	122.5
Heating (kW)	72.13
Cooling (kW)	194.13

Also, for these cases, like in Case-A, disturbances are considered only in the source stream temperatures, and changes in the design parameters are investigated with respect to resiliency (i.e., RDRI). When the design parameters with respect to RDRI for Case-B1 (Figures 6.32, 6.33, 6.34) are considered, the following features can be seen. i) The area of

exchanger 2 and the areas of utility exchangers increase from zero-resiliency up to maximum-resiliency (MRDRI). ii) The area of exchanger 3 decreases from zero-resiliency up to MRDRI. iii) The area of exchanger 1 increases from zero-resiliency up to 10 K, and then decreases up to MRDRI. The dominant factor on the capital cost is the area of exchanger 1 and thus the trajectory of the total area of the network is similar to exchanger 1. The total area of the network increases from zero-resiliency up to 10 K, and then decreases up to MRDRI. iv) Utility consumptions and, hence, the utility costs increase from zero-resiliency up to MRDRI. That is, the retrofit design done with respect to expected disturbances, with any desired magnitude of RDRI greater than zero, requires more utility at the nominal operating conditions (nominal operating conditions correspond to zero value of RDRI). v) In the RDRI range of 0 - 10 K, the capital and operating costs increase together. After 10 K, when capital cost decreases, operating cost continues to increase. vi) The MRDRI value of this bypassed-structure is (Structure-B1) 14.4 K and the BRDRI value is zero.

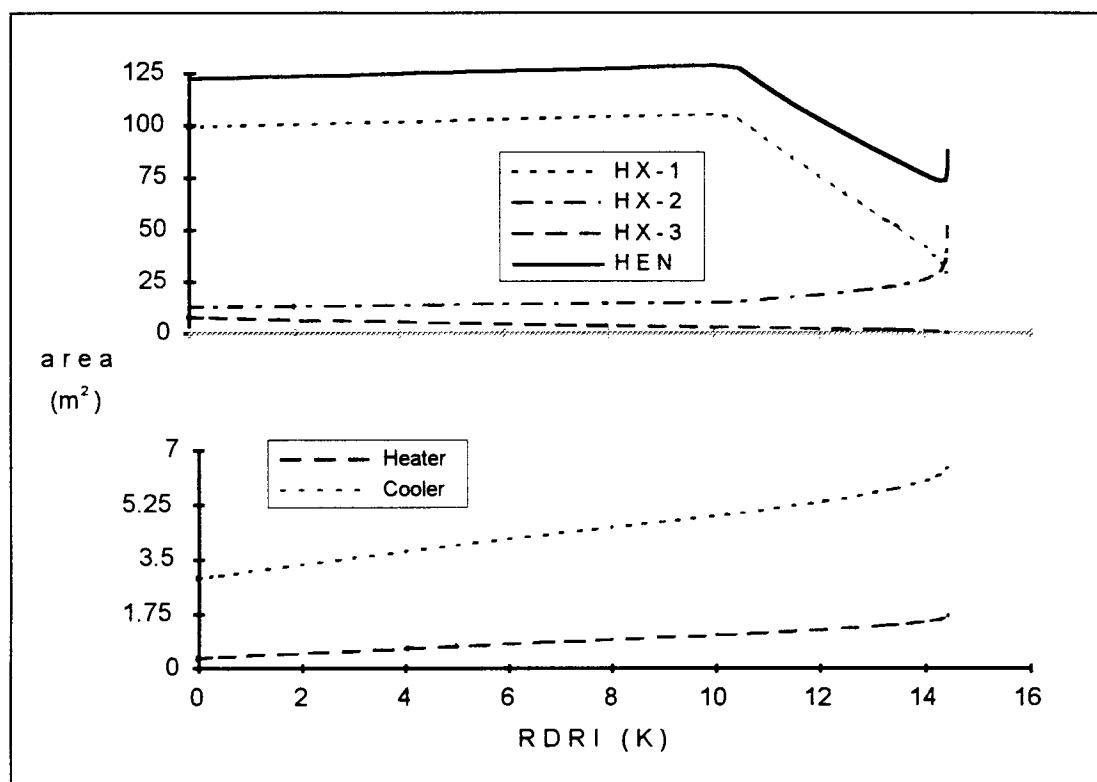


FIGURE 6.32. Changes in areas of heat exchangers and HEN for Case-B1.

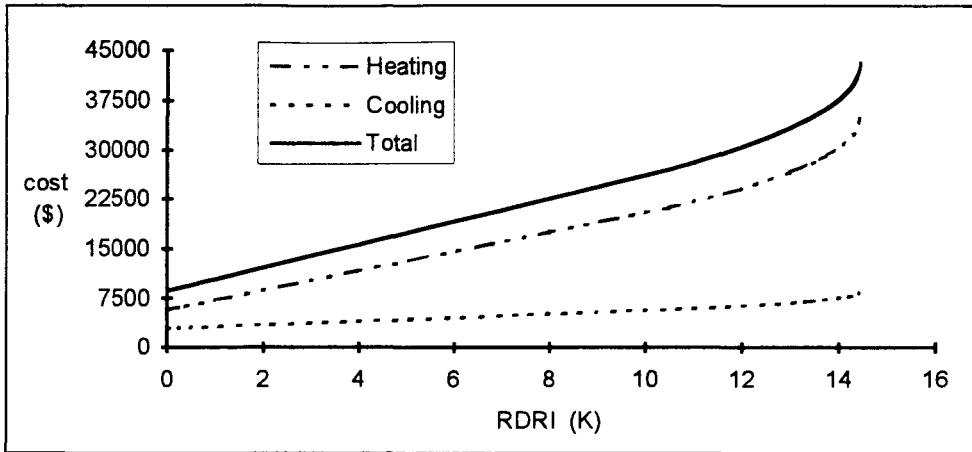


FIGURE 6.33. Changes in utility costs for Case-B1.

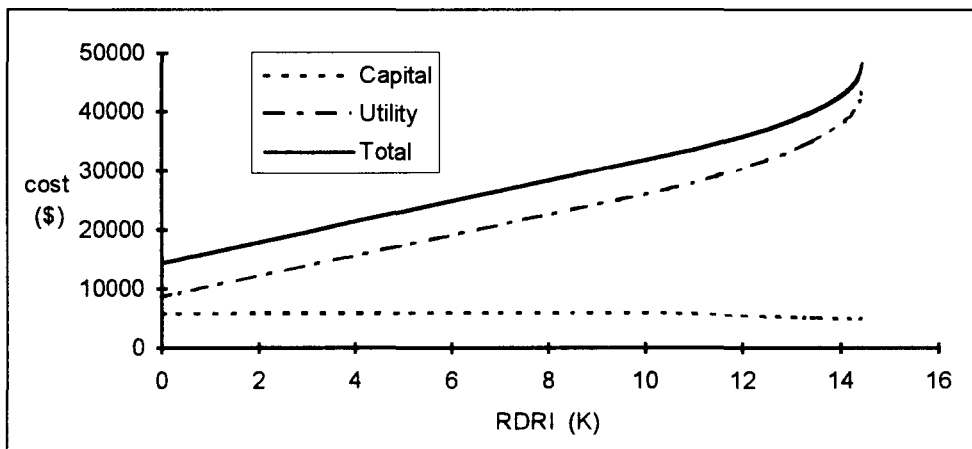


FIGURE 6.34. Changes in costs for Case-B1.

For the second case considered (Case-B2), the following observations can be made (Figures 6.35, 6.36, 6.37). I) The design parameters do not change up to 17.3 K (i.e. BRDRI = 17.3 K). II) Areas of exchangers 1 and 3 continuously decrease beginning from BRDRI up to MRDRI. III) Area of exchanger 2 and the areas of the utility exchangers continuously increase beginning from BRDRI up to MRDRI. IV) Utility consumptions and hence the utility costs increases beginning from BRDRI up to MRDRI. V) The MRDRI value of this bypassed-structure (Structure-B2) is 18.6 K.

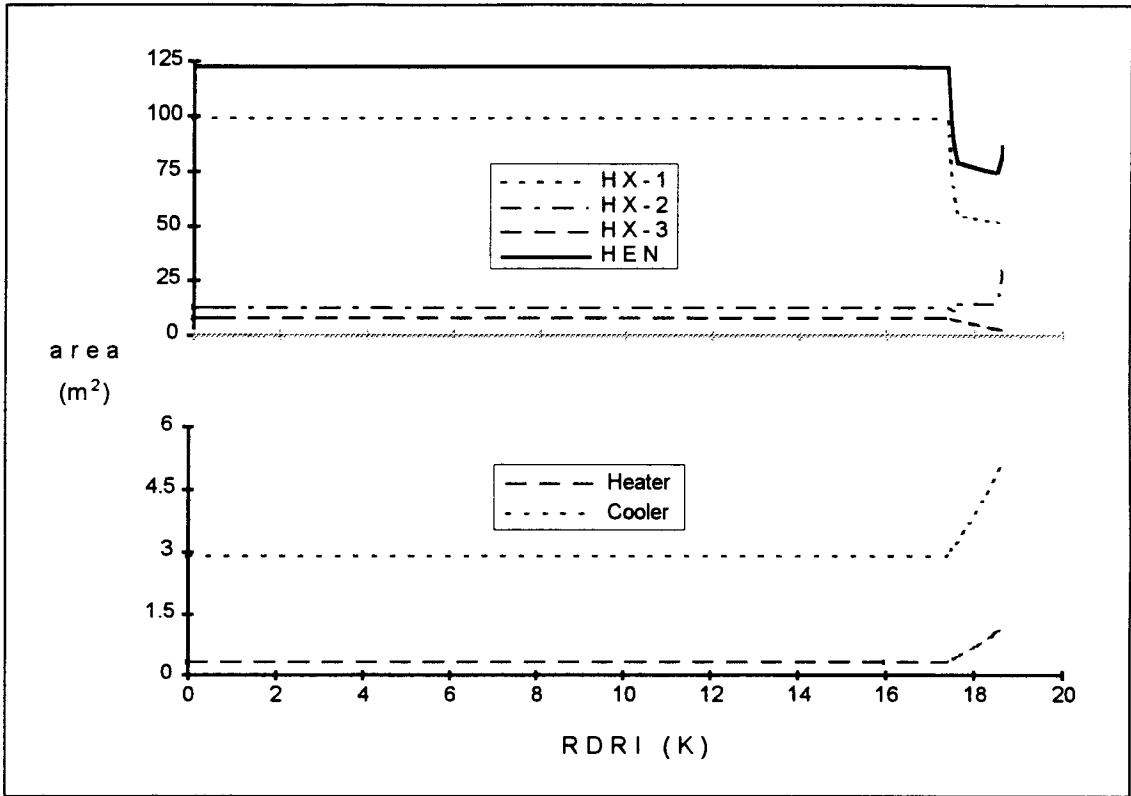


FIGURE 6.35. Changes in areas of heat exchangers and HEN for Case-B2.

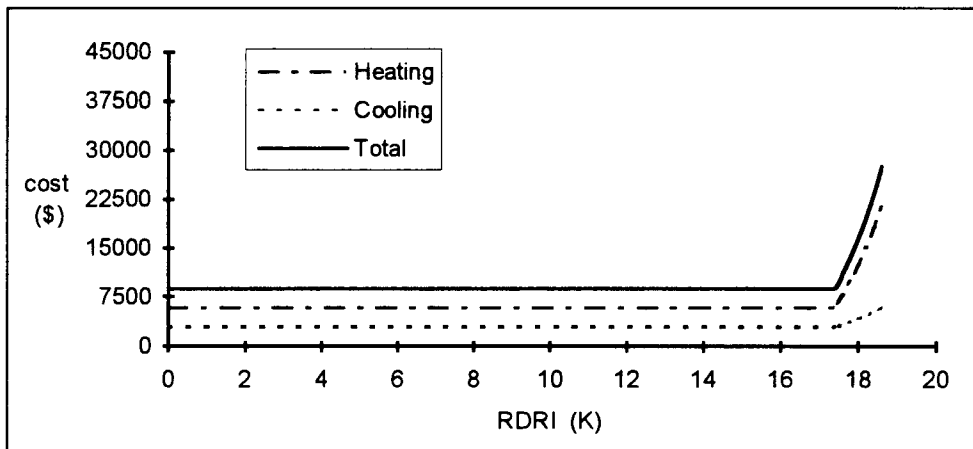


FIGURE 6.36. Changes in utility costs for Case-B2.

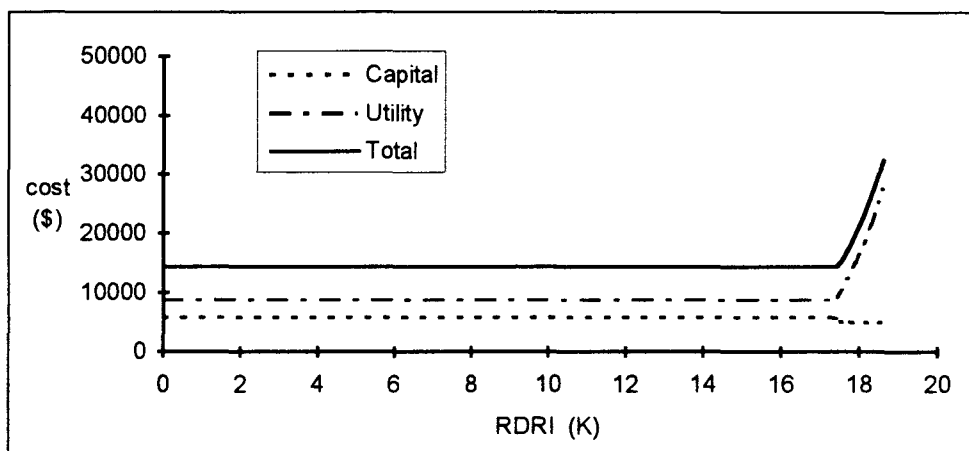


FIGURE 6.37. Changes in costs for Case-B2.

When the analysis of the results of the two bypassed-structures are compared, following conclusions can be made. i) Structure B2 has a BRDRI value, but Structure-B1 has not. That is, Structure-B2 have suitable disturbance propagation paths to direct the disturbances (coming from all possible sources) to the utilities (up to BRDRI). On the other hand, for Structure-B1, there is no way to prevent the effects of the disturbances coming from hot-stream 2 and cold-stream 2 on the target of cold-stream 2 without changing the areas of exchangers. This explicitly means that the nominal bypass fractions are never zero for the resilient design for bypassed-structure 1. ii) The BRDRI value of structure 2 is greater than the MRDRI value of structure 1. This means that by simply inserting two bypasses (hot-side on exchanger 1 and cold-side on exchanger 3) to the original design, the network gains a resiliency value which is greater than the maximum resiliency value which can be obtained by retrofitting the bypassed-structure 1. It should also be indicated that, when such comparison is made, the cost of bypass(es) should also be taken into account. iii) In both cases, resilient design has caused an increase in areas of some exchangers and a decrease in others. This shows the complex nonlinear relationship between the areas of exchangers.

The effect of taking into account the areas of utility exchangers is considerably small on the overall cost. Same bypassed-cases have also been evaluated when the capital-cost term of the utility exchangers in the general objective function is not considered. For this consideration, the initial design parameters are as given in Table 6.7. Results are presented in Figures 6.38 - 6.43 and are very close to the previous ones.

TABLE 6.7. Initial design (zero-resiliency) values for the example structure without considering areas of utility exchangers.

$A_1$ (m <sup>2</sup> )	99.0
$A_2$ (m <sup>2</sup> )	12.5
$A_3$ (m <sup>2</sup> )	7.7
$A_T$ (m <sup>2</sup> )	119.2
Heating (kW)	72.14
Cooling (kW)	194.15

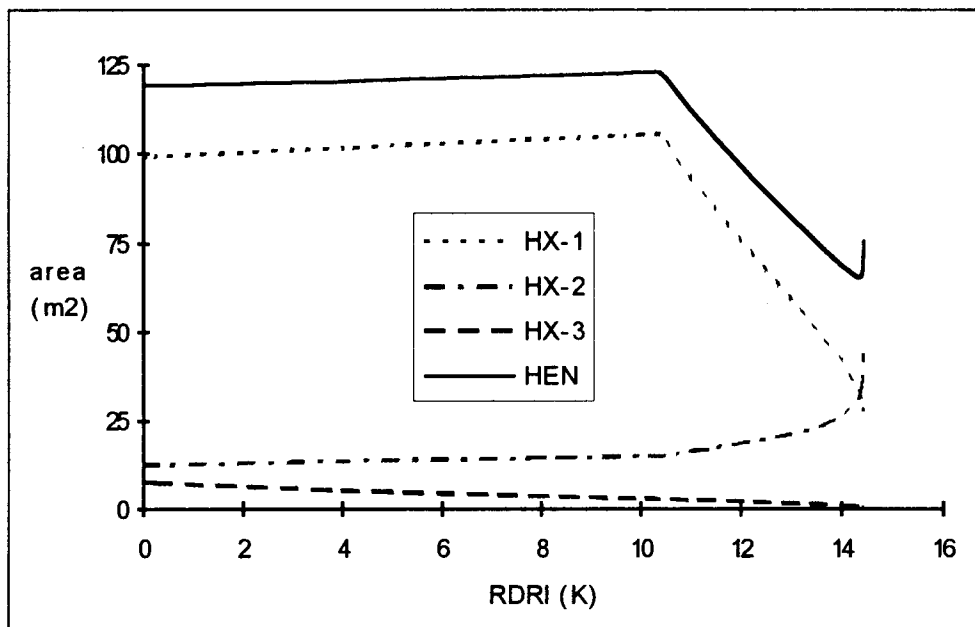


FIGURE 6.38. Changes in the areas of heat exchangers and HEN without considering the areas of utility exchangers for Case-B1.

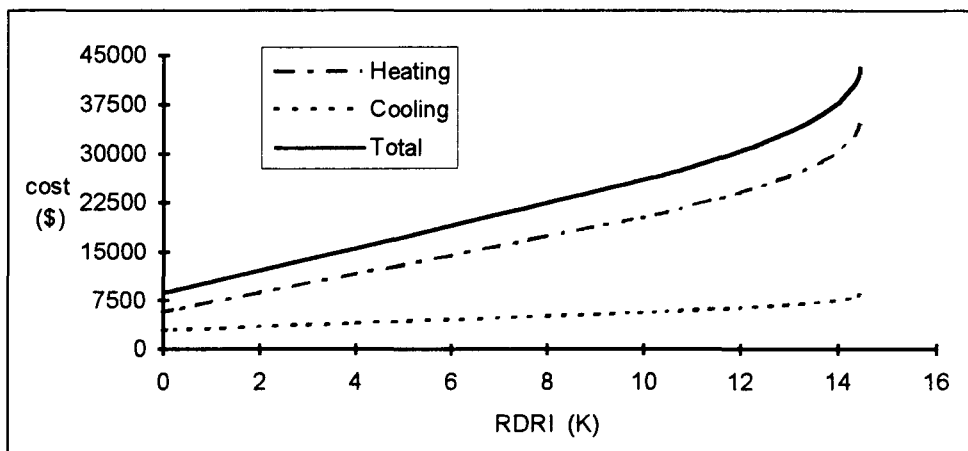


FIGURE 6.39. Changes in utilities without considering the areas of utility exchangers for Case-B1.

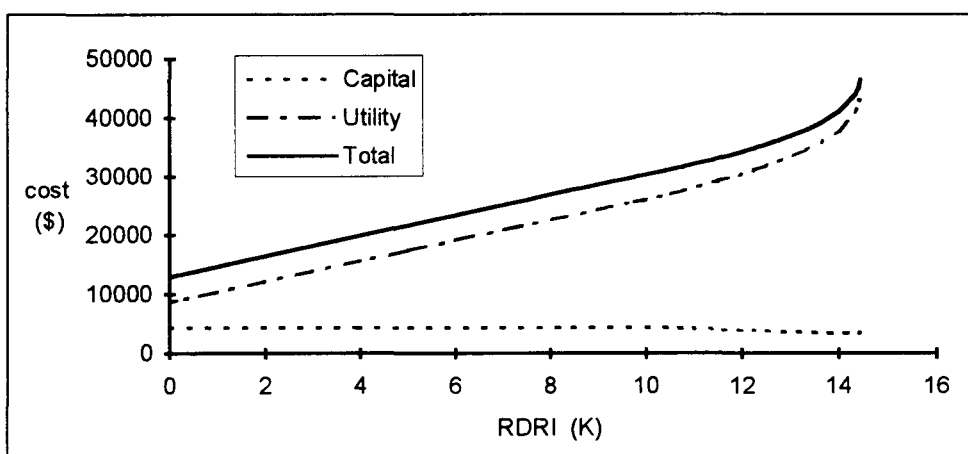


FIGURE 6.40. Changes in costs without considering the areas of utility exchangers for Case-B1.

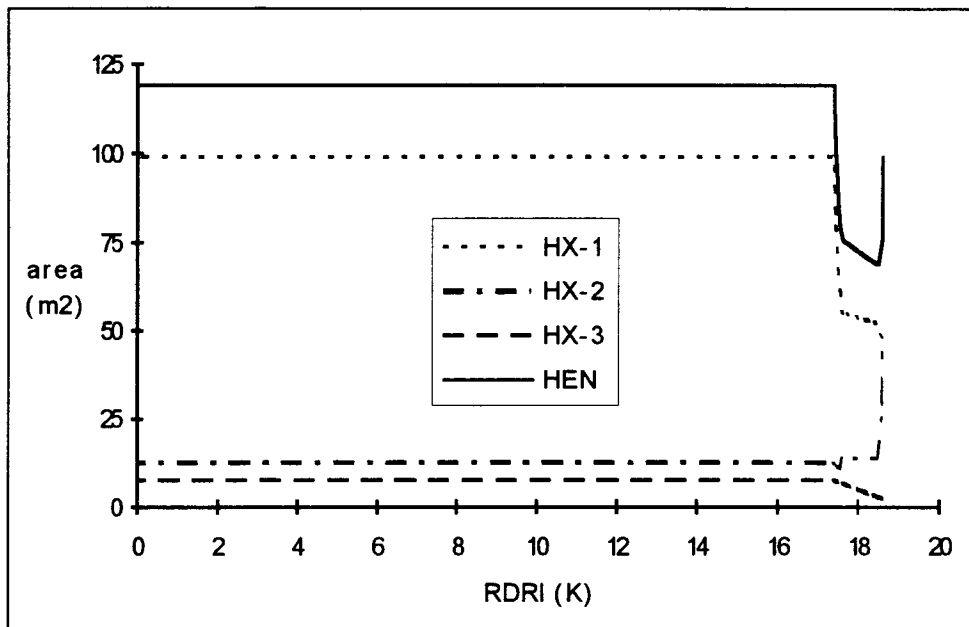


FIGURE 6.41. Changes in the areas of heat exchangers and HEN without considering areas of utility exchangers for Case-B2.

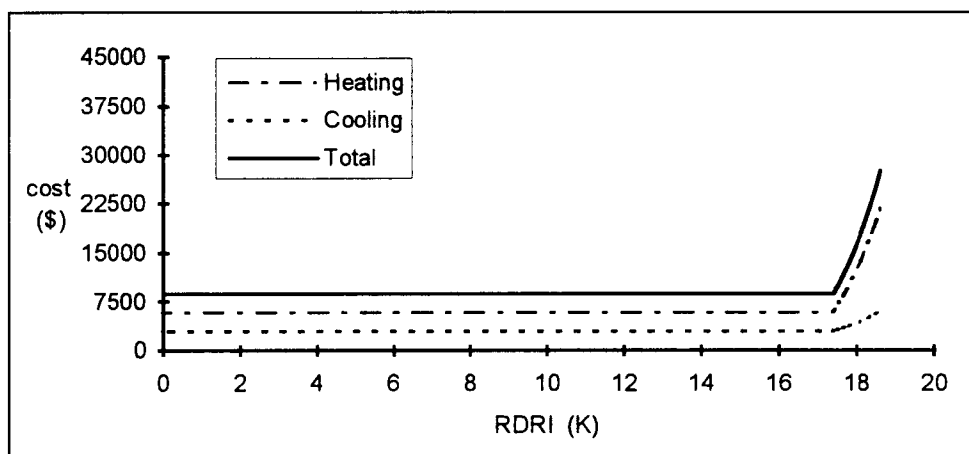


FIGURE 6.42. Changes in utilities without considering the areas of utility exchangers for Case-B2.

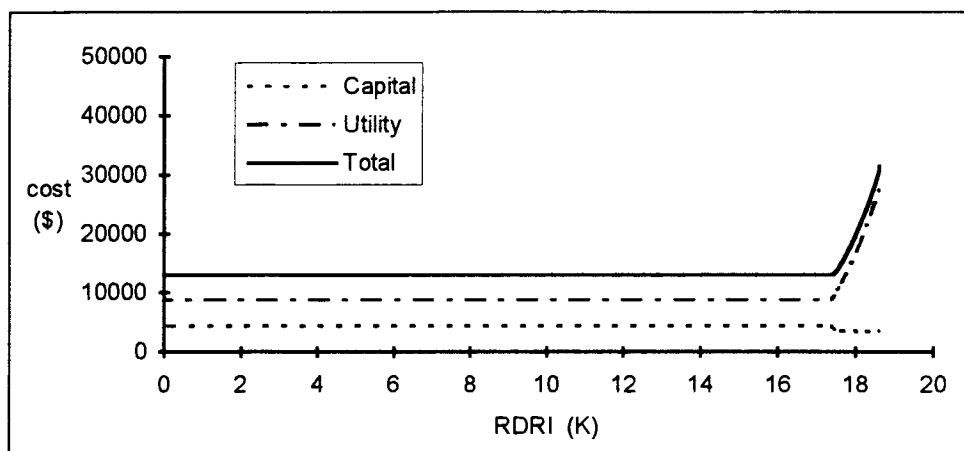


FIGURE 6.43. Changes in costs without considering the areas of utility exchangers for Case-B2.

### 6.3. Comparison of the Conventional Approaches for Controllable Design of HENs with the RDRI-Based Optimal Resilient Retrofit Design

Up to now, some authors who have studied the control of HENs proposed two approaches to gain resiliency when locating control variables (bypasses) for a specified HEN structure. The first approach is to consider the presence of the bypasses after the original design or to consider the bypasses in the synthesis step without taking into account the area changes in the design stage. The second approach is to place bypasses with a heuristic value (e.g., a nominal 10 per cent opening) in the design stage. Herein, the results of the optimal-resilient-retrofit-design approach proposed in this study are compared with the results of the conventional ones.

For demonstration, the bypassed-structure B2 of the previous section (Case-B2 of Section 6.2, Figure 6.31), is used. The economic parameters used in the objective function

are the same as in Case-B2 (as given in Table 6.5). In Table 6.8, parameters for the zero-nominal-bypass fractions design and the design for 10 per cent nominal bypass fractions for the set of economic parameters given in Table 6.5, are tabulated. It should be noted that the design for the zero nominal bypass fractions given in Table 6.8 is identical to the initial (nominal) design given in Table 6.6. Recalling that this design has a 17.3 K BRDRI value, it is feasible in the RDRI range of 0 - 17.3 (i.e., DRI value of this design is 17.3 K). Using a heuristic 10 per cent value for the bypass fractions results in a 21 per cent increase in total exchanger areas, 3 per cent increase in total utility cost and 5 per cent increase in total annualized cost, although the DRI value of this design (second column of Table 6.8) is still 17.3 K. Also, although the cost of the optimal retrofit design with a desired RDRI value of 17.5 K (third column of Table 6.8), is slightly cheaper than the cost of design based on 10 per cent nominal bypass fractions, it has a slightly greater resiliency. If the design for the zero-nominal-bypass-fraction is compared with the optimal retrofit design with a desired RDRI value of 17.5 K (first and third columns of Table 6.8), the design for the zero-nominal-bypass-fractions has only a 17.3 K DRI resiliency value. Furthermore, with the optimal-retrofit-design approach, it is possible to obtain a 18.6 K resiliency (MRDRI) with that structure for the proposed configuration of bypasses.

TABLE 6.8. Design parameters obtained by different design criterion.

	<b>design for zero nominal bypass fractions</b>	<b>design for 10 per cent nominal bypass fractions</b>	<b>optimal resilient retrofit design for RDRI = 17.5 K</b>
$A_1$ (m <sup>2</sup> )	99.13	121.59	68.15
$A_2$ (m <sup>2</sup> )	12.49	14.80	11.43
$A_3$ (m <sup>2</sup> )	7.66	8.03	7.19
$A_H$ (m <sup>2</sup> )	0.33	0.34	0.39
$A_C$ (m <sup>2</sup> )	2.90	2.93	3.06
$A_T$ (m <sup>2</sup> )	<b>122.51</b>	<b>147.68</b>	<b>90.21</b>
<b>Capital Cost (\$)</b>	<b>5,735</b>	<b>6,207</b>	<b>5,129</b>
Heating Utility Cost (\$)	5,770	5,986	6,802
Cooling Utility Cost (\$)	2,912	2,952	3,105
<b>Total Utility Cost (\$)</b>	<b>8,682</b>	<b>8,938</b>	<b>9,907</b>
<b>TAC (\$)</b>	<b>14,417</b>	<b>15,145</b>	<b>15,036</b>
<b>DRI (K)</b>	<b>17.3</b>	<b>17.3</b>	<b>17.5</b>

#### 6.4. Heat-Capacity-Flowrate-Based RDRI

In the previous sections, RDRI values were evaluated on the basis of the source-stream temperatures. Here, an example network structure (adopted from Grossmann and Morari (1983), and Colberg and Morari (1988)) shown in Figure 6.44 is evaluated for the RDRI values based on the heat-capacity-flowrate (HCF). Maximum disturbance magnitudes for the *structure*, considering the source of disturbance in the heat-capacity-

flowrate, are tabulated in Table 6.9. Heat-capacity-flowrate-based flexibility index of the structure is 2.3 kW/K and the network is limited in disturbance directions (+ + -) and (+ - -).

Optimal resilient retrofit of the example structure is investigated in the RDRI range of 0 - 2.3 kW/K, when both of the exchangers have double bypasses (on hot and cold sides). The objective of the retrofit is thought as the minimization of the total annualized cost without considering the effect of the heater area. The economic parameters used in the objective function and the initial design values are as given in Table 6.10. The increase in the areas of the HEN, relative to those of the initial design as a function of RDRI are given in Figure 6.45. The operating cost of this structure does not change up to MRDRI value. It can be said that evaluating the network for temperature-based RDRI together with heat-capacity based RDRI in optimal design may give more robust retrofit designs. This example will be reevaluated in the Section 7.3 based on the temperature disturbances in source-streams as well.

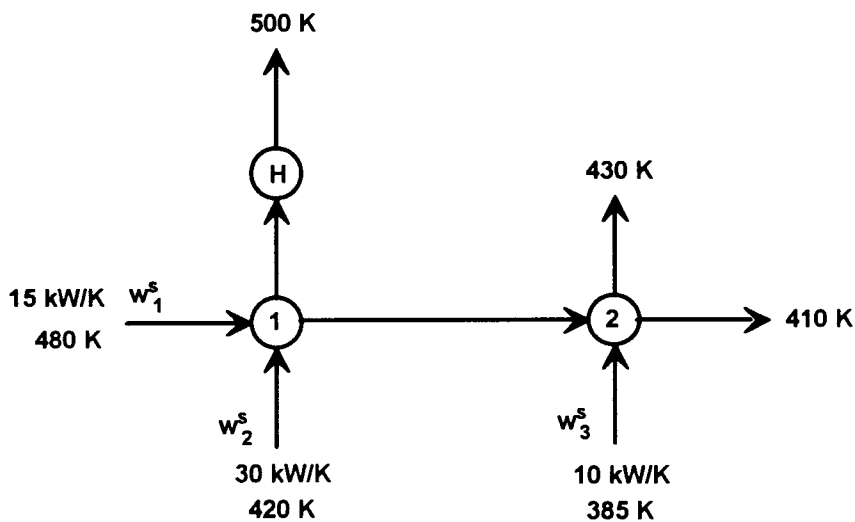


FIGURE 6.44. Example structure used for the HCF-based retrofit evaluation.

TABLE 6.9. Maximum disturbance magnitudes for each disturbance direction based on HCF.

$w_1^s$	$w_2^s$	$w_3^s$	Maximum Disturbance Magnitude	Active Constraints
+	+	+	unbounded	
+	+	-	<b>2.308</b>	HX-2 $\Delta T_{\min}$
+	-	+	14.118	HX-1 $\Delta T_{\min}$
+	-	-	<b>2.308</b>	HX-2 $\Delta T_{\min}$
-	+	+	5.217	HX-1 load
-	+	-	6.000	HX-2 $\Delta T_{\min}$
-	-	+	5.217	HX-1 load
-	-	-	6.000	HX-2 $\Delta T_{\min}$

TABLE 6.10. Economic parameters and initial (nominal) design costs.

$\alpha$	150 \$/m <sup>2</sup>	$A_1$ (m <sup>2</sup> )	25.99
$\beta$	1	$A_2$ (m <sup>2</sup> )	34.36
$\gamma$	0.25	Annualized Capital Cost (\$)	5013
$C_{HU}$	80 \$/kW-year	Operating Cost (\$)	144000
$C_E$	5500 \$	Total Annualized Cost (\$)	149013

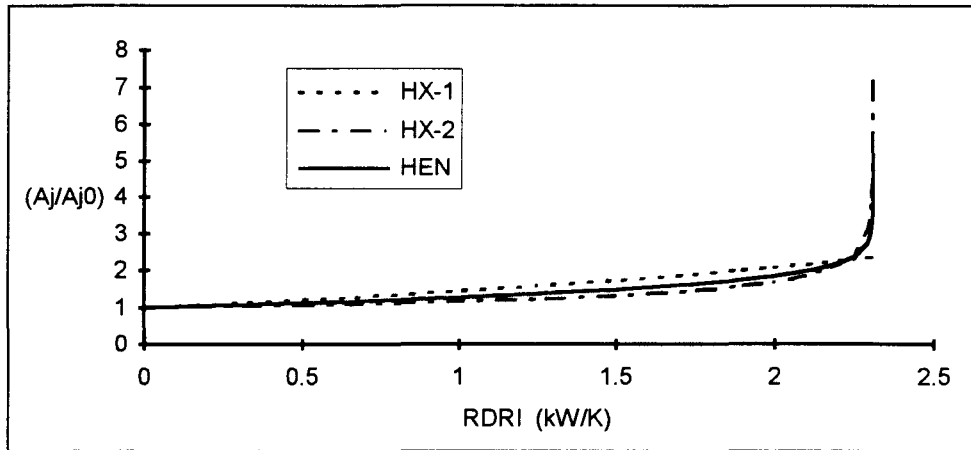


FIGURE 6.45. Increases in the areas of heat exchangers and HEN for the example structure.

## **7. EFFECT OF SOME CONTROL VARIABLES AND DESIGN PARAMETERS ON OPTIMAL RESILIENT RETROFIT DESIGN**

In this chapter, the effects of the splits, the target specifications and the capital-recovery factor on the resilient retrofit design are investigated.

### **7.1. The Effect of Split-Fraction on the Retrofit Design**

Herein, the effect of not considering the split fraction as a manipulated variable on the retrofit design is demonstrated on the splitted-structure example used in Chapter 6 (Figure 6.1). The relationship between the flexibility index and the split fraction for the example structure is as shown in Figure 7.1. It may be expected to get higher resiliencies when a fixed split fraction in the range of (0.55 - 0.66) is selected.

In the examples presented in this section, the objective function is taken as the minimization of the total annualized cost excluding investment costs of utilities, and the economic parameters used for the retrofit evaluation are the same as used in Case-B in Section 6.2 (Table 6.5). All examples are evaluated for one bypass configuration as shown in Figure 7.2 (i.e., hot-side bypass for exchanger 1 together with cold-side bypass for exchanger 3). In Figure 7.3, zero-resiliency design ( $RDRI = DRI = 0$  K) costs as a function of the split fraction are shown. In Figures 7.4 - 7.8, changes in the areas of the exchangers and costs with respect to RDRI are shown for different constant split-fraction values. In Table 7.1, MRDRI values for different split fractions and in Table 7.2, the costs of the optimal resilient designs for different fixed-split-fractions and for different RDRI values are given. The results presented show how the selection of the split-fraction value affects the

resiliency and economy of the network. For this particular example, if the possible maximum resiliency is desired, 0.661 appears to be the best value of split-fraction for providing greatest resiliency at the lowest cost.

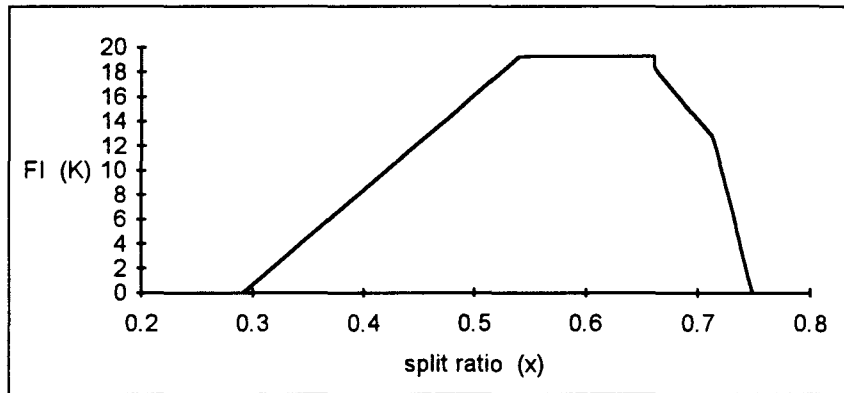


FIGURE 7.1. The relationship between the split-ratio and the flexibility index for the example structure.

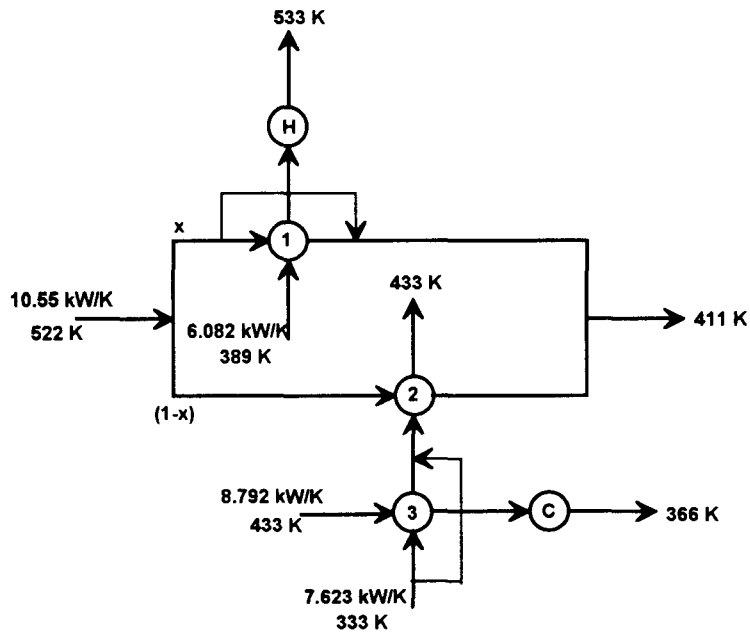


FIGURE 7.2. Example bypassed-structure studied to demonstrate the effect of selecting fixed split ratios ( $x$ ) on the optimal resilient design.

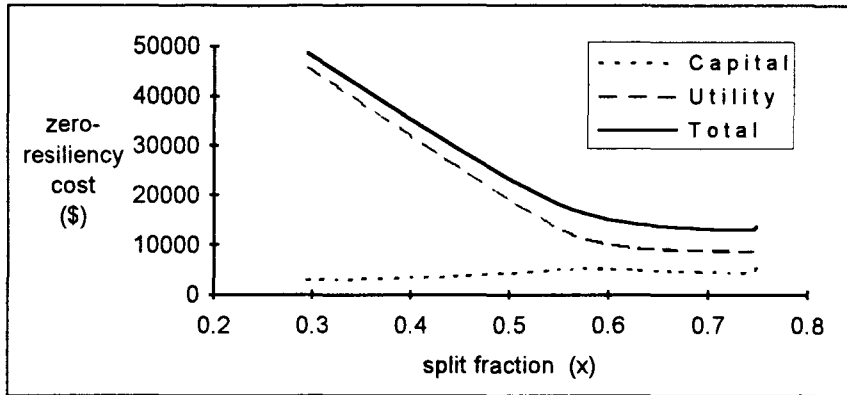


FIGURE 7.3. Zero-resiliency design costs with respect to split fraction for the example bypassed-structure (shown in Figure 7.2).

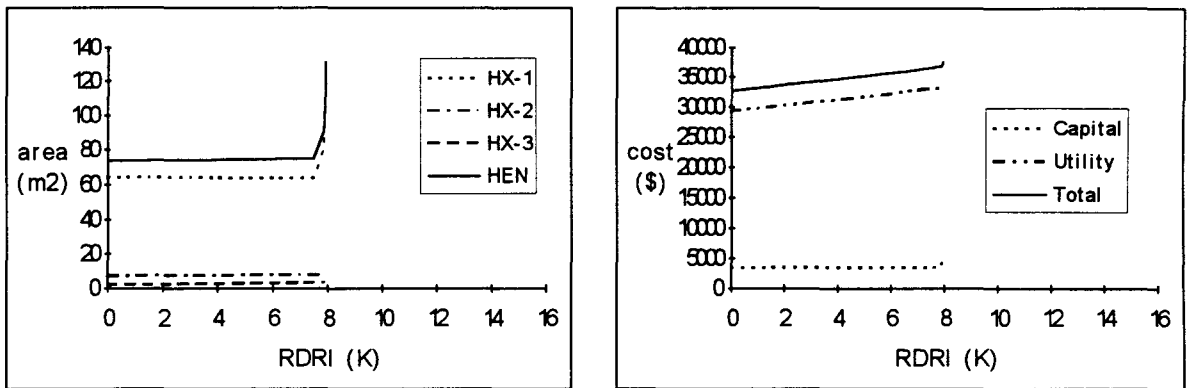


FIGURE 7.4. Design parameters with respect to resiliency for fixed split fraction 0.42.

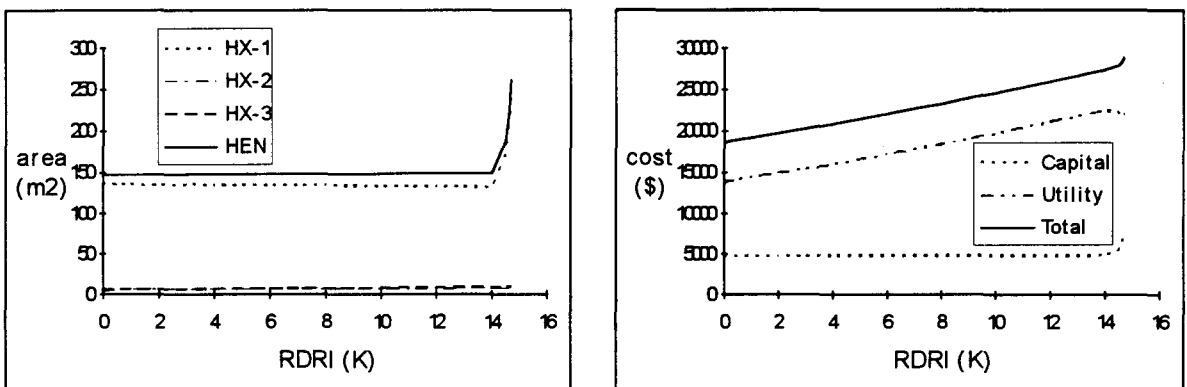


FIGURE 7.5. Design parameters with respect to resiliency for fixed split fraction 0.545.

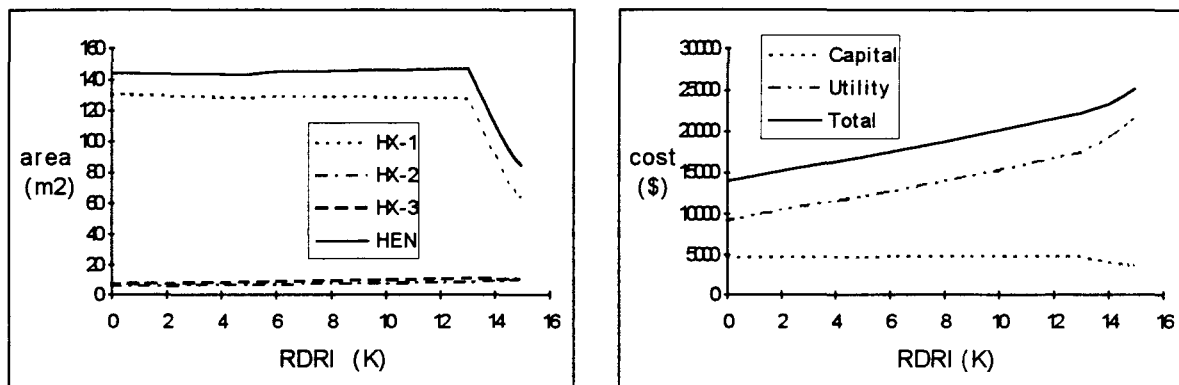


FIGURE 7.6. Design parameters with respect to resiliency for fixed split fraction 0.639.

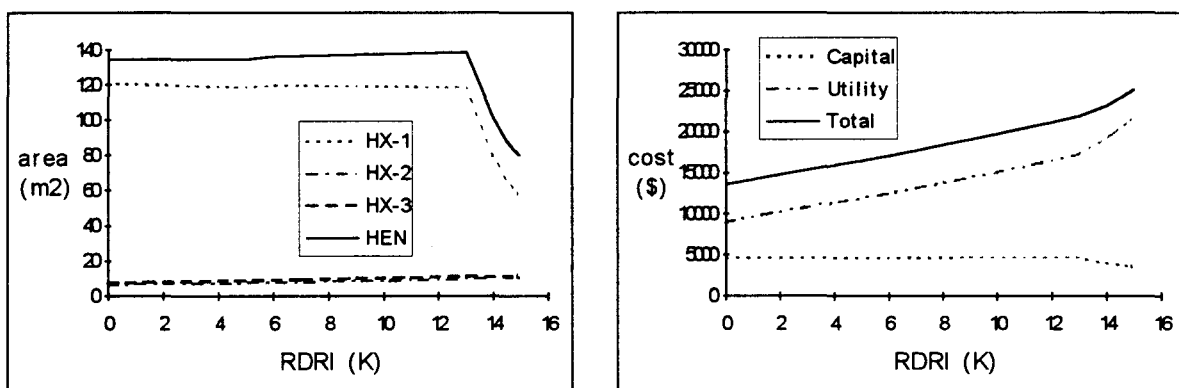


FIGURE 7.7. Design parameters with respect to resiliency for fixed split fraction 0.661.

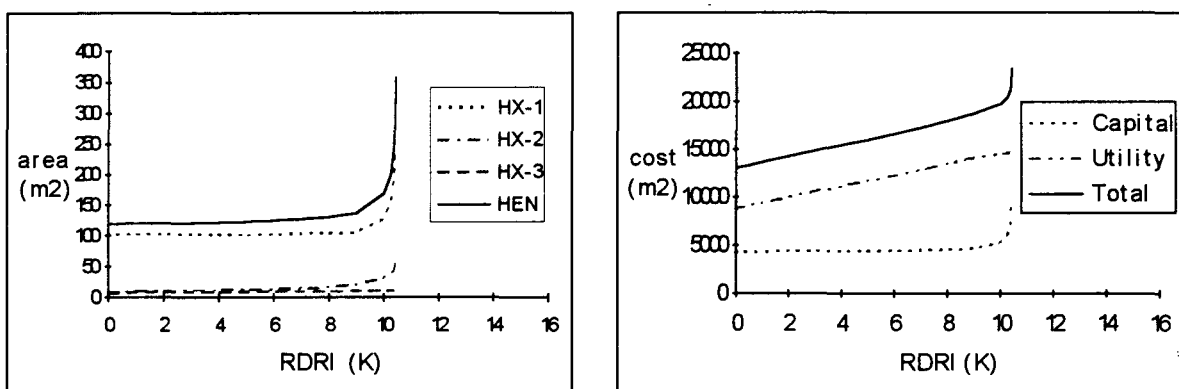


FIGURE 7.8. Design parameters with respect to resiliency for fixed split fraction 0.72.

TABLE 7.1. Different fixed-split-fraction values vs. MRDRI.

split fraction	MRDRI (K)
0.300	0.0
0.420	7.9
0.545	14.7
0.639	15.0
0.661	15.0
0.720	10.4
0.750	0.0

TABLE 7.2. Total annualized cost (\$) of the designs for different fixed-split-fraction values and for different RDRI values.

		x				
		0.420	0.545	0.639	0.661	0.720
R	0 K	32,795	18,689	13,989	13,605	13,037
D	5 K	35,252	21,465	16,884	16,515	16,007
R	10 K	infeasible	24,594	20,109	19,743	19,728
I	15 K	infeasible	infeasible	25,237	25,155	infeasible

## 7.2. The Effect of Split-Mixing-Point Temperature on the Retrofit Design

In the previous cases of the example structure, the temperatures of the split branches were kept free, implicitly assuming that the mixing would be ideal. Here, however, considering possible significant differences in temperatures of the split branches, which

may reduce the performance of control action in operation, the effect of split-remix temperature on the resilient design is investigated for the same splitted-structure example (Figure 7.9). The difference in temperature of split branches is limited to three different values and the results are presented. Like in Case-A in Chapter 6, objective function is taken as the minimization of total area of heat exchangers, ( $\min (A_1+A_2+A_3)$ ), and the MER conditions are desired for the nominal operating conditions (i.e., inlet temperatures of utilities are considered as hard targets at zero-disturbance direction). Including such a constraint which limits the temperature differences in split branches in the split-remix points in design not only increases the cost but also limits the MRDRI value (Figures 7.10, 7.11, 7.12, 7.13). On the other hand, consideration of lower values of  $\Delta T_{mx}$  may increase the controllability of the network. It can be stipulated also that the trade-off between the controllability and controllable/resilient design should be carefully investigated for networks containing stream splits.

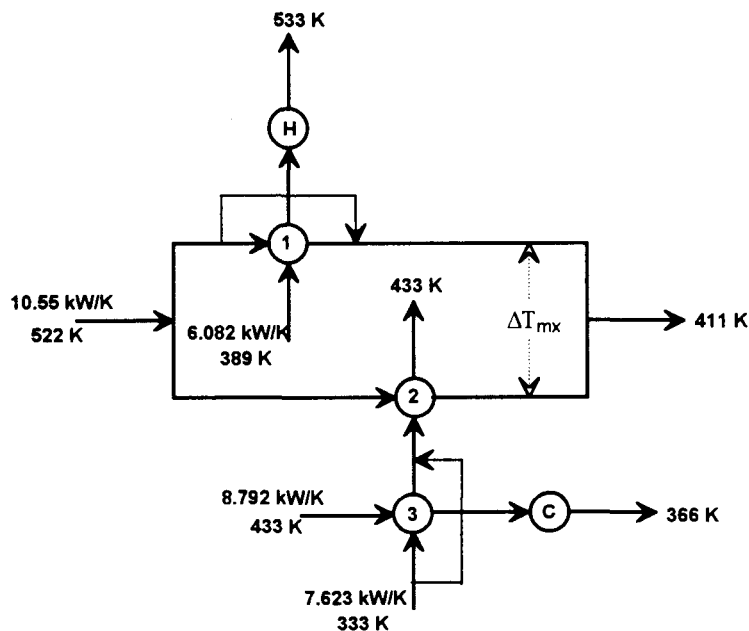


FIGURE 7.9. Example bypassed-structure studied to demonstrate the effect of temperature difference in the split branches on the resilient design.

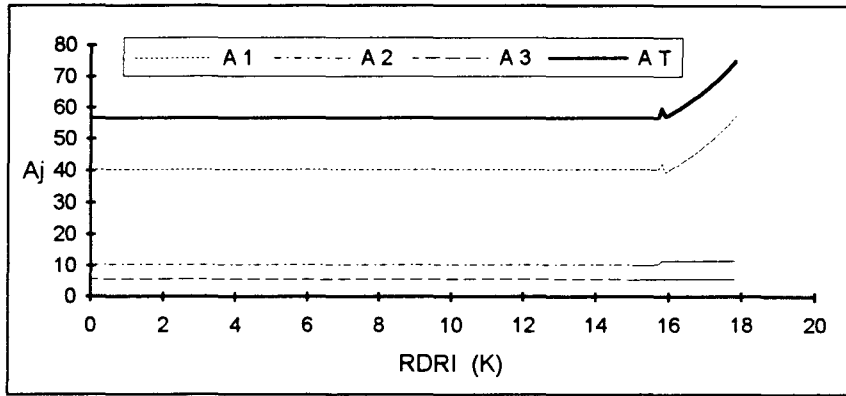


FIGURE 7.10. Increases in the areas of heat exchangers and HEN for unconstrained  $\Delta T_{\text{mx}}$  (Case-A20).

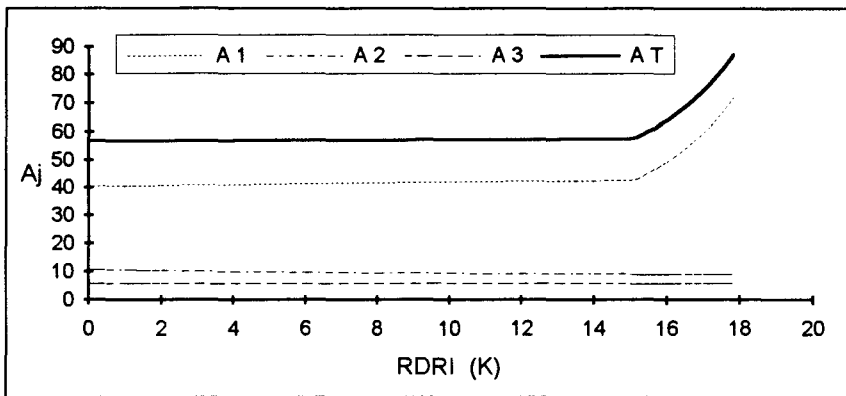


FIGURE 7.11. Increases in the areas of exchangers and HEN for  $\max \Delta T_{\text{mx}} = 30 \text{ K}$ .

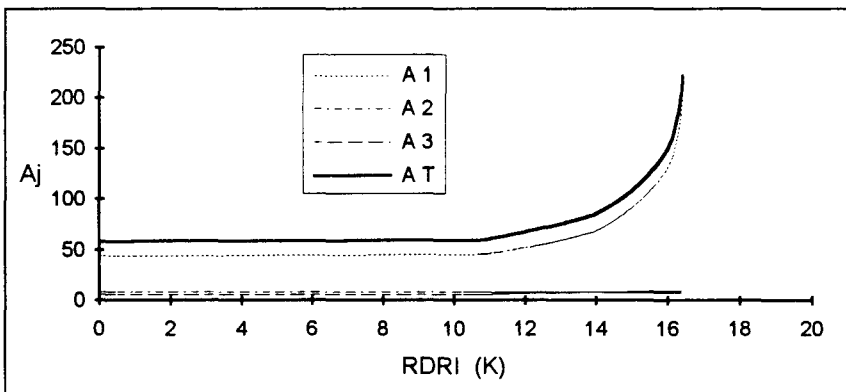


FIGURE 7.12. Increases in the areas of exchangers and HEN for  $\max \Delta T_{\text{mx}} = 15 \text{ K}$ .

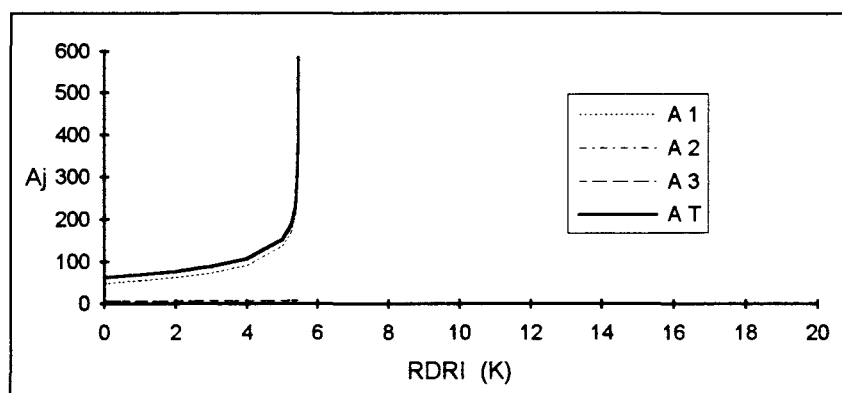


FIGURE 7.13. Increases in the areas of exchangers and HEN for  $\max \Delta T_{\text{mx}} = 0$  K.

### 7.3. The Effect of Target Specifications on the Retrofit Design

In this section, an example network structure which was also used in Section 6.4, as adopted from Grossmann and Morari (1983), and Colberg and Morari (1988) and shown in Figure 7.14, is investigated to show the effect of target specifications on the resilient design with the proposed formulation. The network has two exchangers and a heater. The target of cold-stream 1 can be adjusted by heater. The overall heat-transfer coefficients are taken as  $0.8 \text{ kW/m}^2\text{K}$  for all exchangers. This structure is evaluated for two cases. In Case-C targets are considered as hard targets, and in Case-D two targets are taken as soft (target of hot stream,  $T_{h,1} \leq 410$ , and target of cold-stream 2,  $T_{c,2} \geq 430$ ). For each case, structural flexibility of the network and the active constraints for each disturbance direction, are tabulated in Table 7.3 and Table 7.4. Temperature-based feasibility spaces for each case are shown in Figure 7.15 and Figure 7.16. Both of the structures are limited in source-stream directions  $+++$  and  $-++$ , corresponding to the minimum of the maximum disturbance magnitudes. The temperature-based flexibility indexes are 12 K for Case-C and 13.3 K for Case-D.

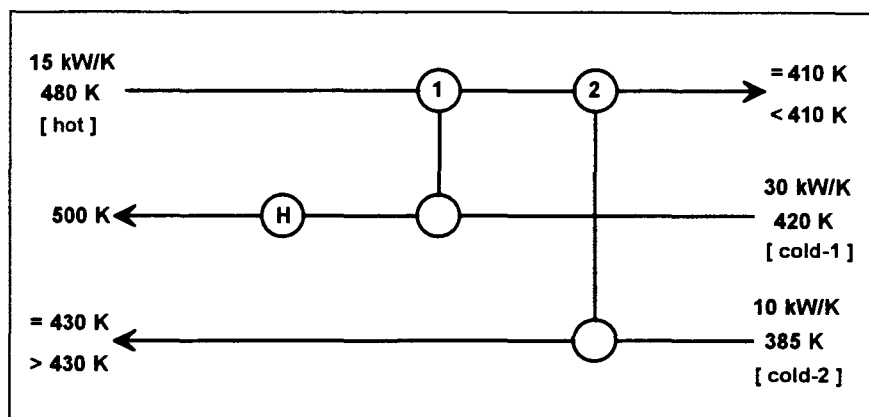


FIGURE 7.14. Example network with soft and hard target-temperature constraints.

TABLE 7.3. Maximum disturbance magnitudes for each disturbance direction for Case-C (hard targets).

$T_1^s$	$T_2^s$	$T_3^s$	maximum disturbance magnitude (K)	Active Constraints
+	+	+	12.0	HX-1 $\Delta T_{\min}$
+	+	-	51.4	heater-load, $T_{c,1} = 500\text{K}$
+	-	+	15.0	HX-2 $\Delta T_{\min}$
+	-	-	unbounded	
-	+	+	12.0	HX-1 $\Delta T_{\min}$
-	+	-	24.0	HX-1 load
-	-	+	15.0	HX-2 $\Delta T_{\min}$
-	-	-	24.0	HX-1 $\Delta T_{\min}$

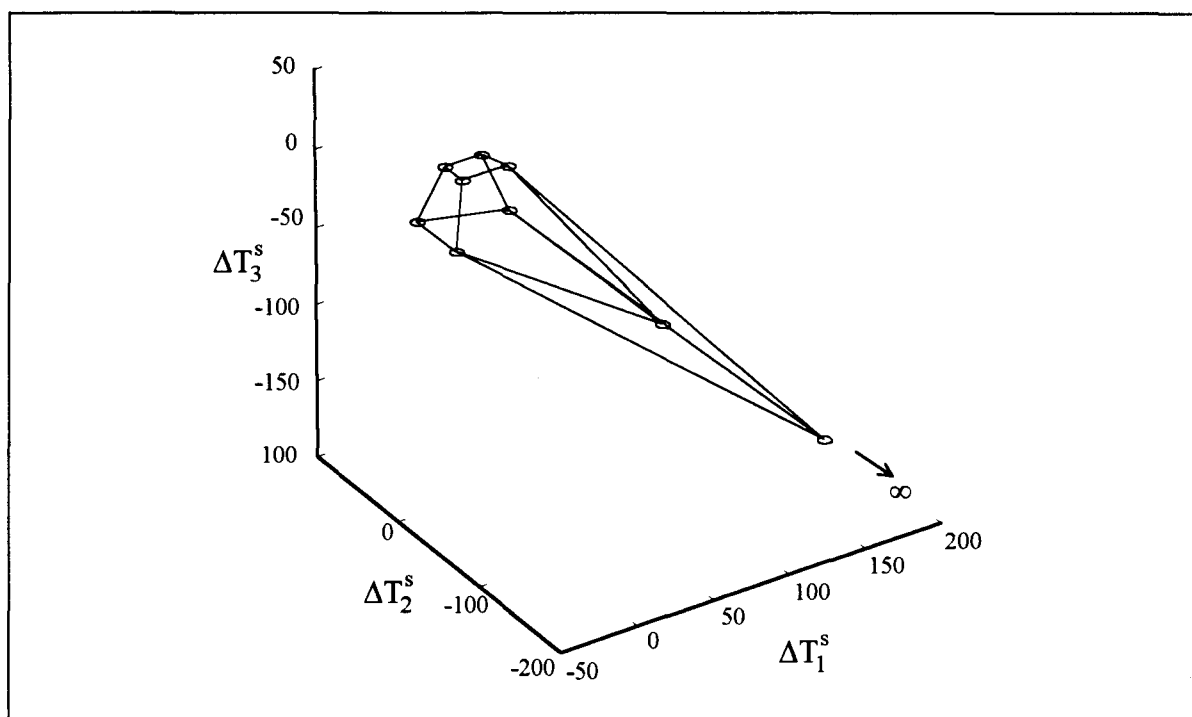


FIGURE 7.15. Temperature-based feasibility region of the example structure for Case-C.

TABLE 7.4. Maximum disturbance magnitudes for each disturbance direction for Case D (soft targets).

$T_1^s$	$T_2^s$	$T_3^s$	maximum disturbance magnitude (K)	Active Constraints		
+	+	+	13.3	HX-1 $\Delta T_{\min}$	HX-2 $\Delta T_{\min}$	$T_{h,1}^T=410$
+	+	-	80.0	HX-1 load		
+	-	+	15.0	HX-2 $\Delta T_{\min}$	$T_{h,1}^T=410$	$T_{c,2}^T=430$
+	-	-	unbounded			
-	+	+	13.3	HX-1 $\Delta T_{\min}$	HX-2 $\Delta T_{\min}$	$T_{h,1}^T=410$
-	+	-	30.0	HX-1 $\Delta T_{\min}$	HX-1 load	
-	-	+	15.0	HX-2 $\Delta T_{\min}$	$T_{h,1}^T=410$	$T_{c,2}^T=430$
-	-	-	50.0	HX-2 $\Delta T_{\min}$	HX-1 load	$T_{c,2}^T=430$

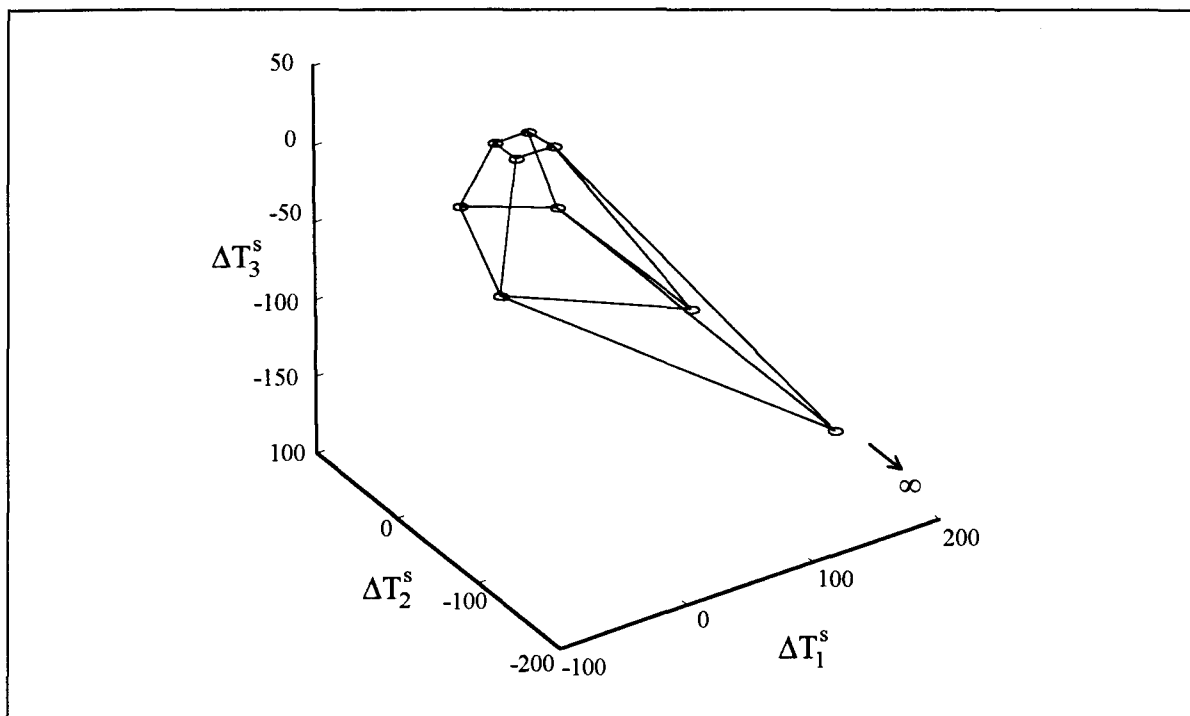


FIGURE 7.16. Temperature-based feasibility region of the example structure for Case-D.

### 7.3.1. Case-Study for Hard Targets, (Case-C)

Herein, the example problem (Figure 7.14) is analyzed for the possible bypass configurations when all the targets are hard. The economic parameters used in evaluating the example and costs of nominal (zero-resiliency) design are given in Table 7.5. In Figures 7.17 - 7.25, the increase in the areas of the exchangers and the total area of the HEN, relative to those of the initial designs, and the increase in the annualized capital cost as a function of RDRI for different bypass configurations are shown. Operating cost does not change throughout the RDRI range studied in these bypass configurations.

TABLE 7.5. Economic parameters and zero-resiliency-design costs.

$\alpha$	150 \$/m <sup>2</sup>	$A_1$ (m <sup>2</sup> )	25.99
$\beta$	1	$A_2$ (m <sup>2</sup> )	34.36
$\gamma$	0.25	Annualized Capital Cost (\$)	5,013
$C_{HU}$	80 \$/kW-year	Operating Cost (\$)	144,000
$C_E$	5,500 \$	Total Annualized Cost (\$)	149,013

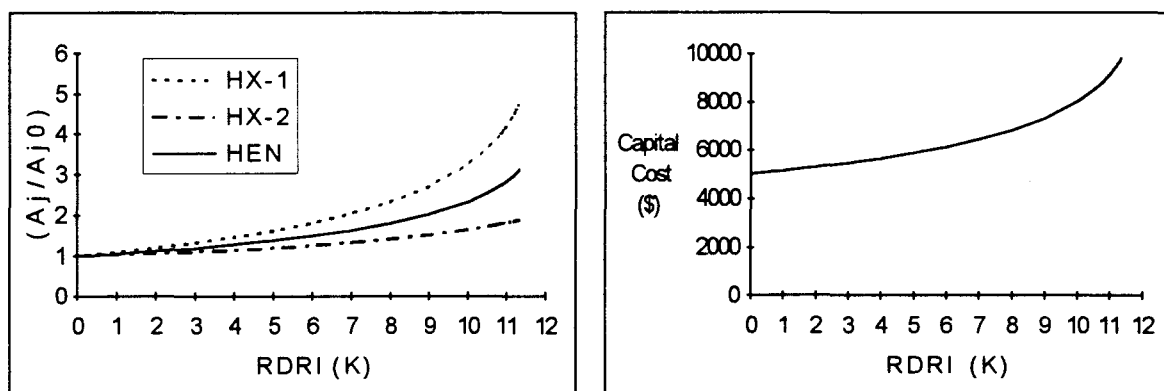


FIGURE 7.17 Changes in the areas and capital cost for the example network structure with a hot-side bypass on HX-1 and a hot-side bypass on HX-2.

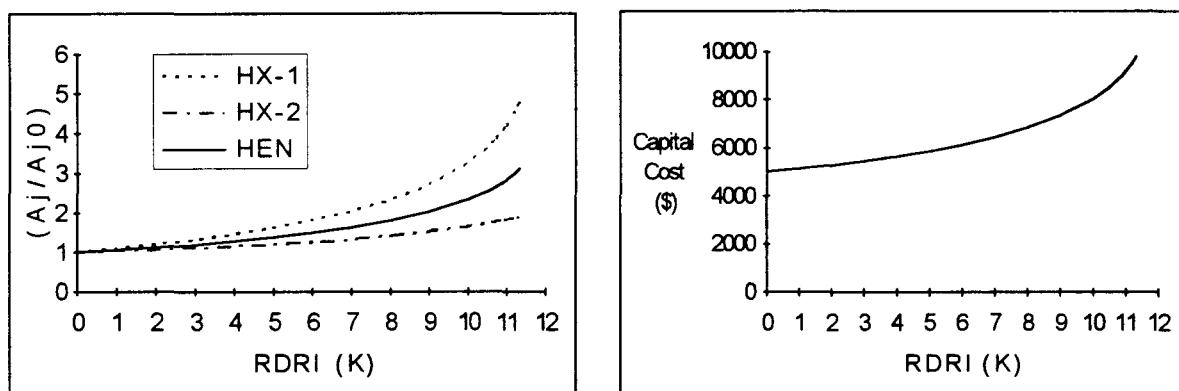


FIGURE 7.18. Changes in the areas and capital cost for the example network structure with a hot-side bypass on HX-1 and a cold-side bypass on HX-2.

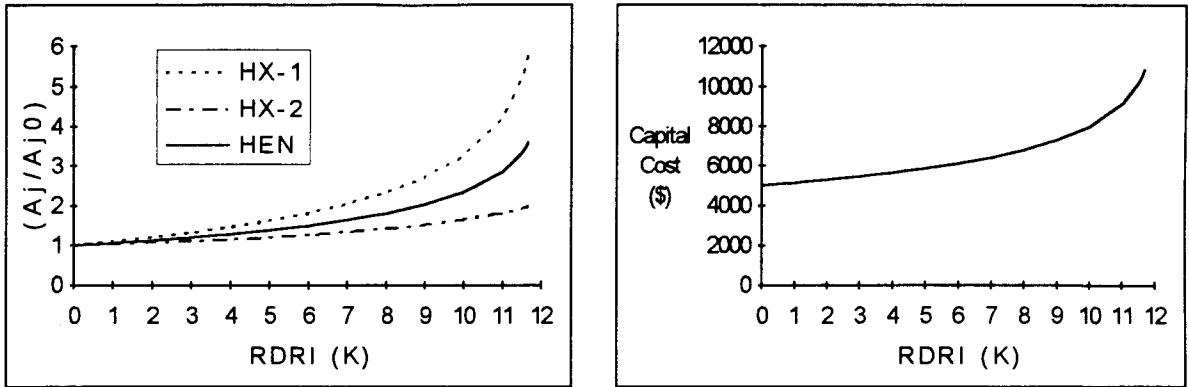


FIGURE 7.19. Changes in the areas and capital cost for the example network structure with a cold-side bypass on HX-1 and a hot-side bypass on HX-2.

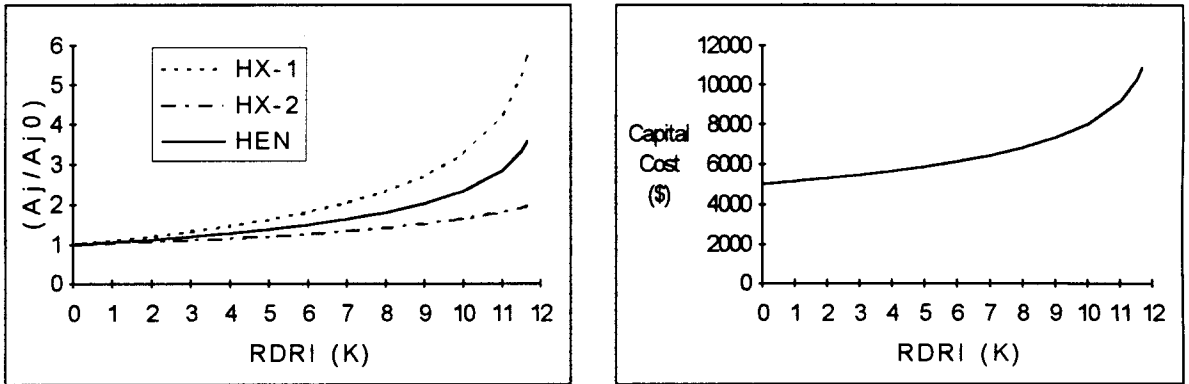


FIGURE 7.20. Changes in the areas and capital cost for the example network structure with a cold-side bypass on HX-1 and a cold-side bypass on HX-2.

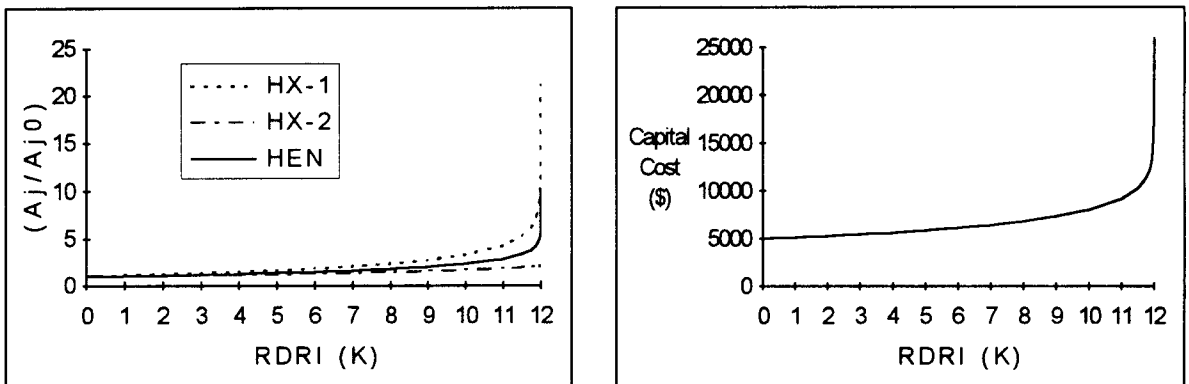


FIGURE 7.21. Changes in the areas and capital cost for the example network structure with a hot- and cold-side bypass on HX-1 and a hot-side bypass on HX-2.

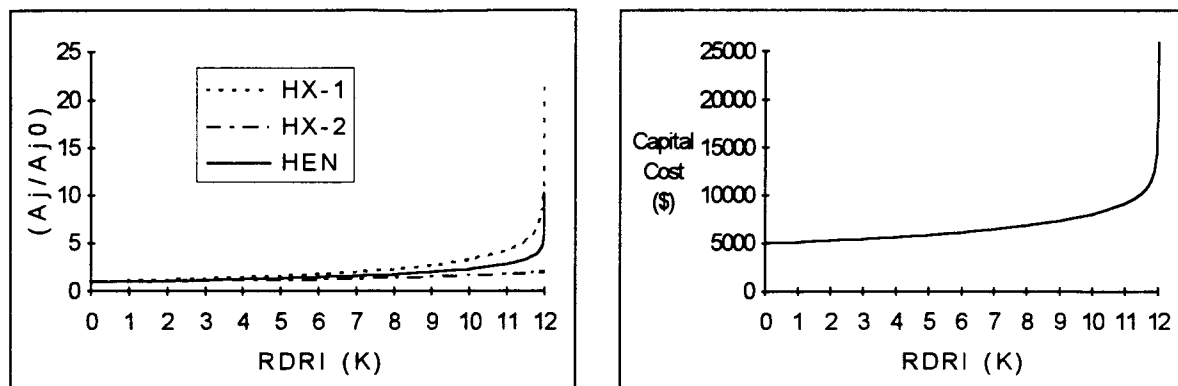


FIGURE 7.22. Changes in the areas and capital cost for the example network structure with a hot- and cold-side bypass on HX-1 and a cold-side bypass on HX-2.

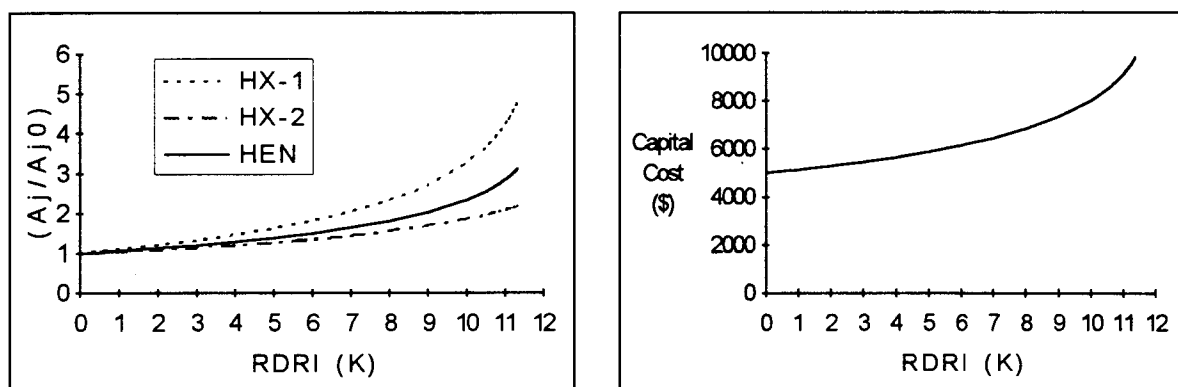


FIGURE 7.23. Changes in the areas and capital cost for the example network structure with a hot-side bypass on HX-1 and a hot- and cold-side bypass on HX-2.

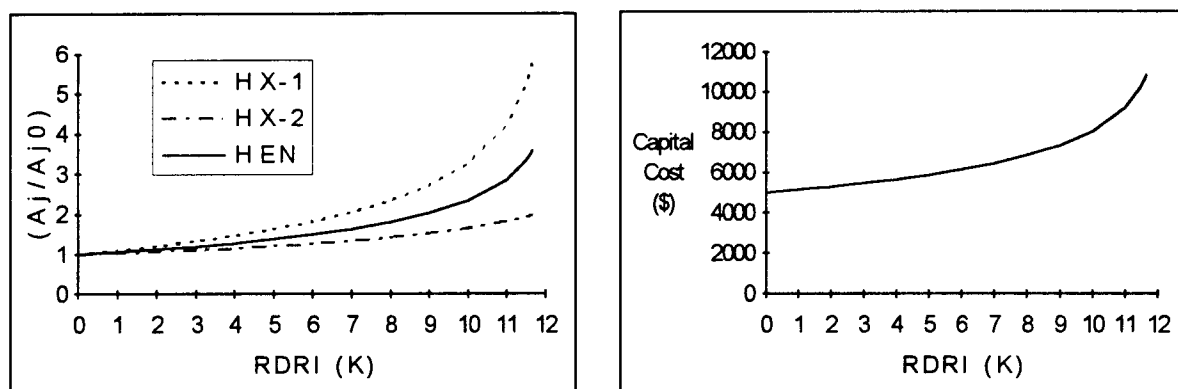


FIGURE 7.24. Changes in the areas and capital cost for the example network structure with a cold-side bypass on HX-1 and a hot- and cold-side bypass on HX-2.

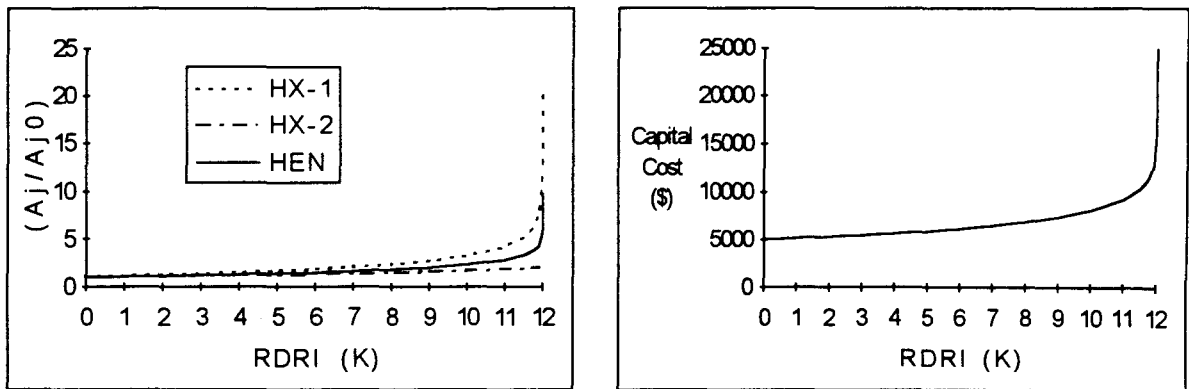


FIGURE 7.25. Changes in the areas and capital cost for the example network structure when all exchangers has double (hot-/cold-side) bypasses.

TABLE 7.6. Bypass placements vs. maximum RDRI values.

Bypasses	MRDRI (K)	Bypasses	MRDRI (K)
No bypass	0	$u_{h,1}$ & $u_{c,2}$ & $u_{h,2}$	11.326
$u_{h,1}$	0	$u_{h,1}$ & $u_{h,2}$	11.329
$u_{c,1}$	0	$u_{c,1}$ & $u_{h,2}$	11.658
$u_{h,2}$	0	$u_{c,1}$ & $u_{c,2}$	11.658
$u_{c,2}$	0	$u_{c,1}$ & $u_{h,2}$ & $u_{c,2}$	11.658
$u_{h,1}$ & $u_{c,1}$	0	$u_{h,1}$ & $u_{c,1}$ & $u_{h,2}$	12.000
$u_{h,2}$ & $u_{c,2}$	0	$u_{h,1}$ & $u_{c,1}$ & $u_{c,2}$	12.000
$u_{h,1}$ & $u_{c,2}$	11.326	all	12.000

Maximum RDRI values for different bypass configurations are tabulated in Table 7.6. Examining the table, (although in this example the differences are small) it can be seen that placing the bypass(es) for an exchanger on the stream which has higher heat-capacity-flowrate, may provide more resilient network design(s). This is the opposite of the

controllability-related heuristics of HENs proposed by Mathisen (1994) who claimed that placing the bypass(es) on streams which has smaller heat-capacity-flowrates gives good control characteristics. This shows the trade-off between controllability and controllable resilient designs of HENs.

### 7.3.2. Case-Study for Soft Targets, (Case-D)

Here, the targets of the HEN are considered as soft targets as given in Figure 7.14, (target of hot stream,  $T_{h,1} \leq 410$ , and target of cold-stream 2,  $T_{c,2} \geq 430$ ). Soft targets, as will be seen, provide greater flexibility to design. In Figure 7.26, the relationship between areas of the exchangers is shown. Points in this figure are obtained by modifying the optimization problem used for finding DRI value of the network, so that fixing the DRI value to zero and also fixing one variable (e.g., area of exchanger-1) and searching for the minimum and then the maximum value of the other variable (e.g. area of exchanger-2) subject to constraints, for this fixed value of the first variable. Then, by scanning the feasible region of one variable, the graph is constructed. The inside of the contour is both the feasible- and the flexible-design region, and the contour indicates the design values of areas for zero-resiliency design (for  $DRI = 0$ ). The nonlinearity of the relation between the areas should be noticed. This nonlinear relationship between exchanger areas shows that oversizing the area of one or more exchanger in the network as independent of the rest(s) may not guarantee a resilient HEN design. Also, it should be noted that any design point on the contour (i.e. zero-resiliency design) will be determined by the trade-off between the capital and the operating costs for a given set of economic parameters.

In Figure 7.27, the relationship between the areas of the exchangers for different DRI values, and the minimum total area curve is shown. The curves are obtained using the procedure described in the previous paragraph using different DRI values other than zero.

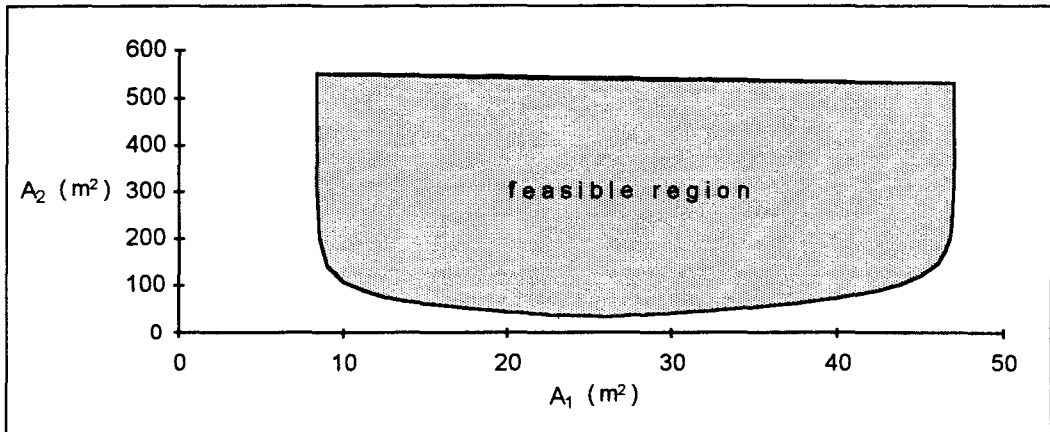


FIGURE 7.26. Relationship between the areas of the exchangers for the example structure when the targets of the HEN are treated as soft.

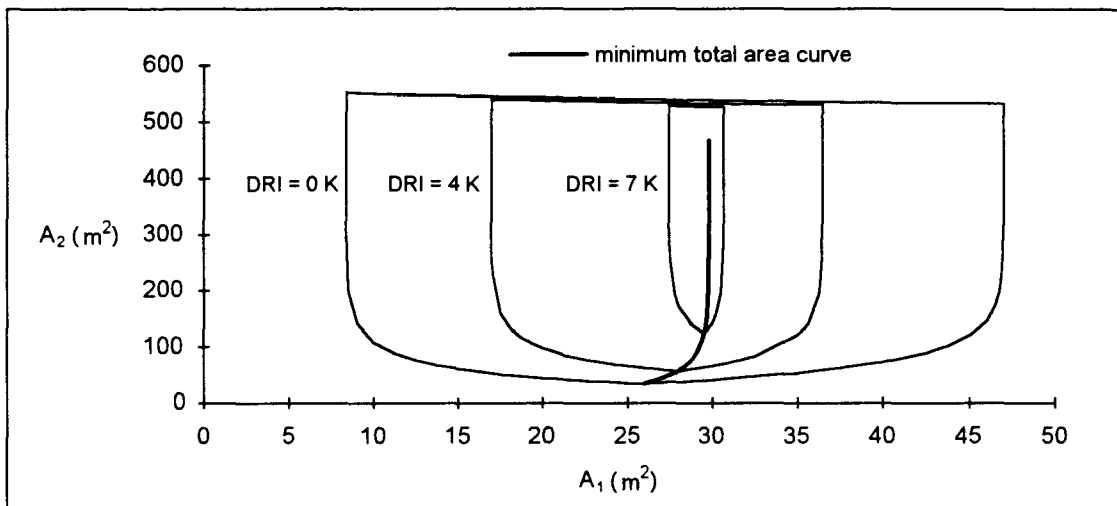


FIGURE 7.27. Relationship between the areas of the exchangers for different DRI values.

In Figures 7.28 - Figure 7.30, changes in the areas of the exchangers and changes in costs with respect to RDRI values for the HEN having no bypass and with two different bypass configurations are shown. The economic parameters are the same as those used in Case-C (Table 7.5) and costs of the base design are given in Table 7.7.

TABLE 7.7. Costs of zero-resiliency (initial) design.

$A_1$ (m <sup>2</sup> )	43.39
$A_2$ (m <sup>2</sup> )	97.87
Annualized Capital Cost (\$)	8,047
Operating Cost (\$)	133,429
Total Annualized Cost (\$)	141,476

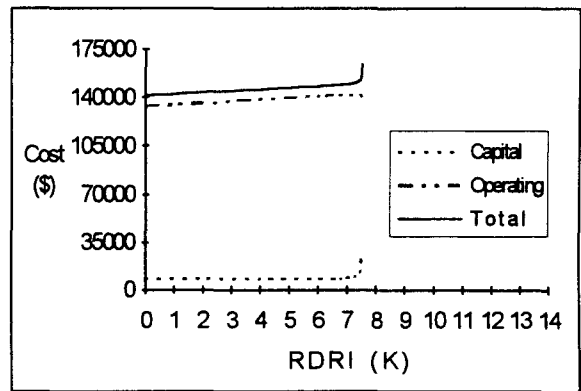
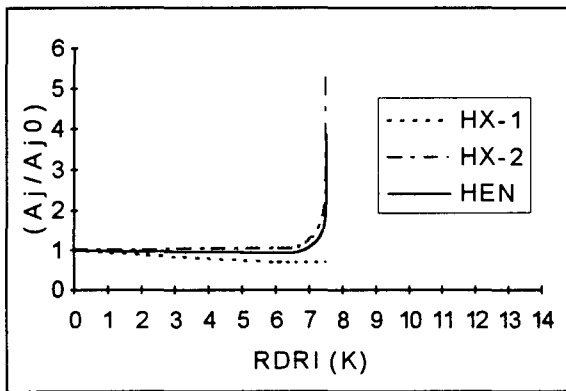


FIGURE 7.28. Changes in areas and costs for the example network structure for the soft-target case when exchangers have no bypasses.

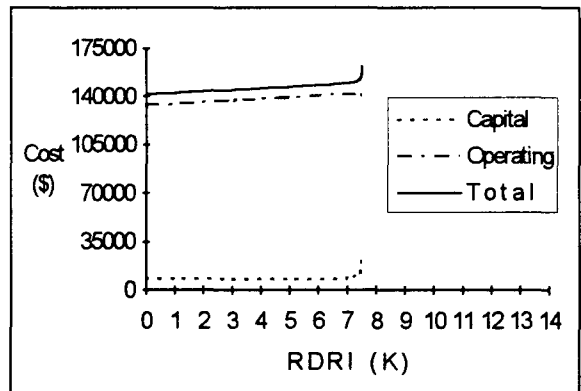
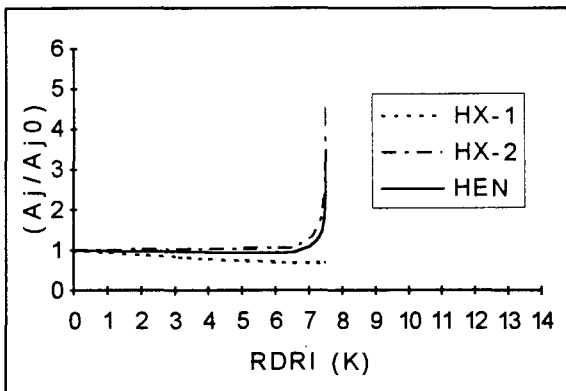


FIGURE 7.29. Changes in areas costs for the example network structure for the soft-target case when exchanger 2 has a hot-side bypass.

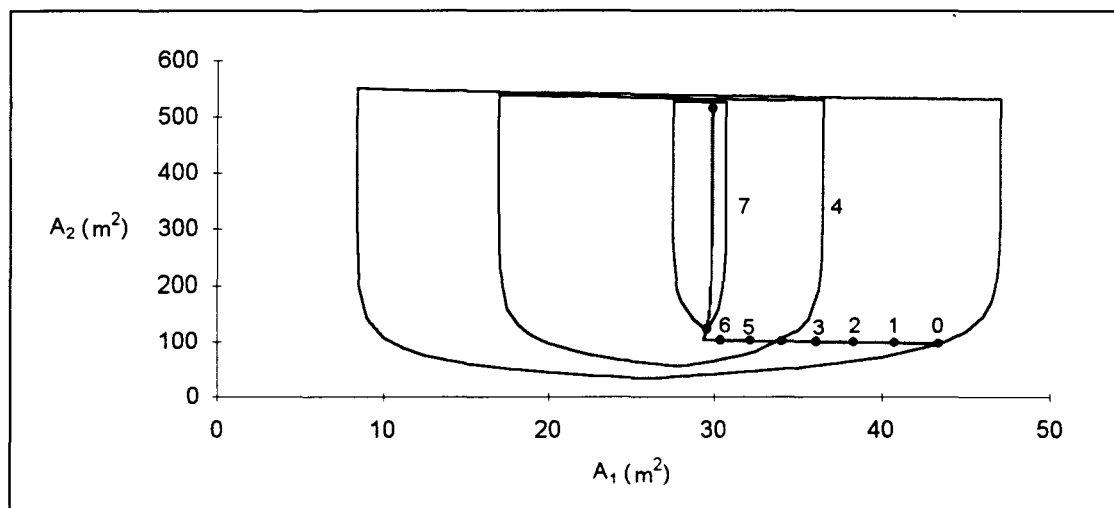


FIGURE 7.30. Changes in the total area of HEN for the example network structure for the soft-target case when exchanger 2 has a hot-side bypass or when exchangers have no bypasses. (numbers indicate the DRI values)

The structure that has no bypass and the structure that has a bypass on the hot side of exchanger-2 (Figure 7.28 and Figure 7.29), have the same trajectories. The structure that has a bypass on the hot side of exchanger-2 has no advantage over the structure without bypass. The area of exchanger 1 decreases slightly up to maximum RDRI value of 7.5 K. Total area of the network (capital cost) decreases up to 6.8 K and then increases (Figure 7.28, Figure 7.29, Figure 7.30). Meanwhile, the operating cost increases up to 6.8 K and then decreases. Up to 6.8 K, the trajectory is determined by the trade-off between the capital and operating cost. From 6.8 K to 7.5 K, the trajectory is in the minimum area curve as can be seen in Figure 7.30.

In Figure 7.31, increases in the areas and costs as a function of RDRI are shown for the example structure that has a cold-side bypass on exchanger 1 and a hot-side bypass on exchanger 2. It should be noted that areas of exchangers (and costs) do not change up to 8.8 K and then increase up to 13.3 K. Up to 8.8 K (BRDRI), original design values do not change. With the use of  $u_{h,2}$  and  $u_{c,1}$  as bypasses, there is no need for any design changes from non-bypassed design, and thus there is no extra cost up to 8.8 K design resiliency (DRI).

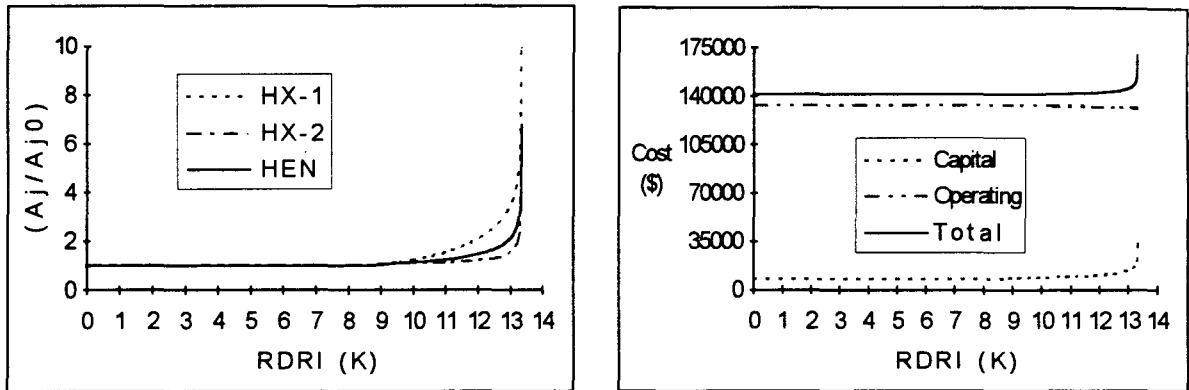


FIGURE 7.31. Changes in the areas costs for the example network structure for the soft-target case when exchanger 1 has a cold-side bypass and exchanger 2 has a hot side bypass.

#### 7.4. The Effect of Capital-Recovery Factor on the Retrofit Design

In this section, the effect of using different capital-recovery factors ( $\gamma$ , Eq. 5.49), in the formulation is demonstrated for the example structure (Case-D) used in the previous section with the bypass configuration where exchanger 1 has a cold-side bypass and exchanger 2 has a hot-side bypass. As can be seen from the results (Figures 7.32, 7.33, 7.34), higher values of capital-recovery factor not only cause higher total annualized costs as logically expected, but also gives lower BRDRI values.

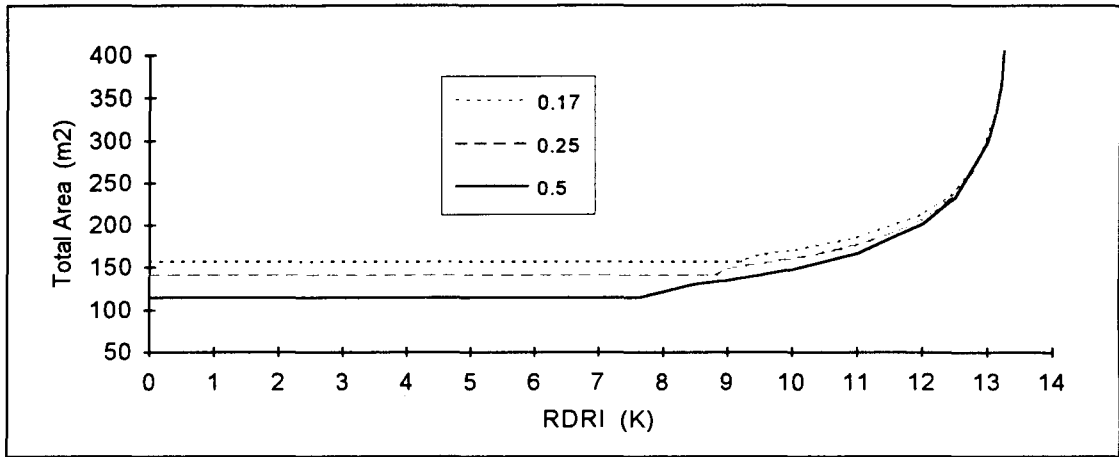


FIGURE 7.32. Total area for different values of capital-recovery factor.

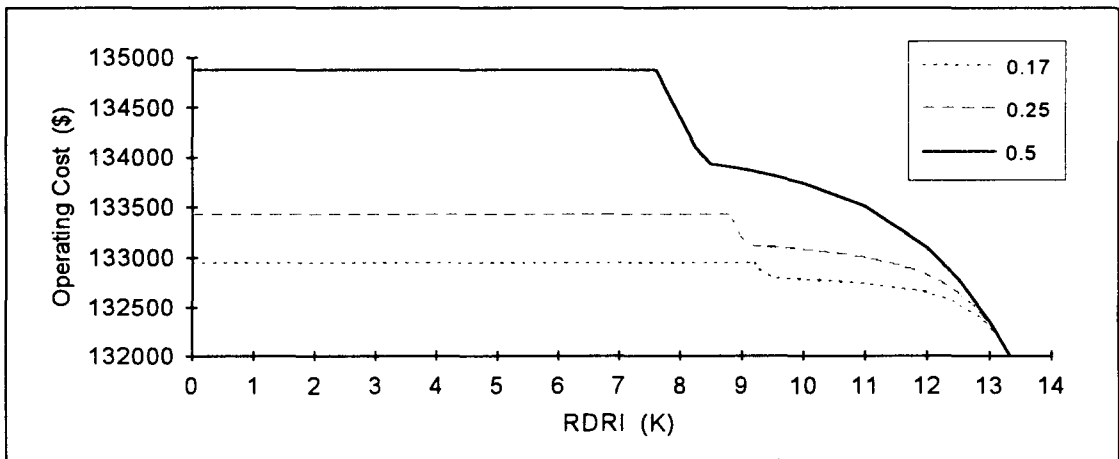


FIGURE 7.33. Operating cost for different values of capital-recovery factor.

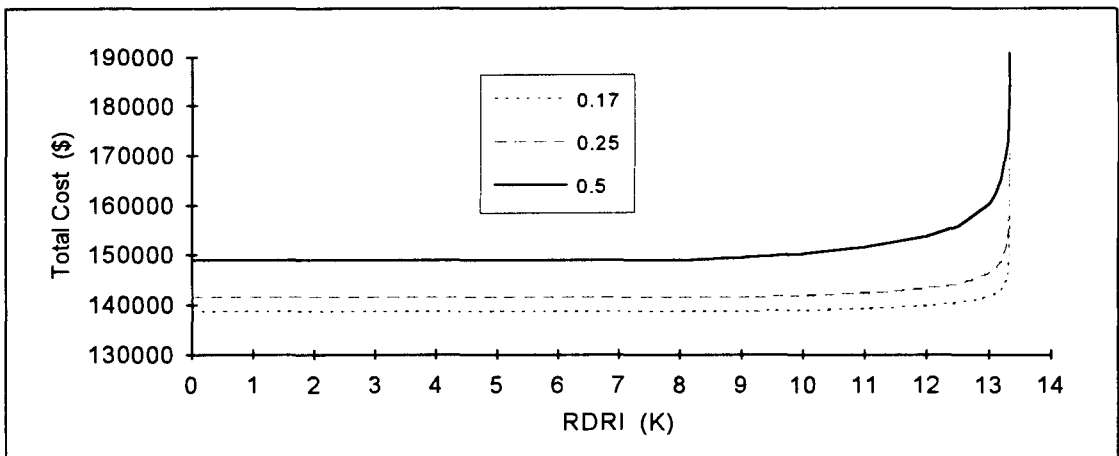


FIGURE 7.34. Total cost for different values of capital-recovery factor.

## 8. CONCLUSIONS AND RECOMMENDATIONS

In this study, a new approach for the resilient/controllable design of heat-exchanger networks has been presented. The proposed technique re-evaluates a predetermined HEN structure for the retrofit design of the HEN which is not only economically at minimum cost but also has the ability to reject the disturbances predefined in *all* possible directions. In other words, the retrofit network designed based on a pre-defined structure is the optimum network for the desired resiliency-target specifications. The definition of a general degree of resiliency (which reflects the expected magnitude of disturbances in temperatures and/or flowrates of source streams) is proposed. The *Retrofit Design Resiliency Index (RDRI)* proposed in this study, defines the expected disturbance range as simultaneous deviation, of identical magnitude for all combinations of the increasing or decreasing directions, from the nominal values of the stream supply temperatures and/or flowrates. The proposed retrofit design formulation evaluates all simultaneous deviations in source streams as a single nonlinear-programming problem, the solution of which, thus guarantees the operability of the HEN within the range of expected disturbances. For the evaluation of the resiliency of a designed HEN, the *Design Resiliency Index (DRI)* is also proposed which determines the value of the maximum permissible equal-in-magnitude, and simultaneous deviations for all possible combinations of disturbance directions in source streams. DRI can be used to check the feasibility of the retrofit design obtained from the proposed formulation for the specified RDRI value. This may be necessary due to a nonunique relationship between DRI and RDRI under some specific conditions.

The objective of the proposed optimization approach is to find the design parameters for a given heat-exchanger structure so that the HEN has a minimum total annualized cost for the desired degree of resiliency. The total-annualized-cost function used in the general formulation, includes two main parts; capital cost (related to the areas of exchangers and utilities) and operating cost (heating and cooling utilities at nominal operating conditions).

The two limiting states of the 'total annualized cost' for a given structure are the 'minimum-total-area network', and 'minimum-utility-cost network' of that structure. The optimal design of a structure for a specified degree of resiliency is in the range of these two limiting states as dependent on the economical parameters.

There are two limiting cost-resiliency trajectories for a specified structure. If the objective is to find the minimum total area of the structure, the cost-resiliency trajectory begins with the possible minimum area of that structure which is the initial design (nonresilient design) and the areas of exchangers increase up to the maximum resiliency (defined by *Maximum Design Resiliency Index, MRDRI*) permitted by the structure. At the maximum resiliency, either the load constraint of an exchanger or/and the minimum approach temperature permitted (if defined) in one disturbance direction becomes active, or the minimum/maximum-input-temperature constraints of the utilities become binding. If the objective is to find the minimum-utility-cost network, the cost-resiliency trajectory is constant throughout all resilient range.

In this study, the relationship between the resiliency and the cost was investigated for several example HEN structures. Base designs of the structures may be the designs obtained from the proposed formulation for the zero-resiliency condition (nonresilient design obtained from the formulation using only the nominal operating conditions) or may be the designs obtained by another technique or with a technique with some specific conditions (e.g., desiring the pinch situation at the nominal operating conditions with a specified minimum-approach-temperature). It is demonstrated that the cost vs. resiliency curve for a HEN problem with specified structure, which begins with the initial design and extends to the maximum degree of resiliency, may take a form as a combination of the following three different characteristic states: I) If the capacity of downstream paths is adequate for directing the disturbances to the utilities and/or to soft-target terminals, the desired resiliency increase does not cause any increase in costs. In terms of definitions developed in this study, the concluding remark of this state is that the DRI value of a network may be greater than the RDRI value used in the retrofit design formulation. Graphs of area vs. RDRI of exchangers show, for some cases, that the areas of exchangers do not change until a specific RDRI value (defined as *Break-Point Design Resiliency Index 'BRDRI'*). For these cases, if

a resilient retrofit design with a RDRI value lower than the BRDRI is aimed for, the resulting retrofit design will turn out to be more resilient, and DRI value of that design will be equal to the value of BRDRI. In other words, the initial design essentially will have a resiliency value indicated by BRDRI. This kind of phenomena are encountered especially when some specific conditions of an initial design are forced to be conserved/kept in the nominal operating conditions of the retrofit design as well. (e.g., by introducing the desired specific conditions of the initial design as hard/soft constraints for the zero-resiliency direction, i.e. nominal operating conditions, of the retrofit design). II) The desire to increase the resiliency may cause the changes in areas of exchangers (increase or decrease) and utility consumption levels (increase or decrease) depending on the trade-off between capital and operating costs for a given set of economic parameters. III) When the utility constraints become active, or there is no economic way, the rejection of the excess disturbance loads may only be achieved then with increase(s) in the heat-exchanger areas, and thus the cost-resiliency trajectory coincides with the 'minimum-area vs. resiliency' trajectory.

It is demonstrated that the resilient retrofit HEN designs do not necessarily have higher total exchanger areas than the original (and/or nonresilient) HENs. This is also true for the individual areas of the exchangers in a network structure. It is possible to get a more resilient network by decreasing the area of one or more exchangers in the network (possibly with a corresponding minor increase in the areas of some other exchangers). Furthermore, the total area of the network may also decrease by increasing the desired value of the resiliency index. This point has been surprisingly overlooked by some authors studied control of heat-exchanger networks. The two common approaches that have been observed in the literature up to now are summarized below.

The first approach is to consider the presence of the manipulated variables (bypass fractions) after the original design or to consider the manipulated variables (bypass fractions) in the synthesis step but without taking into account the area increases in the design stage. These approaches imply that nominal values of bypass-stream openings are zero under the nominal operating conditions and that the bypasses are to be opened only when a disturbance enters the network. The major handicap of this approach for the

control purpose is that the capacity of disturbance rejection is limited since the controls can be applied only in one direction (i.e., by opening the bypasses from their nominal values which are zero towards their values required to reject/re-direct the incoming disturbance).

The second approach, for a specified structure, is to place bypass(es) with a heuristic value (e.g., a nominal 10 per cent opening) in the design step. This approach definitely causes increases in the individual areas of the heat exchangers that are bypassed. The first handicap of this strategy is that the resulting retrofit design may not necessarily guarantee a more resilient network (i.e., does not guarantee a higher value of disturbance rejection capacity). Furthermore, for some exchangers in the network, it may be impossible to get a retrofit design with a 10 per cent bypass opening due to approach-temperature and/or hard constraints. This significantly and unnecessarily limits the number of possible locations of the bypass streams in a network. At that point, it should be mentioned that the selection of locations of the manipulated variables (bypasses) is important for the dynamic control objectives as well, and some authors claim that placing bypasses on final (end-of-network) exchangers with a direct effect on the target should be preferred. However, the placement of bypasses with, say, 10 per cent nominal opening value to such locations, that are heuristically favorable with respect to dynamic control objectives, may be impossible after the design due to above-mentioned constraints. A further handicap of this strategy is that resiliency gained by such a direct bypass placement does not depend on any specification about the expected disturbance range in source streams. In other words, such designs do not aim for satisfying the target-resiliency constraints, and hence, the capacity of disturbance rejection maximum/overall disturbance magnitude that can be tolerated by the network can only be determined after the design has been completed. Since such designs are not based on target-resiliency specifications (or a resiliency measure) and since no economical parameters for the capital and operating cost are considered, it can be possible to say only after the design has been completed that 'how much resiliency gained at how much cost'. Definitely, the retrofit designs obtained by such an approach are not the most cheapest ones among the designs that provide the same resiliency.

Synthesis/design methods proposed for HENs in the literature do not take into account the resiliency of the final design. It has been thought that only the investigation of

'flexibility' of alternative structures is adequate. This may be only a guide for the selection of alternative structures since such 'flexibility measures' should only be thought as the upper limits for the designs that can be obtained from that structure. Resilient designs are necessary not only for enlarging the operability range of the network, but also to obtain designs which can be controlled during operation. Since the standard HEN-generating algorithms do not consider adequacy of the number of manipulated variables for the control action, the control variables and resiliency specifications/constraints must be included in the retrofit design stage. In this respect, HEN problems are the typical examples where the design and control considerations have to be considered together. The approach presented in this study aims to combine the design and control considerations in the most economical way by incorporating manipulated variables in the retrofit-design stage. The relationship between the number and the location of bypasses (degrees of freedom assigned in the design stage), resiliency, and cost has been investigated and demonstrated for a predefined structure. It is shown that the same degree of resiliency can be gained for different number of manipulated variables and also for alternative placement of manipulated variables. Choosing a structure that has minimum number of bypasses may be one criterion when selecting between the alternatives satisfying the same degree of desired resiliency in an economical point of view. On the other hand, selection of a structure that has more bypasses than the minimum (for the specified resiliency degree) may provide some extra advantages in the dynamic control action (e.g., in the case where one or more target(s) are to be kept strictly hard in the operation) by providing more alternative disturbance-propagation paths (created by the increased degrees of freedom). In these situations, the criterion may be the selection of a bypass configuration between the alternatives which will satisfy not only the resiliency targets at minimum cost, but also the dynamic control objectives. In this study, the effect of the selection of manipulated variables on the dynamic control performance was not addressed. Actually, a retrofit objective considering the triple trade-offs between resiliency, dynamic control performance, and cost will give more robust designs.

The proposed retrofit-design approach is limited to the known structures which has been obtained via standard HEN synthesis methods. The presented approach offers the assessment of alternative structures, by incorporating the control variables, with regard to

resiliency/control objectives. There are numerous alternative solution structures/designs to be investigated due to the combinatorial nature of a typical HEN problem. In the future, a general HEN-problem-solution approach may be developed that simultaneously considers the resiliency, and dynamic control objectives and performance, and that will find a unique (or a limited number of) solution(s) under the specified resiliency and control-performance criteria.

## **APPENDICES**

## APPENDIX A

**The GAMS code for the evaluation of the Flexibility Index via linear programming formulation of the example heat-exchanger network given in Chapter 3 (Figure 3.1).**

```

$OFFSYMLIST
OFFSYMREF
OFFFUELLIST
OFFFUELXREF
OPTION DECIMALS=5, LIMROW=0, LIMCOL=0, SYSOUT=OFF, SOLPRINT=OFF;

SCALAR
WH1   / 30 /
WH2   / 45 /
WC1   / 40 /
WC2   / 60 /
T6    / 453 /
DTMIN / 0  /;

VARIABLES
S , T1S , T2S , T3S , T4S , T1 , T2 , T3 , T4 , T5 , T7 , T8 ;

EQUATIONS
SPOZ ,
EQ1 , EQ2 , EQ3 , EQ4 ,
LH1 , LH2 , LH3 , LH4 ,
LC1 , LC2 , LC3 , LC4 ,
MAH1 , MAH2 , MAH3 , MAH4 ,
MAC1 , MAC2 , MAC3 , MAC4 ,
SP1 , SP2 , SP3 , SP4 ,
HT1 , CL1 , CL2 ;

EQ1 .. WH1*(T1S-T1) + WC2*(T4-T2) =E= 0 ;
EQ2 .. WH2*(T2S-T3) + WC2*(T4S-T4) =E= 0 ;
EQ3 .. WH1*(T1-T5) + WC1*(T8-T6) =E= 0 ;
EQ4 .. WH2*(T3-T7) + WC1*(T3S-T8) =E= 0 ;

LH1 .. T1S =G= T1 ;
LH2 .. T2S =G= T3 ;
LH3 .. T1 =G= T5 ;
LH4 .. T3 =G= T7 ;

LC1 .. T2 =G= T4 ;
LC2 .. T4 =G= T4S ;

```

```

LC3 .. T6 =G= T8 ;
LC4 .. T8 =G= T3S ;

MAH1 .. T4 - T1 =L= -1*DTMIN ;
MAH2 .. T4S - T3 =L= -1*DTMIN ;
MAH3 .. T8 - T5 =L= -1*DTMIN ;
MAH4 .. T3S - T7 =L= -1*DTMIN ;

MAC1 .. T2 - T1S =L= -1*DTMIN ;
MAC2 .. T4 - T2S =L= -1*DTMIN ;
MAC3 .. T6 - T1 =L= -1*DTMIN ;
MAC4 .. T8 - T3 =L= -1*DTMIN ;

HT1 .. T2 =L= 513 ;
CL1 .. T5 =G= 353 ;
CL2 .. T7 =G= 313 ;

SP1 .. T1S =E= 573 + S ;
SP2 .. T2S =E= 473 + S ;
SP3 .. T3S =E= 313 + S ;
SP4 .. T4S =E= 413 + S ;

SPOZ .. S =G= 0;

MODEL PRG301 /ALL/ ;
SOLVE PRG301 USING LP MAXIMIZING S ;
DISPLAY S.L ;
DISPLAY T1S.L ;
DISPLAY T2S.L ;
DISPLAY T3S.L ;
DISPLAY T4S.L ;
DISPLAY T1.L ;
DISPLAY T2.L ;
DISPLAY T3.L ;
DISPLAY T4.L ;
DISPLAY T5.L ;
DISPLAY T7.L ;
DISPLAY T8.L ;

```

## APPENDIX B

**The GAMS code for the solution of the optimization problem defined in Chapter 4.**

```

$OFFDIGIT
  OPTION ITERLIM = 100000 ;
*OPTION SOLPRINT = OFF ;
*OPTION SYSOUT  = OFF ;
*OPTION OPTCR   = 0 ;
*OPTION LIMROW  = 0 ;
*OPTION LIMCOL  = 0 ;

SCALAR
  WH1 / 1000 /
  WH2 / 1500 /
  WC1 / 3000 /
  WC2 / 2000 /
*SET 0
*T1S / 583 /
*T2S / 620 /
*T3S / 313 /
*T4S / 388 /
*SET 1
  T1S / 588 /
  T2S / 625 /
  T3S / 308 /
  T4S / 383 /
*SET 2
*T1S / 589 /
*T2S / 626 /
*T3S / 307 /
*T4S / 382 /

  U1 / 1000 /
  U2 / 1000 /
  U3 / 1000 /
  A1 / 1.3862943611 /
  A2 / 4.2498200158 /
  A3 / 10.3187158170 /

*DTMIN / 10 /;
  DTMIN / 0 /;

VARIABLES
  OBJ ,

```

T1T , T2T , T3T , T4T ,  
 T1 , T2 , T3 , T4 , T5 , T6 , T7 , T8 ,  
 UH1 , UH2 , UH3 , UC1 , UC2 , UC3 ,  
 DT11 , DT12 , DT21 , DT22 , DT31 , DT32 ,  
 DTLM1 , DTLM2 , DTLM3 ,  
 BHEX1 , BCEX1 , BTEX1 ,  
 BHEX2 , BCEX2 , BTEX2 ,  
 BHEX3 , BCEX3 , BTEX3 ,  
 WUH1 , WUH2 , WUH3 ,  
 WUC1 , WUC2 , WUC3 ;

## EQUATIONS

EOBJ ,  
 EC01 , EC02 , EC03 , EC04 , EC05 , EC06 ,  
 EC07 , EC08 , EC09 , EC10 , EC11 , EC12 ,  
 IC01 , IC02 , IC03 , IC04 , IC05 , IC06 ,  
 IC07 , IC08 , IC09 , IC10 , IC11 , IC12 ,  
 AC01 , AC02 , AC03 , AC04 , AC05 ,  
 AC06 , AC07 , AC08 , AC09 ,  
 AB01 , AB02 , AB03 ,  
 AB04 , AB05 , AB06 ,  
 AB07 , AB08 , AB09 ,  
 BF01 , BF02 , BF03 ,  
 BF04 , BF05 , BF06 ;

## \*SCENARIO 1

\*T2T.LO = 321 ;  
 \*T2T.UP = 325 ;  
 \*T4T.LO = 398 ;  
 \*T4T.UP = 402 ;  
 \*T1T.LO = 561 ;  
 \*T1T.UP = 565 ;  
 \*T3T.LO = 391 ;  
 \*T3T.UP = 395 ;

## \*SCENARIO 2

T2T.LO = 319.0 ;  
 T2T.UP = 327.0 ;  
 T4T.LO = 396.0 ;  
 T4T.UP = 404.0 ;  
 T1T.LO = 562.5 ;  
 T1T.UP = 563.5 ;  
 T3T.LO = 392.5 ;  
 T3T.UP = 393.5 ;

## \*SCENARIO 3

\*T2T.LO = 322.5 ;  
 \*T2T.UP = 323.5 ;  
 \*T4T.LO = 399.5 ;  
 \*T4T.UP = 400.5 ;  
 \*T1T.LO = 559.0 ;  
 \*T1T.UP = 567.0 ;  
 \*T3T.LO = 389.0 ;  
 \*T3T.UP = 397.0 ;

T1.L = 563 ;  
 T2.L = 563 ;  
 T3.L = 563 ;

```

T4.L = 323 ;
T5.L = 393 ;
T6.L = 400 ;
T7.L = 553 ;
T8.L = 553 ;

*INITIAL BYPASS FRACTION SET 1
UH1.L = 0 ;
UC1.L = 0 ;
UH2.L = 0 ;
UC2.L = 0 ;
UH3.L = 0 ;
UC3.L = 0 ;

*INITIAL BYPASS FRACTION SET 2
*UH1.L = 0.5 ;
*UC1.L = 0.5 ;
*UH2.L = 0.5 ;
*UC2.L = 0.5 ;
*UH3.L = 0.5 ;
*UC3.L = 0.5 ;

EOBJ .. OBJ =E=
          + ABS((T1T-563))
          + ABS((T2T-323))
          + ABS((T3T-393))
          + ABS((T4T-400));

EC01 .. WH1*(1-UH1)*(T1S-T1) + WC2*(1-UC1)*(T8 -T3) =E= 0 ;
EC02 .. WH1*(1-UH1)*(T1S-T1) - U1*A1*DTLM1 =E= 0 ;
EC03 .. WH1*(1-UH2)*(T2 -T4) + WC1*(1-UC2)*(T3S-T5) =E= 0 ;
EC04 .. WH1*(1-UH2)*(T2 -T4) - U2*A2*DTLM2 =E= 0 ;
EC05 .. WH2*(1-UH3)*(T2S-T6) + WC2*(1-UC3)*(T4S-T7) =E= 0 ;
EC06 .. WH2*(1-UH3)*(T2S-T6) - U3*A3*DTLM3 =E= 0 ;

EC07 .. UH1*T1S + (1-UH1)*T1 - T2 =E= 0 ;
EC08 .. UC1*T8 + (1-UC1)*T3 - T1T =E= 0 ;
EC09 .. UH2*T2 + (1-UH2)*T4 - T2T =E= 0 ;
EC10 .. UC2*T3S + (1-UC2)*T5 - T3T =E= 0 ;
EC11 .. UH3*T2S + (1-UH3)*T6 - T4T =E= 0 ;
EC12 .. UC3*T4S + (1-UC3)*T7 - T8 =E= 0 ;

IC01 .. T1 - T1S =L= 0 ;
IC02 .. T8 - T3 =L= 0 ;
IC03 .. T4 - T2 =L= 0 ;
IC04 .. T3S - T5 =L= 0 ;
IC05 .. T6 - T2S =L= 0 ;
IC06 .. T4S - T7 =L= 0 ;

IC07 .. T1S - T3 =G= DTMIN ;
IC08 .. T1 - T8 =G= DTMIN ;
IC09 .. T2 - T5 =G= DTMIN ;
IC10 .. T4 - T3S =G= DTMIN ;
IC11 .. T2S - T7 =G= DTMIN ;
IC12 .. T6 - T4S =G= DTMIN ;

AC01 .. DT11 =E= T1S - T3 ;
AC02 .. DT12 =E= T1 - T8 ;

```

```

AC03 .. DTLM1 =E= ((DT11+1E-7-DT12)/((LOG((DT11+1E-7)/(DT12)))));
DT11.LO = 0.00001;
DT12.LO = 0.00001;

AC04 .. DT21 =E= T2 - T5 ;
AC05 .. DT22 =E= T4 - T3S ;
AC06 .. DTLM2 =E= ((DT21+1E-7-DT22)/((LOG((DT21+1E-7)/(DT22)))));
DT21.LO = 0.00001;
DT22.LO = 0.00001;

AC07 .. DT31 =E= T2S - T7 ;
AC08 .. DT32 =E= T6 - T4S ;
AC09 .. DTLM3 =E= ((DT31+1E-7-DT32)/((LOG((DT31+1E-7)/(DT32)))));
DT31.LO = 0.00001;
DT32.LO = 0.00001;

BF01 .. WUH1 =E= WH1*UH1 ;
BF02 .. WUH2 =E= WH1*UH2 ;
BF03 .. WUH3 =E= WH2*UH3 ;

BF04 .. WUC1 =E= WC2*UC1 ;
BF05 .. WUC2 =E= WC1*UC2 ;
BF06 .. WUC3 =E= WC2*UC3 ;

AB01 .. BHEX1 =E= WH1*(1-UH1)*(T1S-T1) ;
AB02 .. BCEX1 =E= -1*WC2*(1-UC1)*(T8 -T3) ;
AB03 .. BTEX1 =E= U1*A1*DTLM1 ;

AB04 .. BHEX2 =E= WH1*(1-UH2)*(T2 -T4) ;
AB05 .. BCEX2 =E= -1*WC1*(1-UC2)*(T3S-T5) ;
AB06 .. BTEX2 =E= U2*A2*DTLM2 ;

AB07 .. BHEX3 =E= WH2*(1-UH3)*(T2S-T6) ;
AB08 .. BCEX3 =E= -1*WC2*(1-UC3)*(T4S-T7) ;
AB09 .. BTEX3 =E= U3*A3*DTLM3 ;

UH1.LO = 0 ;
UH2.LO = 0 ;
UH3.LO = 0 ;
UC1.LO = 0 ;
UC2.LO = 0 ;
UC3.LO = 0 ;

UH1.UP = 0.999999999 ;
UH2.UP = 0.999999999 ;
UH3.UP = 0.999999999 ;
UC1.UP = 0.999999999 ;
UC2.UP = 0.999999999 ;
UC3.UP = 0.999999999 ;

MODEL PRG401 /ALL/;
SOLVE PRG401 USING DNLP MINIMIZING OBJ;

FILE MM /PRG401.RES/;
PUT MM;
PUT 'OBJ = ',OBJ.L:14:10//
PUT 'T1S = ',T1S:14:10/
PUT 'T2S = ',T2S:14:10/
PUT 'T3S = ',T3S:14:10/

```

```
PUT 'T4S = ',T4S:14:10//
PUT 'T1 = ',T1.L:14:10/
PUT 'T2 = ',T2.L:14:10/
PUT 'T3 = ',T3.L:14:10/
PUT 'T4 = ',T4.L:14:10/
PUT 'T5 = ',T5.L:14:10/
PUT 'T6 = ',T6.L:14:10/
PUT 'T7 = ',T7.L:14:10/
PUT 'T8 = ',T8.L:14:10//
PUT 'T1T = ',T1T.L:14:10/
PUT 'T2T = ',T2T.L:14:10/
PUT 'T3T = ',T3T.L:14:10/
PUT 'T4T = ',T4T.L:14:10//
PUT 'UH1 = ',UH1.L:14:10/
PUT 'UC1 = ',UC1.L:14:10/
PUT 'UH2 = ',UH2.L:14:10/
PUT 'UC2 = ',UC2.L:14:10/
PUT 'UH3 = ',UH3.L:14:10/
PUT 'UC3 = ',UC3.L:14:10//
PUT 'WUH1 = ',WUH1.L:10:3/
PUT 'WUC1 = ',WUC1.L:10:3/
PUT 'WUH2 = ',WUH2.L:10:3/
PUT 'WUC2 = ',WUC2.L:10:3/
PUT 'WUH3 = ',WUH3.L:10:3/
PUT 'WUC3 = ',WUC3.L:10:3//
PUT 'BHEX1 = ',BHEX1.L:10:3
PUT ' BCEX1 = ',BCEX1.L:10:3
PUT ' BTEX1 = ',BTEX1.L:10:3/
PUT 'BHEX2 = ',BHEX2.L:10:3
PUT ' BCEX2 = ',BCEX2.L:10:3
PUT ' BTEX2 = ',BTEX2.L:10:3/
PUT 'BHEX3 = ',BHEX3.L:10:3
PUT ' BCEX3 = ',BCEX3.L:10:3
PUT ' BTEX3 = ',BTEX3.L:10:3//
```

## APPENDIX C

**The GAMS code for the solution of the optimization problem defined in Chapter 6.**

```

$OFFDIGIT
OPTION ITERLIM = 100000 ;
OPTION SOLPRINT = OFF ;
OPTION SYSOUT = OFF ;
OPTION OPTCR = 0 ;
OPTION LIMROW = 0 ;
OPTION LIMCOL = 0 ;

SETS
I / 0*16 /;

SCALAR
S / 0 /;

SCALAR
WH1 / 8.792 /
WH2 / 10.550 /
WC1 / 7.623 /
WC2 / 6.082 /
U1 / 1.000 /
U2 / 1.000 /
U3 / 1.000 /
UHT / 1.428571/
UCL / 1.000 /
CE / 5500 /
ALFA / 150 /
GAMA / 0.125/
CH / 80 /
CC / 15 /
TCUI / 300 /
TCUO / 320 /
THUI / 680 /
THUO / 680 /
DTMIN / 0 /;

PARAMETER T1(I) , T2(I) , T3(I) , T4(I) ;
T1('0') = 522 ;
T1('1') = 522 + S;
T1('2') = 522 + S;
T1('3') = 522 + S;
T1('4') = 522 + S;

```

T1('5') = 522 + S;  
T1('6') = 522 + S;  
T1('7') = 522 + S;  
T1('8') = 522 + S;  
T1('9') = 522 - S;  
T1('10') = 522 - S;  
T1('11') = 522 - S;  
T1('12') = 522 - S;  
T1('13') = 522 - S;  
T1('14') = 522 - S;  
T1('15') = 522 - S;  
T1('16') = 522 - S;

T2('0') = 389 ;  
T2('1') = 389 + S;  
T2('2') = 389 + S;  
T2('3') = 389 + S;  
T2('4') = 389 + S;  
T2('5') = 389 - S;  
T2('6') = 389 - S;  
T2('7') = 389 - S;  
T2('8') = 389 - S;  
T2('9') = 389 + S;  
T2('10') = 389 + S;  
T2('11') = 389 + S;  
T2('12') = 389 + S;  
T2('13') = 389 - S;  
T2('14') = 389 - S;  
T2('15') = 389 - S;  
T2('16') = 389 - S;

T3('0') = 433 ;  
T3('1') = 433 + S;  
T3('2') = 433 + S;  
T3('3') = 433 - S;  
T3('4') = 433 - S;  
T3('5') = 433 + S;  
T3('6') = 433 + S;  
T3('7') = 433 - S;  
T3('8') = 433 - S;  
T3('9') = 433 + S;  
T3('10') = 433 + S;  
T3('11') = 433 - S;  
T3('12') = 433 - S;  
T3('13') = 433 + S;  
T3('14') = 433 + S;  
T3('15') = 433 - S;  
T3('16') = 433 - S;

T4('0') = 333 ;  
T4('1') = 333 + S;  
T4('2') = 333 - S;  
T4('3') = 333 + S;  
T4('4') = 333 - S;  
T4('5') = 333 + S;  
T4('6') = 333 - S;  
T4('7') = 333 + S;  
T4('8') = 333 - S;  
T4('9') = 333 + S;

```

T4('10') = 333 - S;
T4('11') = 333 + S;
T4('12') = 333 - S;
T4('13') = 333 + S;
T4('14') = 333 - S;
T4('15') = 333 + S;
T4('16') = 333 - S;

```

## VARIABLES

```

A1 , A2 , A3 , AH , AC , AT ,
COSTHEAT , COSTCOOL , COSTCAPE , COSTCAPH , COSTCAPC , COSTTOT ,
UH1(I) , UH2(I) , UH3(I) , UC1(I) , UC2(I) , UC3(I) , X1(I) ,
T5(I) , T6(I) , T7(I) , T9(I) , T10(I) , T11(I) ,
T12(I) , T13(I) , T14(I) ,
T8(I) , T15(I) , T16(I) , T17(I) ,
DT11(I) , DT12(I) , DT21(I) , DT22(I) , DT31(I) , DT32(I) ,
DTH1 , DTH2 , DTC1 , DTC2 ,
DTLM1(I) , DTLM2(I) , DTLM3(I) , DTLMHT , DTLMCL;

```

## EQUATIONS

```

E0 , EH , EC , ECH , ECC , ECP , ETA,
EHA , EHA1 , EHA2 , EHA3 , ECA , ECA1 , ECA2 , ECA3 ,
E1(I) , E2(I) , E3(I) , E4(I) , E5(I) , E6(I) , E7(I) , E8(I) ,
E9(I) , E10(I) , E11(I) , E12(I) , E13(I) ,
E14(I) , E15(I) , E16(I) , E17(I) , E18(I) , E19(I) , E20(I) , E21(I) ,
E22(I) ,
C1(I) , C2(I) , C3(I) , C4(I) , C5(I) , C6(I) , C7(I) ,
C8(I) , C9(I) , C10(I) , C11(I) , C12(I) , C13(I) , C14(I) ,
C15(I) , C16(I) , C17(I) , C18(I) , C19(I) , C20(I) ;

```

```

$INCLUDE 'PRG601.INI'

```

```

T17.LO(I) = 411;
T17.UP(I) = 411;
T16.LO(I) = 433;
T16.UP(I) = 433;

```

```

T8.UP('0') = 533;
T8.UP('1') = 533;
T8.UP('2') = 533;
T8.UP('3') = 533;
T8.UP('4') = 533;
T8.UP('5') = 533;
T8.UP('6') = 533;
T8.UP('7') = 533;
T8.UP('8') = 533;
T8.UP('9') = 533;
T8.UP('10') = 533;
T8.UP('11') = 533;
T8.UP('12') = 533;
T8.UP('13') = 533;
T8.UP('14') = 533;
T8.UP('15') = 533;
T8.UP('16') = 533;

```

```

T15.LO('0') = 366;
T15.LO('1') = 366;
T15.LO('2') = 366;
T15.LO('3') = 366;

```

```

T15.LO('4') = 366;
T15.LO('5') = 366;
T15.LO('6') = 366;
T15.LO('7') = 366;
T15.LO('8') = 366;
T15.LO('9') = 366;
T15.LO('10') = 366;
T15.LO('11') = 366;
T15.LO('12') = 366;
T15.LO('13') = 366;
T15.LO('14') = 366;
T15.LO('15') = 366;
T15.LO('16') = 366;

ETA .. AT =E= A1+A2+A3+AH+AC;
E0 .. COSTTOT =E= COSTCAPE+COSTHEAT+COSTCOOL+COSTCAPH+COSTCAPC;
ECP .. COSTCAPE =E= (GAMA*((CE+ALFA*A1)+(CE+ALFA*A2)+(CE+ALFA*A3)));
ECH .. COSTCAPH =E= (GAMA*((CE+ALFA*AH)));
ECC .. COSTCAPC =E= (GAMA*((CE+ALFA*AC)));
EH .. COSTHEAT =E= CH*(WC2*(533-T8('0')));
EC .. COSTCOOL =E= CC*(WH1*(T15('0')-366));
EHA .. (WC2*(533-T8('0')) - (AH*UHT*DTLMHT)) =E= 0;
ECA .. (WH1*(T15('0')-366) - (AC*UCL*DTLMCL)) =E= 0;

EHA1 .. DTH1 =E= (THUO - T8('0'));
EHA2 .. DTH2 =E= (THUI - 533);
*EHA3 .. DTLMHT =E= 0.5*(DTH1+DTH2);
*EHA3 .. DTLMHT =E= (0.5*DTH1*DTH2*(DTH1+DTH2)+1E-6)**0.33333333;
EHA3 .. DTLMHT =E= ((DTH1+1E-7-DTH2)/((LOG((DTH1+1E-7)/(DTH2)))));
DTH1.LO = 0.00001;
DTH2.LO = 0.00001;

ECA1 .. DTC1 =E= (T15('0') - TCUO);
ECA2 .. DTC2 =E= (366 - TCUI);
*ECA3 .. DTLMCL =E= 0.5*(DTC1+DTC2);
*ECA3 .. DTLMCL =E= (0.5*DTC1*DTC2*(DTC1+DTC2)+1E-6)**0.33333333;
ECA3 .. DTLMCL =E= ((DTC1+1E-7-DTC2)/((LOG((DTC1+1E-7)/(DTC2)))));
DTC1.LO = 0.00001;
DTC2.LO = 0.00001;

E1(I) .. WH2*X1(I)*(1-UH1(I))*(T1(I)-T5(I))
        +WC2*(1-UC1(I))*(T2(I)-T7(I)) =E= 0;
E2(I) .. WH2*X1(I)*(1-UH1(I))*(T1(I)-T5(I))
        -U1*A1*DTLM1(I) =E= 0;
E3(I) .. WH2*(1-X1(I))*(1-UH2(I))*(T1(I)-T9(I))
        +WC1*(1-UC2(I))*(T14(I)-T11(I)) =E= 0;
E4(I) .. WH2*(1-X1(I))*(1-UH2(I))*(T1(I)-T9(I))
        -U2*A2*DTLM2(I) =E= 0;
E5(I) .. WH1*(1-UH3(I))*(T3(I)-T12(I))
        +WC1*(1-UC3(I))*(T4(I)-T13(I)) =E= 0;
E6(I) .. WH1*(1-UH3(I))*(T3(I)-T12(I))
        -U3*A3*DTLM3(I) =E= 0;

E7(I) .. UH1(I)*T1(I) + (1-UH1(I))*T5(I) - T6(I) =E= 0;
E8(I) .. UC1(I)*T2(I) + (1-UC1(I))*T7(I) - T8(I) =E= 0;
E9(I) .. UH2(I)*T1(I) + (1-UH2(I))*T9(I) - T10(I) =E= 0;
E10(I) .. UC2(I)*T14(I) + (1-UC2(I))*T11(I) - T16(I) =E= 0;
E11(I) .. UH3(I)*T3(I) + (1-UH3(I))*T12(I) - T15(I) =E= 0;
E12(I) .. UC3(I)*T4(I) + (1-UC3(I))*T13(I) - T14(I) =E= 0;

```

E13(I) ..  $X1(I)*T6(I) + (1-X1(I))*T10(I) - T17(I) =E= 0;$

E14(I) ..  $DT11(I) =E= (T1(I) - T7(I) );$

E15(I) ..  $DT12(I) =E= (T5(I) - T2(I) );$

E16(I) ..  $DTLM1(I) =E= ((DT11(I)+1E-7-DT12(I))/$   
 $((LOG((DT11(I)+1E-7)/(DT12(I))))));$

DT11.LO(I) = 0.00001;

DT12.LO(I) = 0.00001;

E17(I) ..  $DT21(I) =E= (T1(I) - T11(I));$

E18(I) ..  $DT22(I) =E= (T9(I) - T14(I));$

E19(I) ..  $DTLM2(I) =E= ((DT21(I)+1E-7-DT22(I))/$   
 $((LOG((DT21(I)+1E-7)/(DT22(I))))));$

DT21.LO(I) = 0.00001;

DT22.LO(I) = 0.00001;

E20(I) ..  $DT31(I) =E= (T3(I) - T13(I));$

E21(I) ..  $DT32(I) =E= (T12(I) - T4(I) );$

E22(I) ..  $DTLM3(I) =E= ((DT31(I)+1E-7-DT32(I))/$   
 $((LOG((DT31(I)+1E-7)/(DT32(I))))));$

DT31.LO(I) = 0.00001;

DT32.LO(I) = 0.00001;

C1(I) ..  $T1(I) - T5(I) =G= 0;$

C2(I) ..  $T7(I) - T2(I) =G= 0;$

C3(I) ..  $T1(I) - T9(I) =G= 0;$

C4(I) ..  $T11(I) - T14(I) =G= 0;$

C5(I) ..  $T3(I) - T12(I) =G= 0;$

C6(I) ..  $T13(I) - T4(I) =G= 0;$

C7(I) ..  $T1(I) - T17(I) =G= 0;$

C8(I) ..  $T1(I) - T6(I) =G= 0;$

C9(I) ..  $T1(I) - T10(I) =G= 0;$

C10(I) ..  $T3(I) - T15(I) =G= 0;$

C11(I) ..  $T8(I) - T2(I) =G= 0;$

C12(I) ..  $T16(I) - T14(I) =G= 0;$

C13(I) ..  $T14(I) - T4(I) =G= 0;$

C14(I) ..  $T16(I) - T4(I) =G= 0;$

C15(I) ..  $T1(I) - T7(I) =G= DTMIN;$

C16(I) ..  $T5(I) - T2(I) =G= DTMIN;$

C17(I) ..  $T1(I) - T11(I) =G= DTMIN;$

C18(I) ..  $T9(I) - T14(I) =G= DTMIN;$

C19(I) ..  $T3(I) - T13(I) =G= DTMIN;$

C20(I) ..  $T12(I) - T4(I) =G= DTMIN;$

A1.LO = 0;

A2.LO = 0;

A3.LO = 0;

AH.LO = 0;

AC.LO = 0;

AT.LO = 0;

UH1.LO(I) = 0;

UH2.LO(I) = 0;

UH3.LO(I) = 0;

UC1.LO(I) = 0;

UC2.LO(I) = 0;

UC3.LO(I) = 0;

```
UH1.UP(I) = 0.999999;
UH2.UP(I) = 0;
UH3.UP(I) = 0;
```

```
UC1.UP(I) = 0;
UC2.UP(I) = 0;
UC3.UP(I) = 0.999999;
```

```
X1.LO(I) = 0.000001;
X1.UP(I) = 0.999999;
```

```
MODEL PRG601 /ALL/;
SOLVE PRG601 USING NLP MINIMIZING COSTTOT;
```

```
FILE MM /PRG601.RES/;
PUT MM;
PUT 'S =',S:14:9/
PUT 'A1 =',A1.L:14:10
PUT ' A2 =',A2.L:14:10
PUT ' A3 =',A3.L:14:10/
PUT ' AH =',AH.L:14:10
PUT ' AC =',AC.L:14:10/
PUT 'AT =',AT.L:14:10/
PUT 'COSTHEAT = ',COSTHEAT.L:16:3/
PUT 'COSTCOOL = ',COSTCOOL.L:16:3/
PUT 'COSTCAPH = ',COSTCAPH.L:16:3/
PUT 'COSTCAPC = ',COSTCAPC.L:16:3/
PUT 'COSTCAPE = ',COSTCAPE.L:16:3/
PUT 'COSTTOT = ',COSTTOT.L:16:3/
```

```
LOOP(I,
PUT 'X1 = ',X1.L(I):14:10/
PUT 'UH1 = ',UH1.L(I):14:10/
PUT 'UC1 = ',UC1.L(I):14:10/
PUT 'UH2 = ',UH2.L(I):14:10/
PUT 'UC2 = ',UC2.L(I):14:10/
PUT 'UH3 = ',UH3.L(I):14:10/
PUT 'UC3 = ',UC3.L(I):14:10/
PUT 'T5 = ',T5.L(I):14:10/
PUT 'T6 = ',T6.L(I):14:10/
PUT 'T7 = ',T7.L(I):14:10/
PUT 'T8 = ',T8.L(I):14:10/
PUT 'T9 = ',T9.L(I):14:10/
PUT 'T10 = ',T10.L(I):14:10/
PUT 'T11 = ',T11.L(I):14:10/
PUT 'T16 = ',T16.L(I):14:10/
PUT 'T13 = ',T13.L(I):14:10/
PUT 'T14 = ',T14.L(I):14:10/
PUT 'T12 = ',T12.L(I):14:10/
PUT 'T15 = ',T15.L(I):14:10/
PUT 'T17 = ',T17.L(I):14:10//
);
```

```
FILE MMM /PRG601.INI/;
PUT MMM;
PUT 'A1.L = ',A1.L:20:10,';'/
PUT 'A2.L = ',A2.L:20:10,';'/
```

```

PUT 'A3.L    = ',A3.L:20:10,';' /
PUT 'AH.L    = ',AH.L:20:10,';' /
PUT 'AC.L    = ',AC.L:20:10,';' /
PUT 'AT.L    = ',AT.L:20:10,';' /
PUT 'COSTCAPE.L    = ',COSTCAPE.L:20:10,';' /
PUT 'COSTCAPH.L    = ',COSTCAPH.L:20:10,';' /
PUT 'COSTCAPC.L    = ',COSTCAPC.L:20:10,';' /
PUT 'COSTHEAT.L    = ',COSTHEAT.L:20:10,';' /
PUT 'COSTCOOL.L    = ',COSTCOOL.L:20:10,';' /
PUT 'COSTTOT.L    = ',COSTTOT.L:20:10,';' /

LOOP(I,
PUT 'T5.L("I.TL:2,") = ',T5.L(I):14:9,';' /
PUT 'T6.L("I.TL:2,") = ',T6.L(I):14:9,';' /
PUT 'T7.L("I.TL:2,") = ',T7.L(I):14:9,';' /
PUT 'T8.L("I.TL:2,") = ',T8.L(I):14:9,';' /
PUT 'T9.L("I.TL:2,") = ',T9.L(I):14:9,';' /
PUT 'T10.L("I.TL:2,") = ',T10.L(I):14:9,';' /
PUT 'T11.L("I.TL:2,") = ',T11.L(I):14:9,';' /
PUT 'T12.L("I.TL:2,") = ',T12.L(I):14:9,';' /
PUT 'T13.L("I.TL:2,") = ',T13.L(I):14:9,';' /
PUT 'T14.L("I.TL:2,") = ',T14.L(I):14:9,';' /
PUT 'T15.L("I.TL:2,") = ',T15.L(I):14:9,';' /
PUT 'T16.L("I.TL:2,") = ',T16.L(I):14:9,';' /
PUT 'T17.L("I.TL:2,") = ',T17.L(I):14:9,';' /

PUT 'X1.L("I.TL:2,") = ',X1.L(I):14:9,';' /

PUT 'UH1.L("I.TL:2,") = ',UH1.L(I):14:9,';' /
PUT 'UC1.L("I.TL:2,") = ',UC1.L(I):14:9,';' /
PUT 'UH2.L("I.TL:2,") = ',UH2.L(I):14:9,';' /
PUT 'UC2.L("I.TL:2,") = ',UC2.L(I):14:9,';' /
PUT 'UH3.L("I.TL:2,") = ',UH3.L(I):14:9,';' /
PUT 'UC3.L("I.TL:2,") = ',UC3.L(I):14:9,';' /
);

FILE MMMM /PRG601.OUT/;
PUT MMMM;
PUT S:7:3,','
PUT A1.L:7:2,','
PUT A2.L:7:2,','
PUT A3.L:7:2,','
PUT AH.L:7:2,','
PUT AC.L:7:2,','
PUT AT.L:8:2,','
PUT COSTCAPH.L:9:2,','
PUT COSTCAPC.L:9:2,','
PUT COSTCAPE.L:9:2,','
PUT COSTHEAT.L:9:2,','
PUT COSTCOOL.L:9:2,','
PUT COSTTOT.L:11:2,','

```

## REFERENCES

- Chen J. J. J. (1988). "Comments on Improvement on a Replacement for the Logarithmic Mean" , *Chemical Engineering Science*, **42**, 1635.
- Colberg R. D., M. Morari, (1988). "Analysis and Synthesis of Resilient Heat Exchanger Networks," in J. Wei, J.L. Anderson, K.B. Bischoff, J.H. Seinfeld (Eds.) *Advances in Chemical Engineering*, **14**, 1-93, Academic Press, USA.
- Dolan W. B., P. T. Cummings, M. D. Le Van (1989). "Process Optimization via Simulated Annealing," *American Institute of Chemical Engineers Journal*, **35**, 725-736.
- Dolan W. B., P. T. Cummings, M.D. Le Van (1990). "Algorithmic Efficiency of Simulated Annealing for Heat Exchanger Network Design," *Computers and Chemical Engineering*, **14**, 1039-1050.
- Floudas C. A., I. E. Grossmann (1986). "Synthesis of Flexible Heat Exchanger Networks for Multiperiod Operation," *Computers and Chemical Engineering*, **10**, 153-168.
- Floudas C. A., A. R. Ciric, I. E. Grossmann (1986). "Automatic Synthesis of Optimum Heat Exchanger Network Configurations," *American Institute of Chemical Engineers Journal*, **32**, 276-290.
- Floudas C. A., I. E. Grossmann (1987a). "Synthesis of Flexible Heat Exchanger Networks with Uncertain Flowrates and Temperatures," *Computers and Chemical Engineering*, **11**, 319-336.

Floudas C. A., I. E. Grossmann (1987b). "Automatic Generation of Multiperiod Heat Exchanger Network Configurations," *Computers and Chemical Engineering*, **11**, 123-142.

Floudas C. A., A. R. Ciric (1989). "Strategies for Overcoming Uncertainties in Heat Exchanger Networks," *Computers and Chemical Engineering*, **13**, 1133-1152.

Georgiou A., C. A. Floudas (1989a). "An Optimization Model for the Generic Rank Determination of Structural Matrices," *International Journal of Control*, **49**, 1633-1644.

Georgiou A., C. A. Floudas (1989b). "Simultaneous Process Synthesis and Control: Minimization of Disturbance Propagation in Heat Exchanger Networks," *Third International Conference of Computer-Aided Process Design (FOCAPD)*, pp. 435-450, Snowmass Village, Colorado, USA.

Grossmann I. E., M. Morari (1983). "Operability, Resiliency and Flexibility - Process Design Objectives for a Changing World," *Proceedings of the Second International Conference on Foundations of Computer-Aided Process Design*, pp. 937-953, Snowmass Village, Colorado, USA.

Grossmann I. E., C. A. Floudas (1987). "Active Constraint Strategy for Flexibility Analysis in Chemical Processes," *Computers and Chemical Engineering*, **11**, 675-693.

Hohmann E. C. (1971). "Optimum Networks for Heat Exchange," Ph.D. Thesis, University of South California, LA, USA.

Huang Y. L., L. T. Fan (1992). "Distributed Strategy for Integration of Process Design and Control: A Knowledge Engineering Approach to the Incorporation of Controllability into Exchanger Network Synthesis," *Computers and Chemical Engineering*, **16**, 497-522.

Kirkpatrick S., C. D. Gelatt, M. P. Vecchi (1983). "Optimization by Simulated Annealing," *Science*, **220**, 671.

Konukman A. E. Ş, U. Akman, M. C. Çamurdan (1992). "Synthesis of Dynamic Resilience of Heat Exchanger Networks," *Proceedings of Turkish VIII th National Symposium on Chemistry and Chemical Engineering*, İstanbul, 7 - 11 September 1992, **Vol. IV**, 363-368.

Konukman A. E. Ş, U. Akman, M. C. Çamurdan (1994). "Optimal Design of Resilient and Controllable Heat Exchanger Networks," *Proceedings of the First Turkish Chemical Engineering Congress*, Ankara, 13-16 September 1994, **Vol. I**, 342-349.

Konukman A. E. Ş., U. Akman, H. Ütebay, M. C. Çamurdan (1995a). "Effects of Bypass-Stream Manipulations on Disturbance-Propagation Paths in Heat Exchanger Networks," *DOĞA-Turkish Journal of Engineering and Environmental Sciences*, **19**, 43-51.

Konukman A. E. Ş, U. Akman, M. C. Çamurdan (1995b). "Optimal Design of Controllable Heat-Exchanger Networks under Multi-Directional Resiliency-Target Constraints," *Computers and Chemical Engineering*, **Suppl. 19**, 149-153.

Kotjabasakis E., B. Linnhoff (1986). "Sensitivity Tables in the Design of Flexible Processes: 1. How much Contingency in Heat Exchanger Networks is Cost-Effective?," *Chem. Eng. Res. Des.*, **24**, 197-211.

Lee K. F., A. H. Masso, D. F. Rudd (1970). "Branch and Bound Synthesis of Integrated Process Designs," *Industrial and Engineering Chemistry Fundamentals*, **9**, 48.

Linnhoff B., J. R. Flower (1978a). "Synthesis of Heat Exchanger Networks: I. Systematic Generation of Energy Optimal Networks," *American Institute of Chemical Engineers Journal*, **24**, 633-642.

Linnhoff B., J. R. Flower (1978b). "Synthesis of Heat Exchanger Networks: II. Evolutionary Generation of Networks with Various Criteria of Optimality," *American Institute of Chemical Engineers Journal*, **24**, 642-654.

Linnhoff B., D. W. Townsend, D. Boland, G. F. Hewitt, B. E. A. Thomas, A. R. Guy, R. H. Marsland (1982). *A User Guide on Process Integration for the Efficient Use of Energy*, Pergamon Press, NY.

Linnhoff B., E. Hindmarsh (1983). "The Pinch Design Method for Heat Exchanger Networks," *Chemical Engineering Science*, **38**, 745-763.

Linnhoff B., E. Kotjabasakis (1986). "Downstream Paths for Operable Process Design," *Chemical Engineering Progress*, **82**, May, 23-28.

Masso A. H., D. F. Ruud (1969). "The Synthesis of System Designs. II. Heuristic Structuring," *American Institute of Chemical Engineers Journal*, **15**, 10-17.

Mathisen K. W., S. Skogestad, E. A. Wolf (1991). "Controllability of Heat Exchanger Networks," paper 152n, presented at *Annual Meeting of the American Institute of Chemical Engineers*, LA, USA.

Mathisen K. W., S. Skogestad, T. Gundersen (1992). "Optimal Bypass Placement in Heat Exchanger Networks," paper 67e, presented at *Spring Meeting of the American Institute of Chemical Engineers*, New Orleans, USA.

Mathisen K. W., S. Skogestad (1992). "Design, Operation and Control of Resilient Heat Exchanger Networks," paper 141g, presented at *Annual Meeting of the American Institute of Chemical Engineers*, Miami, USA.

Mathisen K. W. (1994). "Integrated Design and Control of Heat Exchanger Networks," Ph.D. Thesis, University of Trondheim, Norway.

Nishida N., Y. A. Liu, L. Lapidus (1977). "Studies in Chemical Process Design and Synthesis: III. A Simple and Practical Approach to the Optimal Synthesis of Heat Exchanger Networks," *American Institute of Chemical Engineers Journal*, **23**, 77-93.

Papalexandri K. P., E. N. Pistikopoulos (1993). "A Multiperiod MINLP Model for Improving the Flexibility of Heat Exchanger Networks," *Computers and Chemical Engineering, Suppl.* **17**, 111-116.

Papoulias S. A., I. E. Grossmann (1983a). "A Structural Optimization Approach in Process Synthesis - I. Utility Systems," *Computers and Chemical Engineering*, **7**, 695-706.

Papoulias S. A., I. E. Grossmann (1983b). "A Structural Optimization Approach in Process Synthesis - II Heat Recovery Networks," *Computers and Chemical Engineering*, **7**, 707-721.

Papoulias S. A., I. E. Grossmann (1983c). "A Structural Optimization Approach in Process Synthesis - III. Total Processing Systems," *Computers and Chemical Engineering*, **7**, 723-734.

Paterson W. R. (1984). "A Replacement for the Logarithmic Mean," *Chemical Engineering Science*, **39**, 1635, 1984.

Raghavan S. (1977). "Heat Exchanger Network Synthesis: A Thermodynamic Approach," Ph.D. Thesis, Purdue University, Lafayette, USA.

Saboo A. K., M. Morari, D. C. Woodcock (1985). "Design of Resilient Processing Plants - VIII A Resilience Index for Heat Exchanger Networks," *Chemical Engineering Science*, **40**, 1553-1565.

Swaney R. E., I. E. Grossmann (1985). "An Index for Operational Flexibility in Chemical Process Design. Part II: Computational Algorithms," *American Institute of Chemical Engineers Journal*, **31**, 631-641.

Yee T. F., I. E. Grossmann (1990). "Simultaneous Optimization Models for Heat Integration - II. Heat Exchanger Network Synthesis," *Computers and Chemical Engineering*, **14**, 1165-1183.

Yee T. F., I. E. Grossmann, Z. Kravanja (1990a). "Simultaneous Optimization Models for Heat Integration - I. Area and Energy Targeting and Modeling of Multi-Stream Exchangers," *Computers and Chemical Engineering*, **14**, 1151-1164.

Yee T. F., I. E. Grossmann, Z. Kravanja (1990b). "Simultaneous Optimization Models for Heat Integration - III. Process and Heat Exchanger Network Optimization," *Computers and Chemical Engineering*, **14**, 1185-1200.

## REFERENCES NOT CITED

Ahmad S., B. Linnhoff, R. Smith (1990). "Cost Optimum Heat Exchanger Networks - 2. Targets and Design for Detailed Capital Cost Models," *Computers and Chemical Engineering*, **14**, 751-767.

Calandranis J., G. Stephanopoulos (1988). "A Structural Approach to the Design of Control Systems in Heat Exchanger Networks," *Computers and Chemical Engineering*, **12**, 651-669.

Cerda J., M. R. Galli, N. Camusis, M. A. Isla (1990). "Synthesis of Flexible Heat Exchanger Networks - I. Convex Networks," *Computers and Chemical Engineering*, **14**, 197-211.

Cerda J., M. R. Galli (1990). "Synthesis of Flexible Heat Exchanger Networks - II. Nonconvex Networks with Large Temperature Variations," *Computers and Chemical Engineering*, **14**, 197-211.

Cerda J., M. R. Galli (1991). "Synthesis of Flexible Heat Exchanger Networks - III. Temperature and Flowrate Variations," *Computers and Chemical Engineering*, **15**, 7-24.

Chen B., J. Shen, Q. Sun, S. Hu (1989). "Development of an Expert System for Synthesis of Heat Exchanger Networks," *Computers and Chemical Engineering*, **13**, 1221-1227.

Ciric A. R., C. A. Floudas (1989). "A Retrofit Approach for Heat Exchanger Networks," *Computers and Chemical Engineering*, **13**, 703-715.

Ciric A. R., C. A. Floudas (1990). "A Mixed Integer Nonlinear Programming Model for Retrofitting Heat-Exchanger Networks," *Industrial and Engineering Chemistry Research*, **29**, 239-251.

Ciric A. R., C. A. Floudas (1991). "Heat Exchanger Network Synthesis without Decomposition," *Computers and Chemical Engineering*, **15**, 385-396.

Colberg R. D., M. Morari, D. W. Townsend (1989). "A Resilience Target for Heat Exchanger Network Synthesis," *Computers and Chemical Engineering*, **13**, 821-837.

Duran M. A., I. E. Grossmann (1986). "A Mixed-Integer Nonlinear Programming Algorithm for Process System Synthesis," *American Institute of Chemical Engineers Journal*, **32**, 592-606.

Floudas C. A., A. Aggarwal, A. R. Ciric (1989). "Global Optimum Search for Nonconvex NLP and MINLP Problems," *Computers and Chemical Engineering*, **13**, 1117-1132.

Grossmann I. E., K. P. Halemane, R. E. Swaney (1983). "Optimization Strategies for Flexible Chemical Processes," *Computers and Chemical Engineering*, **7**, 439-462.

Gundersen T., L. Næss (1988). "The Synthesis of Cost Optimal Heat Exchanger Networks. An Industrial Review of the State of the Art," *Computers and Chemical Engineering*, **12**, 503-530.

Gundersen T., I. E. Grossmann (1990). "Improved Optimization Strategies for Automated Heat Exchanger Network Synthesis Through Physical Insights," *Computers and Chemical Engineering*, **14**, 925-944.

Halemane K. P., I. E. Grossmann (1983). "Optimal Process Design Under Uncertainty," *American Institute of Chemical Engineers Journal*, **29**, 425-433.

Jezowski J. (1992). "SYNHEN: Microcomputer Directed Package of Programs for Heat Exchanger Network Synthesis," *Computers and Chemical Engineering*, **16**, 691-706.

Linnhoff B., S. Ahmad (1990). "Cost Optimum Heat Exchanger Networks - I. Minimum Energy and Capital Using Simple Models for Capital Cost," *Computers and Chemical Engineering*, **14**, 729-750.

Luus R. (1993). "Optimization of Heat Exchanger Networks," *Industrial and Engineering Chemistry Research*, **32**, 2633-2635.

Mathisen K. W., M. Morari, S. Skogestad (1994). "Dynamic Models for Heat Exchanger Networks," *Computers and Chemical Engineering*, **Suppl. 18**, 459-463.

Marselle D. F., M. Morari, D. F. Rudd (1982). "Design of Resilient Processing Plants - II. Design and Control of Energy Management Systems," *Chemical Engineering Science*, **37**, 259-270.

Papalexandri K. P., E. N. Pistikopoulos (1994). "Synthesis and Retrofit Design of Operable Heat Exchanger Networks. 1. Flexibility and Structural Controllability Aspects," *Industrial and Engineering Chemistry Research*, **33**, 1718-1737.

Papalexandri K. P., E. N. Pistikopoulos (1994). "Synthesis and Retrofit Design of Operable Heat Exchanger Networks. 2. Dynamics and Control Structure Considerations," *Industrial and Engineering Chemistry Research*, **33**, 1738-1755.

Papastratos S., A. Isambert, D. Depeyre (1993). "Computerized Optimum Design and Dynamic Simulation of Heat Exchanger Networks," *Computers and Chemical Engineering*, **S 17**, 329-334.

Qassim R. Y., C. S. Silveira (1988). "Heat Exchanger Network Synthesis: The Goal Programming Approach," *Computers and Chemical Engineering*, **12**, 1163-1165.

Qeseda I., I. E. Grossmann (1993). "Global Optimum Algorithm for Heat Exchanger Networks," *Industrial and Engineering Chemistry Research*, **32**, 487-499.

Ratnam R., V. S. Patwardhan (1991). "Sensitivity Analysis for Heat Exchanger Networks," *Chemical Engineering Science*, **46**, 451-458.

Saboo A.K., M. Morari (1984). "Design of Resilient Processing Plants - IV Some New Results on Heat Exchanger Network Synthesis," *Chemical Engineering Science*, **39**, 579-592.

Saboo A. K., M. Morari, R. D. Colberg (1987a). "Resilience Analysis of Heat Exchanger Networks - I. Temperature Dependent Heat Capacities," *Computers and Chemical Engineering*, **11**, 399-408.

Saboo A. K., M. Morari, R. D. Colberg (1987b). "Resilience Analysis of Heat Exchanger Networks - II. Stream Splits and Flowrate Variations," *Computers and Chemical Engineering*, **11**, 457-468.

Trivedi K. K., B. K. O'Neill, J. R. Roach, R. M. Wood (1989). "A New Dual-Temperature Design Method for the Synthesis of Heat Exchanger Networks," *Computers and Chemical Engineering*, **13**, 667-685.

Trivedi K. K., B. K. O'Neill, J. R. Roach, R. M. Wood (1990). "Systematic Energy Relaxation in MER Heat Exchanger Networks," *Computers and Chemical Engineering*, **14**, 601-611.

Umeda T., J. Itoh, K. Shiroko (1978). "Heat Exchange System Synthesis," *Chemical Engineering Progress*, **74**, July, 70-76.

Yee T. F., I. E. Grossmann (1991). "A Screening and Optimization Approach for the Retrofit of the Heat-Exchanger Networks," *Industrial and Engineering Chemistry Research*, **30**, 146-162.